



8-1987

# Development of Dynamic Non-Hortonian Watershed Models for Steeply Sloping Forested Watersheds: Application to Eastern Kentucky

Digital Object Identifier: <https://doi.org/10.13023/kwrri.rr.168>

Lindell E. Ormsbee  
*University of Kentucky*, [lindell.ormsbee@uky.edu](mailto:lindell.ormsbee@uky.edu)

Abdul Q. Khan  
*University of Kentucky*

**Right click to open a feedback form in a new tab to let us know how this document benefits you.**

Follow this and additional works at: [https://uknowledge.uky.edu/kwrri\\_reports](https://uknowledge.uky.edu/kwrri_reports)

 Part of the [Forest Sciences Commons](#), [Geology Commons](#), [Hydrology Commons](#), and the [Water Resource Management Commons](#)

## Repository Citation

Ormsbee, Lindell E. and Khan, Abdul Q, "Development of Dynamic Non-Hortonian Watershed Models for Steeply Sloping Forested Watersheds: Application to Eastern Kentucky" (1987). *KWRRI Research Reports*. 37.  
[https://uknowledge.uky.edu/kwrri\\_reports/37](https://uknowledge.uky.edu/kwrri_reports/37)

This Report is brought to you for free and open access by the Kentucky Water Resources Research Institute at UKnowledge. It has been accepted for inclusion in KWRRI Research Reports by an authorized administrator of UKnowledge. For more information, please contact [UKnowledge@lsv.uky.edu](mailto:UKnowledge@lsv.uky.edu).

DEVELOPMENT OF DYNAMIC NON-HORTONIAN  
WATERSHED MODELS FOR STEEPLY SLOPING  
FORESTED WATERSHEDS: Application to  
Eastern Kentucky

By

Lindell E. Ormsbee  
Principal Investigator

Abdul Q. Khan  
Research Assistant

Project Number: G-1019-02 , G-1227-02\* (A-104-KY)

Agreement Number(s): 14-08-0001-G1019 (FY 1985)  
14-08-0001-G1227 (FY 1986)

Period of Project: July 1985 - June 1987

Water Resources Research Institute  
University of Kentucky  
Lexington, Kentucky

The work upon which this report is based was supported in part by funds provided by the United States Department of the Interior, Washington, D.C., as authorized by the Water Resources Research Act of 1984. Public Law 98-242.

August 1987

## **DISCLAIMER**

The contents of this report do not necessarily reflect the views and policies of the United States Department of the Interior, Washington, D.C., nor does mention of trade names or commercial products constitute their endorsement or recommendation for use by the U.S. Government.

## ABSTRACT

A comprehensive conceptual watershed model is developed to simulate the hydrologic response of steeply sloping forested watersheds. Two non-Hortonian and two Hortonian models were first tested with data from selected watersheds in West Virginia and eastern Kentucky in order to understand the different mechanisms of flow responsible for storm hydrograph generation in this type of watersheds. The two non-Hortonian models tested were the kinematic storage model (Sloan et al. 1983) and the saturation deficit model (Beven and Wood, 1983). Both models were unable to adequately reproduce the observed hydrographs in the four forested watersheds considered in this research. The two Hortonian models tested were Clark's unit hydrograph model and Snyder's unit hydrograph model. These two models were able to reproduce the observed hydrographs only through model calibration with unrealistic parameter values.

Based on the conclusions from the testing of the two non-Hortonian and the two Hortonian models, a simple conceptual comprehensive watershed model was developed for predicting storm hydrograph from small, steeply sloping forested watersheds. The conceptual model incorporates all types of flow processes including macropore flow (quick response subsurface flow). An evaluation of the resulting model was made using the data from the previously mentioned four watersheds in West Virginia and eastern Kentucky. The model predicted with reasonable accuracy the response of these watersheds to precipitation. The results indicate that the model is capable of simulating the hydrologic response of this type of watersheds while at the same time depicting the actual flow mechanism in play.

Descriptors: Forested Watersheds, Water Management, Watershed Management  
Runoff Forecasting, Runoff, Forest Hydrology

## **ACKNOWLEDGEMENTS**

The authors wish to thank Dr. G. B. Coltharp for providing hydrologic data for the Little Millseat watershed. The authors also extends their sincere appreciation to Mr. Dale G. Hall for the excellent job he has done in typing the manuscript.

## TABLE OF CONTENTS

Description	Page
ABSTRACT	iii
ACKNOWLEDGEMENTS	iv
LIST OF TABLES	ix
LIST OF FIGURES	x
LIST OF SYMBOLS	xiii
CHAPTER 1 : INTRODUCTION	1
1.1 Problem Statement	1
1.2 Project Objectives	3
1.3 Project Completion	3
1.4 Overview	3
CHAPTER 2 : REVIEW OF THE LITERATURE	5
2.1 Modeling of Rainfall-Runoff Process	5
2.2 Mechanisms of Runoff Generation	5
2.2.1 Hortonian Overland Flow	5
2.2.2 Non-Hortonian Flow	6
2.2.2.1 Subsurface Flow	6
2.2.2.1.1 Macropore Flow	7
2.2.2.1.2 Micropore Flow	8
2.2.2.2 Saturation Overland Flow	9
2.2.2.3 Variable Source Area Concept	9
2.3 Mechanisms of Runoff Routing	11
2.3.1 Simplified Hydraulic Models	13
2.3.2 Hydrologic Models	14
2.3.2 Linearized Models	16

2.4 Models of Watershed Runoff	17
2.5 Mathematical Models of Forested Watershed Runoff	17
2.5.1 Hortonian Type Models	18
2.5.1.1 Conceptual Hortonian Models	19
2.5.1.1.1 Unit Hydrograph Method	19
2.5.1.1.2 Instantaneous Unit Hydrograph Method	20
2.5.1.2 Physically-Based Hortonian Models	21
2.5.1.2.1 Overland Flow Models	21
2.5.2 Variable Source Area Models	22
2.5.2.1 Distributed Physically-Based Models	22
2.5.2.1.1 Hillslope Models	22
2.5.2.1.2 Watershed Models	23
2.5.2.2 Lumped Conceptual Models	23
2.5.2.2.1 Hillslope Model	25
2.5.2.2.2 Watershed Model	28
 CHAPTER 3 : MODEL COMPARISONS	 34
3.1 Introduction	34
3.2 Physiography and Topography	34
3.3 Land Use	40
3.4 Soil Classification	40
3.5 Hydrology	41
3.6 Hydrologic Data	42
3.7 Description of HEC-1	43
3.7.1 Assumptions and Limitation of HEC-1	43
3.7.2 Steps To Use HEC-1	44
3.7.3 Capabilities of HEC-1	44

3.7.4 Modified Version of HEC-1	45
3.8 Non-Hortonian Flow Models	46
3.8.1 Results	46
3.8.2 Discussion of the Results	59
3.9 Hortonian Flow Models	60
3.9.1 Results	60
3.9.2 Discussion of the Results	63
3.10 Parameter Estimation for Hortonian Models	63
3.10.1 Loss Rate Parameters	63
3.10.1.1 Land Use Coefficient	64
3.10.1.2 Infiltration Exponent	64
3.10.1.3 Final Infiltration Rate	64
3.10.1.4 Initial Storage Potential	64
3.10.2 Unit Hydrograph Parameters	65
3.10.2.1 Time of Concentration	66
3.10.2.2 Storage Coefficient	66
3.10.2.3 Time of Lag	66
3.10.2.4 Peaking Coefficient	66
3.10.3 Results	68
3.10.4 Discussion of Results	68
3.11 Conclusions	68
 CHAPTER 4 : A COMPREHENSIVE CONCEPTUAL MODEL FOR FORESTED WATERSHEDS	 70
4.1 Introduction	70
4.2 General Description of the Model	70
4.2.1 Macropore Store	71
4.2.2 Micropore Store	71



4.2.3 Surface Store	72
4.3 Detailed Description of the Model	72
4.3.1 Macropore Storage	72
4.3.2 Micropore Storage	76
4.3.3 Surface Storage	78
4.3.3.1 Hortonian Overland Flow	78
4.3.3.2 Saturation Overland Flow	79
4.3.3.3 Distribution of Overland Flow	79
 CHAPTER 5 : COMPREHENSIVE MODEL RESULTS	 81
5.1 Introduction	81
5.2 Modified Version of HEC-1	81
5.3 Comprehensive Model Application	82
5.3.1 Data Reduction	82
5.3.2 Results	82
5.3.3 Discussion of the Results	91
 CHAPTER 6 : SUMMARY AND CONCLUSIONS	 92
6.1 Summary	92
6.2 Conclusions	94
6.3 Recommendations for Future Research	94
 REFERENCES	 96
 APPENDIX A : Precipitation Hyetographs	 102

## LIST OF TABLES

Table		Page
3.1	Watershed Characteristics	35
3.2a	Optimized Parameters : Non-Hortonian Models	47
3.2b	Statistics of Selected Hydrologic Parameters : Non-Hortonian Models with Optimization	48
3.3a	Optimized Parameters : Hortonian Models	61
3.3b	Statistics of Selected Hydrologic Parameters : Hortonian Models With Optimization	62
3.4	Estimated Parameter Values : Hortonian Models	67
5.1	Estimated Parameter Values : Comprehensive Watershed Model	83
5.2	Optimized Parameters : Comprehensive Watershed Model	84
5.3	Statistics of Selected Hydrologic Parameters : Comprehensive Watershed Model	85

## LIST OF FIGURES

Figure		Page
2.1	Kinematic Storage Model Without Saturation Overland Flow	27
2.2	Kinematic Storage Model With Saturation Overland Flow	27
2.3	Conceptual Representation of Saturation Deficit Model	30
3.1a	Location Map : Crane Creek Watershed, W.Va.	36
3.1b	Topographic Map : Crane Creek Watershed, W.Va.	36
3.2a	Location Map : R.F. Sandlick Creek Watershed, W.Va.	37
3.2b	Topographic Map : R.F. Sandlick Creek Watershed, W.Va.	37
3.3a	Location Map : Little Millseat Watershed, Ky.	38
3.3b	Topographic Map : Little Millseat Watershed, Ky.	38
3.4a	Location Map : Cane branch Watershed, Ky.	39
3.4b	Topographic Map : Cane Branch Watershed, Ky.	39
3.5a	Crane Creek : Storm 1 : Non-Hortonian Models With Optimization	49
3.5b	Crane Creek : Storm 1 : Hortonian Models With Optimization	49
3.6a	Crane Creek : Storm 2 : Non-Hortonian Models With Optimization	50
3.6b	Crane Creek : Storm 2 : Hortonian Models With Optimization	50
3.7a	Crane Creek : Storm 3 : Non-Hortonian Models With Optimization	51
3.7b	Crane Creek : Storm 3 : Hortonian Models With Optimization	51
3.8a	Crane Creek : Storm 4 : Non-Hortonian Models With Optimization	52
3.8b	Crane Creek : Storm 4 : Hortonian Models With Optimization	52

3.9a	R.F. Sandlick Creek : Storm 1 : Non-Hortonian Models With Optimization	53
3.9b	R.F. Sandlick Creek : Storm 1 : Hortonian Models With Optimization	53
3.10a	R.F. Sandlick Creek : Storm 2 : Non-Hortonian Models With Optimization	54
3.10b	R.F. Sandlick Creek : Storm 2 : Hortonian Models With Optimization	54
3.11a	Little Millseat : Storm 1 : Non-Hortonian Models With Optimization	55
3.11b	Little Millseat : Storm 1 : Hortonian Models With Optimization	55
3.12a	Little Millseat : Storm 2 : Non-Hortonian Models With Optimization	56
3.12b	Little Millseat : Storm 2 : Hortonian Models With Optimization	56
3.13a	Little Millseat : Storm 3 : Non-Hortonian Models With Optimization	57
3.13b	Little Millseat : Storm 3 : Hortonian Models With Optimization	57
3.14a	Cane Branch : Storm 1 : Non-Hortonian Models With Optimization	58
3.14b	Cane Branch : Storm 1 : Hortonian Models With Optimization	58
4.1	Comprehensive Watershed Model : Scenario I : Gravity Water Absent	73
4.2	Comprehensive Watershed Model : Scenario II : Gravity Water Present	73
5.1	Crane Creek : Storm 1 : Comprehensive Watershed Model	86
5.2	Crane Creek : Storm 2 : Comprehensive Watershed Model	86
5.3	Crane Creek : Storm 3 : Comprehensive Watershed Model	87
5.4	Crane Creek : Storm 4 : Comprehensive Watershed Model	87

5.5	R.F. Sandlick Creek : Storm 1 : Comprehensive Watershed Model	88
5.6	R.F. Sandlick Creek : Storm 2 : Comprehensive Watershed Model	88
5.7	Little Millseat : Storm 1 : Comprehensive Watershed Model	89
5.8	Little Millseat : Storm 2 : Comprehensive Watershed Model	89
5.9	Little Millseat : Storm 3 : Comprehensive Watershed Model	90
5.10	Cane Branch : Storm 1 : Comprehensive Watershed Model	90
A.1	Precipitation Hyetograph : Crane Creek : Storm 1	103
A.2	Precipitation Hyetograph : Crane Creek : Storm 2	104
A.3	Precipitation Hyetograph : Crane Creek : Storm 3	105
A.4	Precipitation Hyetograph : Crane Creek : Storm 4	106
A.5	Precipitation Hyetograph : R. F. Sandlick Creek : Storm 1	107
A.6	Precipitation Hyetograph : R. F. Sandlick Creek : Storm 2	108
A.7	Precipitation Hyetograph : Little Millseat : Storm 1	109
A.8	Precipitation Hyetograph : Little Millseat : Storm 2	110
A.9	Precipitation Hyetograph : Little Millseat : Storm 3	111
A.10	Precipitation Hyetograph: Cane Branch: Storm 1	112

## LIST OF SYMBOLS

### Symbol

$\alpha$	Constant, hillslope angle, fraction of rainfall running as saturation overland flow
$\alpha_{mp}$	Fraction of precipitation entering the soil macropores
$a$	Constant, upslope area drained per unit width of slope, land use coefficient
$a_p$	Attenuation parameter for peak discharge
$A$	Cross-section area
$AW_{max}$	Maximum value of available water store
$\beta$	Constant, surface slope angle, fraction of rainfall running as Hortonian overland flow
$C$	Constant, Chezy coefficient
$C_g$	Geometric factor of the watershed
$C_o$	Wave Celerity
$C_p$	Peaking coefficient
$C_{mp}$	Macropore storage constant
$C_{ss}$	Micropore flow velocity
$D$	Hillslope soil depth to an impermeable layer
$ET$	Evapotranspiration potential
$EP$	Pan evaporation
$f$	Infiltration rate
$f_c$	Final infiltration rate after prolonged wetting
$\gamma$	Fraction of rainfall running as overland flow (sum of Hortonian overland flow and saturation overland flow)
$g$	Gravitational acceleration
$GI$	Growth index of crops in % of maturity
$GW$	Value of gravity water store

GWmax	Maximum value of gravity water store
h	Depth of water table at outlet
$\partial h/\partial x$	Hydraulic gradient
i	Rainfall excess rate, hydraulic gradient
I	Inflow
I( $\tau$ )	Rainfall excess rate
K	Storage parameter, wave dispersion coefficient, ratio of growth index of crops to pan evaporation
$K_0$	Saturated hydraulic conductivity
$K_s$	Saturated hydraulic conductivity
$\lambda$	Constant
L	Length of channel reach, hillslope length, hydraulic length of the watershed
Ls	Saturated slope length
m	Constant
$\nu$	Kinematic viscosity of water
n	Infiltration exponent
Pmi	Fraction of rainfall which either infiltrates the micropores or runs off as overland flow
Pmp	Input to macropore store
q	Discharge per unit width
$q_0$	Discharge per unit width
$q_v$	Input to saturated zone
$Q_0$	Subsurface recession constant
$Q_b$	Subsurface drainage from the complete basin
$Q_i$	Initial catchment discharge
Qmp	Macropore flow
Qp	Peak discharge

$Q_s$	Micropore flow per unit area
$Q_{mi}$	Micropore flow per unit width
$Q_{uz}$	Total reduction in the catchment average deficit
$R$	Rainfall excess rate, storage coefficient
$S$	Storage, storage potential, saturation deficit
$\bar{S}$	Average storage deficit
$S_1$	Current storage potential
$S_f$	Friction slope
$S_o$	Channel slope
$S_{mp}$	Macropore storage value
$S_{uz}$	Storage in the unsaturated zone in excess of field capacity
$\theta_s$	Saturated water content
$\theta_d$	Water content at field capacity
$t$	Time
$\Delta t$	Time increment
$t_c$	Time of concentration
$t_d$	Time delay per unit of deficit
$T_{lag}$	Time of lag
$T_p$	Time of travel of the wave crest
$u(t-\tau)$	Instantaneous unit hydrograph
$V$	Velocity
$V_0$	Reference flow velocity
$w$	Average speed of flood peak
$x$	Distance, weighting factor
$\Delta x$	Space increment
$y$	Flow depth





## CHAPTER 1

### INTRODUCTION

#### 1.1 Problem Statement :

The development and management of Kentucky's water resources remains a very high priority. In the state of Kentucky, as in other states, a natural conflict exists between the need for economic development and the need to preserve the integrity of the state's water resources. One way to minimize this conflict is through the development and implementation of comprehensive watershed management guidelines. In order to develop such guidelines for natural watersheds there is a strong need for more refined analytical tools.

At the present time the USGS maintains approximately 120 daily-read stream gaging stations in the state of Kentucky. These gaging stations are primarily confined to the larger streams and tributaries of the major river basins. As a result, most of the lower order streams are not monitored. One cost effective method of determining the hydrologic response of such non-gaged watersheds is through the use of mathematical models. These models can be used to predict both watershed discharge and pollutant loadings as either deterministic or stochastic functions of precipitation and other hydrologic variables (Sloan et al., 1983).

Since the 1930's the Horton (1933) infiltration approach to runoff production has dominated hydrology and its applications to the prediction of river discharges (Soil Conservation Service, 1972; Crawford and Linsley, 1966) and in land management (Schawb et al., 1966). In humid regions, such as the Appalachian region of Eastern Kentucky, the infiltration capacity of the soil generally remains high

unless the dense vegetation cover is disturbed. For such watersheds, Horton overland flow is typically confined to areas that have been denuded of their vegetation. For those areas that have not been severely disturbed, Horton overland flow does not occur. At least two processes generate storm runoff in these regions. These two processes of storm runoff are subsurface stormflow, and direct precipitation onto saturated areas. The relative importance of each process varies with topography, soil antecedent wetness, and storm size. Together, these two processes make up the variable source area concept (Dunne et al., 1975).

Despite the widespread observations of non-Hortonian flow in humid watersheds, nearly all existing hydrologic models are based on the Hortonian flow concept. There exists therefore, a strong need for hydrologic watershed models based on the observed mechanisms of saturation overland flow and subsurface flow. Although some attempts have been made at modeling the various mechanisms in the non-Hortonian flow process, there remains a need for the various processes to be combined in a general watershed model for use in the prediction of watershed hydrologic response.

In addition to being important in the accurate prediction of the hydrologic response of a watershed, the use of non-Hortonian models based on the variable-source-area concept is vitally important in the identification and characterization of non-point source pollution. If the runoff from a watershed is dominated by subsurface flow then current hydrologic models based on classical Hortonian runoff theory will offer few valid interpretations of the source and movement of pollutant within the watershed. Although such models may predict mass outputs satisfactorily they will fail to lead to the correct management practice

(Hewlett and Troendle, 1975).

## **1.2 Project Objectives :**

The objective of the proposed research was the development of two hydrologic models for use in the prediction of the hydrologic response of steeply sloping forested watersheds in humid areas. The first model was developed for small upland watersheds while the second model was developed for much larger tributary watersheds.

The original proposal for the project called for the development of a large scale tributary model using the concept of a most probable stream network distribution. However, during the course of the research it was decided that a more useful product could be obtained by incorporating the upland model into an existing comprehensive watershed model such as HEC-1. As a result, the second approach was ultimately used in developing a modeling framework for larger tributary watersheds.

## **1.3 Project Completion :**

Both an upland watershed model and a tributary watershed model have been developed for steeply sloping forested watersheds. The upland watershed model incorporates the flow mechanisms of overland flow, micropore flow and macropore flow. The tributary watershed model consists of a modified version of the HEC-1 watershed model which incorporates the upland watershed model.

## **1.4 Overview :**

Chapter 2 presents a review of the literature dealing with runoff processes and runoff models with an emphasis on the description of physically based variable-source-area models.

In chapter 3, the incorporation of two such models, the Kinematic Storage Model (Sloan et. al, 1983) and the Saturation Deficit Model

(Beven and Wood, 1983) in HEC-1 is described. HEC-1 is a comprehensive hydrologic modeling package developed by the US Army Corps of Engineers, Davis, California. In addition, results obtained using the kinematic storage model and the saturation deficit model are compared with those obtained using models based on Hortonian flow theory (Clark's model and Snyder's model).

Chapter 4 gives a detailed description of a new model which incorporates all the possible runoff generation processes including the macropore component of subsurface flow. This model was also embedded in HEC-1.

In chapter 5, results from the new model are compared with those from the kinematic storage model and the saturation deficit model neither of which accounts for flow in macropores.

Finally, the conclusions resulting from this study are summarized in Chapter 6. Recommendations for future research are also presented in this chapter.

## CHAPTER 2

### REVIEW OF THE LITERATURE

#### 2.1. Modeling of Rainfall-Runoff Process :

The majority of hydrologic watershed models are composed of two basic components. These include the runoff generation mechanism and the runoff routing mechanism.

#### 2.2. Mechanisms of Runoff Generation :

At present there are two major conceptual models of the runoff generation process. The first is based on the Hortonian flow concept introduced by Robert Horton in 1933. The second type of model is based on the variable-source-area concept first formally introduced by Hewlett and Hibbert in 1967.

##### 2.2.1. Hortonian Overland Flow :

Horton overland flow theory postulates that the infiltration capacity of a soil is reduced exponentially under a continuous high-intensity rainfall of long duration. Horton assumed that this decrease was primarily due to the compaction, structural change and inwashing of fine particles at the soil surface. With the progression of the storm, the infiltration capacity of the soil finally decreases to a constant value over the whole watershed. Whenever the rainfall rate exceeds the infiltration rate, overland flow and subsequently surface runoff occurs over the entire catchment area. Overland flow reaches the channels very quickly and leads to the rapid increase in the rising limb of the runoff hydrograph. After the rainfall ceases, the surface runoff decreases, quickly in the initial stages and later gradually, as water recedes in the small channels first followed by that in the larger ones. According to

Horton's flow theory, surface runoff provides the major portion of the storm hydrograph whereas water infiltrating into the soil is responsible for sustaining the long-time recession discharge from the watershed.

From the previous discussion it is clear that the amount of rainfall infiltration into the soil is a key component in the runoff generation process using Horton's theory. Once the infiltration loss has been calculated, rainfall excess can easily be calculated by subtracting the amount of infiltration from the amount of rainfall.

#### **2.2.2. Non-Hortonian Flow :**

In recent years, it has become increasingly evident that the Hortonian flow model is inadequate to explain the response of many catchments where measured infiltration rates are high enough to be only rarely exceeded by storm rainfall intensities. In such a case, the storm hydrograph may either be generated by subsurface flow (Hursh and Brater, 1941; Hewlett and Hibbert, 1967; Weyman, 1973; and Neiber, 1979) or surface flow on areas of soil saturated from below as the water table rises to the soil surface (Dunne and Black, 1970; Dunne et al., 1975; Kirkby et al., 1976; and Beven, 1977). In this regard, it is important to recognize that catchment storm response may involve significant subsurface contributions while runoff contributing areas may be highly dynamic.

##### **2.2.2.1. Subsurface Flow :**

In many catchments, the magnitude and the shape of the storm hydrograph may be dominantly controlled by subsurface flows. Evidence for this comes from areas where little or no overland flow is observed (Hewlett and Hibbert, 1967; and Mosley, 1979). Essentially two basic mechanisms have been proposed to account for the

contribution of subsurface flow to watershed response. These two mechanisms are macropore flow and micropore flow.

#### 2.2.2.1.1. Macropore Flow :

Many investigators including Whipkey (1967), Jones (1975), Corbett (1979) and Mosley (1979,1982) have cited flow through interconnected macro-channels in the soil as being important in the generation of subsurface storm flow. This has either been inferred from the extreme rapidity of the subsurface flow response or directly from observation of flow. Whipkey (1967) first postulated that interconnected macro-channels formed by roots of trees and animal burrows can provide the means for rapid subsurface flow from upper slopes to stream channels. With advanced growth, roots can become major soil forming agents compressing the soil causing local changes in porosity and bulk density (Corbett, 1979). When they decay, they leave openings, resulting in a large increase in non-capillary porosity (Retzer,1963). Animal burrows which can be extensive in natural watersheds can also act like subsurface pipe networks and can rapidly transport water through soil profile. Soil pipes formed by macropores therefore, impart a system of flow conduits to the soil matrix thereby increasing significantly the effective hydraulic conductivity of the soil although they may contribute only a very small amount to total porosity (Barcello and Nieber, 1982; and Beven and German, 1982).

Several researchers have provided information regarding the significance of soil pipe flow relative to other hydrograph contributions. During one experiment Whipkey (1969) observed outflow to come from a root hole 122 cm below the soil surface 16 minutes after



an application rate of 25 mm per hour had begun. Whipkey then dug trenches across the slope of his plots to brake up the continuity of the existing macropore channels. This reduced the total stream flow to half of that which occurred prior to trenching. Jones (1975) found out that whereas the hydraulic conductivity value of the soil material overlying a soil pipe indicated a time of 12 hours for pipe discharge to initiate, the observed time to peak was only 1.73 hours. Barcello and Nieber (1982) using a computer simulation model found that for the same rainfall and hillslope conditions, soil pipe networks contributed more discharge to storm flow peak than the unpiped hillslope. They also found out that soil pipe networks contributed significantly more discharge than a single soil pipe. Mosley (1982) carried out a series of experiments in an instrumented steep sloping forested watershed in New Zealand. Data for a number of storms indicated that preferred pathways for subsurface flow via macropores in the soil was the predominant mechanism of channel storm flow generation in storms whenever quick flow runoff volume (total runoff volume - delayed subsurface runoff volume) was greater than about 1 mm. He concluded that the saturated hydraulic conductivity of the soil matrix is not a limiting factor on the ability of subsurface flow to generate storm flow. Weyman (1970) also made similar observations under natural rainfall conditions at the base of a brown earth profile in the East Twin catchment in England.

#### **2.2.2.1.2. Micropore Flow :**

In a watershed where there is no well developed system of macropores, Hewlett and Hibbert (1967) suggested the process of displacement to account for the response of subsurface flow to

rainfall. This is known as micropore flow. Hewlett and Hibbert proposed that if the soil is at or above field capacity, precipitation input thickens the water films surrounding the soil particles, causing the release of previously stored water. Each input of precipitation sends a pressure wave along the saturated zones. This wave moves downslope as a pulse and releases previously stored water. If the released water emerges at the surface, it contributes to storm flow. However, it is to be remembered that this contribution is previously stored water and not new water (Sloan et al., 1983).

#### **2.2.2.2. Saturation Overland Flow :**

Saturation overland flow occurs when subsurface flow is no longer capable of releasing all the water that infiltrates into the soil. This results in the increase of the volume of water stored in the soil thus causing the water table to rise to the ground surface. Rain falling on the saturated area then runs off as overland flow. It is to be noted that this saturated area varies through time, both during and before rain storms. Saturation overland flow extends in time initially to low-order tributary channels, then to unchanneled swales and finally to foot of hillslopes. At the end of storm, this saturated area shrinks gradually as the soil slowly drains.

#### **2.2.2.3. Variable Source Area Concept :**

Hewlett (1961) conducted a number of field studies at Coweeta and first proposed the concept of dynamic watershed source areas (i.e., variable source areas). A source area has been defined as that part of the watershed where precipitation is converted to runoff. These areas are often near the stream channel and quickly become saturated during a rainfall event. In the study undertaken by

Hewlett, the drainage of water downslope in soil troughs was studied and it was observed that moisture gradients increased downslope. It was proposed that rain falling after drainage had set up these hydraulic gradients quickly satisfied the water deficits near the channel, saturated the soil and thus setup conditions for storm flow generation. The deficits upslope would take longer to satisfy, but as rainfall continued, the contributing area would expand. He therefore concluded that storm flow was generated from precipitation over saturated areas which began to contribute as deficits are satisfied. Upslope rain subsequently recharged the soil for sustained base flow and the maintenance of the channel wet areas.

Dunne and Black (1970) made a field study of a number of areas in the Sleepers River Experimental Watershed in northeastern Vermont. One of their study areas had a well drained slope and poorly drained soils at the base of the slope. They found that significant amount of runoff occurred only from small wet area at the base of the slope. Its low storage capacity was quickly filled, the surface was intersected by the water table and then the source area behaved as an impervious area. Dunne and Black also applied artificial storms of high return periods to the watershed. Similar mechanisms to those in the natural storms were observed. In one test, rain was applied only to the channel area and a hydrograph similar to natural storms was observed. As the duration was increased, the source area also expanded.

Corbett (1979) studied a small forested watershed in Pennsylvania. After extensive experimentation with the application of artificial rainfall, he concluded that variable source area concept provided the best framework to evaluate a watershed's

response to precipitation. The front portion of the watershed had shallow soils which drained to the channel. However, the back portion had to drain through deep soils to reach the stream. A delay between the response of the front and the back halves of watershed was observed. It was also observed that for dry antecedent moisture conditions the rising limb and the peak of the hydrograph were produced by contributions from precipitation on the channel and the base of the slope only. The lower and middle slopes provided the major portion of the runoff during recession. For wet antecedent moisture conditions, peak flow rates were found to be two to three times greater than those for dry antecedent conditions. There was also a substantial increase in the amount of rainfall converted to quick and delayed flow. Temporary zones of saturation developed during the storm and the development of these areas has an important bearing on how effectively a particular area responded to rainfall.

### 2.3. Mechanisms of Runoff Routing :

The general equations governing unsteady flow in an open channel are known as the St. Venant equations. These equations consist of a conservation of mass equation :

$$\frac{\partial(AV)}{\partial x} + \frac{\partial A}{\partial t} = 0 \quad (2.1)$$

and a conservation of momentum equation :

$$\frac{\partial V}{\partial t} + V \frac{\partial V}{\partial x} + g \left( \frac{\partial y}{\partial x} + S_f - S_0 \right) = 0 \quad (2.2)$$

where  $x$  is the distance along the channel,  $A$  is the cross-section area,  $V$  is the velocity,  $g$  is the gravitational acceleration,  $y$  is the flow depth,  $S_0$  is the channel slope and  $S_f$  is the friction slope.

Equations (2.1) and (2.2) are quasi-linear hyperbolic partial

differential equations which cannot be solved analytically. The variables  $x$  and  $t$  are the independent variables while  $V$  and  $y$  are the dependent variables. The cross section area  $A$  is a known function of  $y$ , and  $S_f$  is a known function of  $V$  and  $y$ .  $S_f$  can be computed using either the Chezy or Manning formula for steady flow.

Runoff routing models based on the complete solution of the St. Venant equations are termed dynamic wave models. Stoker (1953) and Isaacson, et al. (1954) first used the full St. Venant equations to model the routing of floods on the Ohio river. With the increasing availability of high-speed computers, many researchers have developed alternative numerical solution schemes for the complete St. Venant equations. The various dynamic wave models cited in the literature can be divided into essentially two broad groups. The first group consists of the direct methods, where the St. Venant equations are expressed in finite difference form and solutions are obtained for time increment  $(\Delta t)$  and space increment  $(\Delta x)$  along the channel. The second group is the method of characteristics, where the partial differential equations (2.1) and (2.2) are first converted to an equivalent system of four ordinary differential equations. Finite difference approximations are then substituted into these four equations to solve the system (Fread, 1985).

A further classification of the dynamic wave models is possible based on the finite difference scheme used for solving the equations. In an explicit solution scheme, the differential equations are transformed into a set of algebraic equations which can be solved explicitly. In an implicit scheme, the differential equations are transformed into a set of algebraic equations (linear or non-linear) which must be solved simultaneously. If the set of simultaneous equations happen to be non-

linear, they can only be solved using an iterative solution procedure.

Due to the complex nature of the St. Venant equations and the difficulty in obtaining stable solutions, a number of simplified, approximate solution techniques have been developed for channel routing. The approximate methods can be classified as a) Hydraulic, b) Hydrologic and c) Linearized models of the St. Venant equations. A comprehensive review of all three methods has been provided by Fread (1985). A brief discussion of each of these simplifications is presented below.

### 2.3.1. Simplified Hydraulic Models :

Hydraulic models are based on the conservation of mass equation and a simplified form of the conservation of momentum equation. One type of simplified hydraulic model is the kinematic wave model. Interest in this model was sparked by the work of Lighthill and Whitman (1955). The kinematic model uses the following simplified form of the conservation of momentum equation :

$$S_f - S_0 = 0 \quad (2.3)$$

Equation (2.3) essentially states that the momentum of the unsteady flow is assumed to be the same as that of steady uniform flow as described by the Chezy or Manning equation or some other similar expression in which discharge is a single-valued function of stage, e.g.,

$$A = \alpha Q^\beta \quad (2.4)$$

in which A is the cross-sectional area,  $\alpha = [\beta/C^2 S_0]$ ,  $\beta = 2/3$ , and C is the Chezy coefficient. Combining equations (2.3), (2.4) and (2.1) results in the following nonlinear kinematic wave model (Li, et al., 1975) :

$$\frac{\partial Q}{\partial x} + \alpha \beta Q^{\beta-1} \frac{\partial Q}{\partial t} = 0 \quad (2.5)$$

which can be solved by explicit or implicit finite difference methods.

Another simplified hydraulic model is the diffusion wave model which utilizes equation (2.1) and the following simplified form of the momentum equation:

$$S_f - \partial y / \partial x = 0 \quad (2.6)$$

The nonlinear diffusion wave model is a significant improvement over the kinematic model because of the inclusion of the water surface slope term (diffusion effect) of the flood wave. It also allows the specifications of a boundary condition at the downstream extremity of the routing reach to account for backwater effects.

### 2.3.2. Hydrologic Models :

The most widely used method of the hydrologic stream routing models is the Muskingum method originated by McCarthy (1938). The method uses a linear algebraic relationship between the storage and both the inflow  $I$  and the outflow  $Q$ , together with two parameters  $K$  and  $X$ . The Muskingum method is based on the following form of the continuity equation :

$$\frac{dS}{dt} = I - Q \quad (2.7)$$

where the total storage is expressed as

$$S = KQ + K X(I - Q) = K[XI + (1-X)Q] \quad (2.8)$$

or,

$$dS = S_2 - S_1 = K[X(I_2 - I_1) + (1-X)(Q_2 - Q_1)] \quad (2.9)$$

Combining equations (2.7) and (2.9) yields,

$$Q_2 = C_1' I_2 + C_2' I_1 + C_3' Q_1 \quad (2.10)$$

where

$$C_1' = \frac{\Delta t - 2KX}{2K(1-X) + \Delta t}$$

$$C_2' = \frac{\Delta t + 2KX}{2K(1-X) + \Delta t}$$

$$C_3' = \frac{2K(1-X) - \Delta t}{2K(1-X) + \Delta t}$$

The parameter  $X$  with values between 0 and 0.5 is a weighting factor which expresses the relative influence of the inflow  $I$  and the outflow  $Q$ .  $K$  is a storage parameter with dimensions of time and expresses the storage to discharge ratio. Its value is approximately equal to the travel time through the reach.

Cunge (1969) discussed the Muskingum method and extended it. He also showed that the attenuation of the flood wave obtained by the Muskingum method arises from the finite difference equation which replaces the partial differential equations. From equation (2.9) and (2.10):

$$K \frac{d}{dt} [XQ_j + (1-X)Q_{j+1}] = Q_j - Q_{j+1} \quad (2.11)$$

where  $Q_j$  is the inflow to the reach and  $Q_{j+1}$  is the outflow.

Written in finite difference form,

$$\frac{K}{\Delta t} = [XQ_j^{n+1} + (1-X)Q_{j+1}^{n+1} - XQ_j^n - (1-X)Q_{j+1}^n] \quad (2.12)$$

or,

$$\frac{K}{\Delta t} = \frac{1}{2} (Q_j^{n+1} - Q_{j+1}^{n+1} + Q_j^n - Q_{j+1}^n) \quad (2.13)$$

If  $K$  is defined by,

$$K = \Delta x/w \quad (2.14)$$

where  $w$  is the average speed of the flood peak and  $\Delta x$  is the length of the reach, then it can be shown that Eq. (2.13) is a finite difference representation of the kinematic wave equation (2.5). With  $K$  defined as in equation (2.14), it remains to calculate  $X$ . At first



sight there is no obvious form for X, but Cunge observed that by expressing  $Q_j^n$  in terms of their Taylor expansions Eq. (2.13) is also a finite difference representation of the classic diffusion equation,

$$\frac{\partial Q}{\partial t} + w \frac{\partial Q}{\partial x} = m \frac{\partial^2 Q}{\partial x^2} \quad (2.15)$$

where

$$m = (1/2 - X) w \Delta x \quad (2.16)$$

If the diffusion equation is also defined as  $u = (\alpha Q_p)/L$  then,

$$X = 1/2 - \alpha \bar{Q}_p / (L w \Delta x) \quad (2.17)$$

where L is the length of the whole reach which is subdivided into subreaches of length  $\Delta x$ , and  $\bar{Q}_p$  is the average peak discharge. The value of  $\bar{Q}_p$  is the average of the values of  $\bar{Q}_p$  at the upstream and downstream ends of the reach. It can be estimated using

$$\bar{Q}_p = Q_p - 1/2 Q^* \quad (2.18)$$

By examining the second order approximation of the St. Venant equations, Price (1974) was able to obtain the following expression for  $Q^*$  :

$$Q^* = [a_p / (L/T_p)^3] Q_p | d^2 Q_p / dt^2 | \quad (2.19)$$

where  $a_p$  is the attenuation parameter for the peak discharge  $Q_p$  and  $T_p$  is the time of travel of the wave crest over the length L of the reach. Price suggested that the curvature of the hydrograph at the peak may be estimated from,

$$d^2 Q_p / dt^2 = (Q_1 + Q_{-1} - 2Q_p) / (\Delta t^2) \quad (2.20)$$

where  $Q_1$  and  $Q_{-1}$  are the discharges at  $\Delta t$  to either side of the peak and,  $\Delta t$  is equal to one fifth of the time to peak of the hydrograph.

### 2.3.3. Linearized models :

Linearized models of the complete St. Venant equations were

developed by Lighthill and Whitham (1955) and Dooge and Harley (1967). If the equations (2.1) and (2.2) are rewritten for a unit-width channel and in terms of unit discharge ( $q_0$ ) and depth ( $y_0$ ), and then combined and linearized about a reference flow velocity ( $V_0 = q_0/y_0$ ), then the following linearized equation is obtained (Dooge and Harley, 1967) :

$$\begin{aligned} (gy_0^3 - V_0^2) \partial^2 q / \partial x^2 - 2V_0 \partial^2 q / \partial x \partial t - \partial^2 q / \partial t^2 \\ = 3gS_0 \partial q / \partial x + 2g S_0 / V_0 \partial q / \partial t \end{aligned} \quad (2.21)$$

Through further simplification of this equation, the classic diffusion equation may be obtained (Hyami, 1951) :

$$\partial q / \partial t = K \partial^2 q / \partial x^2 - C_0 \partial q / \partial x \quad (2.22)$$

where  $K$  is a wave dispersion coefficient and  $C_0$  is the wave celerity. The instantaneous unit response of the diffusion equation may be expressed as,

$$H(x,t) = (1/4\pi K) (x/t)^{3/2} e^{-[(C_0 t - x)^2 / (4Kt)]} \quad (2.23)$$

in which  $\pi$  is a constant and  $K$  is computed from the expression,

$$K = q_0 / 2S_0 \quad (2.24)$$

where  $q_0$  is the base flow rate and  $S_0$  is the channel bottom slope.

#### 2.4. Models of Watershed Runoff :

There are three classes of model that have been used to study hydrologic processes and systems : physical, analog and mathematical. With the advent of computers and rapid improvement in memory capacity and computation speed, mathematical models are now the most commonly used class of models.

#### 2.5. Mathematical Models of Forested Watershed Runoff :

Mathematical models of watershed runoff can be classified as conceptual or physically-based. They may also be divided into either

lumped or distributed parameter models. Physically based models are based on the physics of the runoff whereas conceptual models are formulated on the basis of a simple arrangement of a relatively small number of elements, each of which itself is a simple representation of a physical relationship. A lumped parameter model assumes that the variations in hydrologic variables within a watershed are negligible and can be taken to be constant. In contrast, distributed parameter models take into account the variations in hydrologic variables in a watershed due to the differences in soil type, topography, land use, rainfall intensity etc. Both Hortonian type models and Variable Source Area models can be described as lumped conceptual or distributed physically-based.

#### **2.5.1. Hortonian Type Models :**

The amount of rainfall infiltration into the soil is a key component in the runoff generation process using Horton's theory. Once the infiltration loss has been calculated, rainfall excess can easily be calculated by subtracting the amount of infiltration from the amount of rainfall. Equations and models available in the literature to predict infiltration can be classified as being either physically based or empirical. Physically based equations attempt to describe the infiltration process by utilizing concepts from soil physics. Among the physically based models are : a) Richard's equation (Philip, 1954) : which is based on Darcy's flow equation and the equation of continuity; b) Philip's model (1957) : which is formulated by considering only the first two terms of the infinite series solution to Richard's equation; and c) The Green-Ampt model (Green and Ampt, 1911) : which is derived by applying Poiseuille's capillary tube

law (assuming soil to be a bundle of capillary tubes) and the equation of continuity for piston type soil moisture profiles.

In contrast to the physically based models, empirical equations use parameters that must be determined from observed infiltration data. Among those are : a) Horton's model (Horton, 1933) : in which infiltration is quantified as a function of initial and final infiltration rate and a decay coefficient which accounts for the decrease in infiltration rate with time; b) Holtan's model (Holtan, 1961) : which predicts infiltration as a function of available water storage; and c) The SCS method (Soil Conservation Service, 1972) : which is an empirical method developed by the Soil Conservation Service to predict rainfall excess directly as function of rainfall and an empirical parameter called the curve number which is a function of the perviousness of the soil surface.

Once rainfall excess has been computed, it can be converted into runoff by either a lumped conceptual or a physically-based model.

#### **2.5.1.1. Conceptual Hortonian Models :**

The most commonly described lumped conceptual techniques in literature are the unit hydrograph method and the instantaneous unit hydrograph method.

##### **2.5.1.1.1. Unit Hydrograph Method :**

Unit hydrograph theory is based on the assumptions of a linear and time-invariant system. A hydrologic system is classified as linear if the principle of superposition is valid. A time-invariant system is one where the parameters do not change with time. The unit hydrograph is defined as a hydrograph produced by a D-hour storm of constant rainfall intensity containing one unit of runoff volume.

The unit hydrograph for a particular watershed may be determined from an observed hydrograph and rainfall excess pattern. Generally, basic streamflow and rainfall data are not available to allow construction of a hydrograph except for a relatively few watersheds; therefore techniques have evolved to generate synthetic unit hydrographs. Among the more well known ones are : a) Snyder Method (Snyder, 1938), b) Clark's Method (Clark, 1945) and c) The SCS Method (Soil Conservation Service, 1972).

#### 2.5.1.1.2. Instantaneous Unit Hydrograph Method :

The Instantaneous unit hydrograph is the limit of the unit hydrograph when the duration tends to zero. Unit hydrograph techniques are applied to a storm by using a convolution equation to develop a composite runoff hydrograph. For a continuous rainfall, discharge  $Q$  is given by,

$$Q = \int_0^t u(t-\tau) I(\tau) d\tau \quad (2.25)$$

where  $I(\tau)$  is the rainfall excess rate and  $u(t-\tau)$  is the lagged instantaneous unit hydrograph. If the rainfall excess and direct runoff observations are known, then the instantaneous unit hydrograph (known as the kernel function) can be determined.

Instantaneous unit hydrographs are sometimes defined by conceptualizing the overland flow as runoff routed through a series of linear reservoirs (Nash, 1957). In the simplest case, the overland flow is approximated by a single linear reservoir. A constant rainfall excess  $i$  is routed through this reservoir to yield a runoff hydrograph. Applying the continuity equation to the reservoir yields,

$$i - Q = dS/dt \quad (2.26)$$

where  $Q$  is the outflow from the reservoir and  $S$  is the storage of the

reservoir. For a linear reservoir,  $S = K Q$  where  $K$  is a storage constant. Therefore, equation (2.26) becomes,

$$dQ/dt + Q/K = i/K \quad (2.27)$$

The solution of eq. (2.27) is

$$Q = i (1 - e^{-t/K}) \quad (2.28)$$

eq. (2.28) gives the rising limb of the hydrograph. If rainfall stops at time  $t = t_0$  then,

$$-Q = K dQ/dt \quad (2.29)$$

If  $Q = Q_0$  at  $t = t_0$  and letting  $\tau = t - t_0$ , eq. (2.29) becomes,

$$dQ/d\tau + Q/K = 0 \quad (2.30)$$

The solution of eq. (2.30) is,

$$Q = Q_0 e^{-\tau/K} \quad (2.31)$$

eq. (2.31) gives the recession limb of the hydrograph.

#### 2.5.1.2. Physically-Based Hortonian Models :

The most extensively used physically-based Hortonian model is the overland flow model.

##### 2.5.1.2.1. Overland Flow Models :

Overland flow is the movement of rainfall excess over the watershed surface to a watershed channel. Overland flow response can be predicted by a combination of the continuity equation and a flow rate function. The equation of continuity can be written as,

$$\partial q/\partial x + \partial y/\partial t = i \quad (2.32)$$

where  $q$  is the discharge per unit width,  $y$  is the flow depth,  $t$  is the time and  $i$  is the rainfall excess per unit area. The flow rate function is usually approximated by uniform flow equation given by,

$$q = a y^b \quad (2.33)$$

where  $a$  and  $b$  are coefficients and  $q$  and  $y$  have been defined

previously. For laminar flow (Linsley et al., 1975),  $a = gS_o/(3\nu)$  and  $b = 3$ . For turbulent flow Manning's equation is used which gives  $a = 1.49 S_o^{1/2}/n$  and  $b = 5/3$ . In the above equations,  $S_o$  is the channel bed slope,  $\nu$  is kinematic viscosity of water and  $n$  is Manning's roughness coefficient.

### **2.5.2. Variable Source Area Models :**

Several researchers have developed mathematical models for use in analyzing the mechanisms of subsurface flow and saturation overland flow. The models may be either distributed physically-based or lumped conceptual.

#### **2.5.2.1. Distributed Physically-Based Models :**

The majority of the physically-based variable source area models are based on the solution of Richard's equation for transient partly saturated flow. Most of them have been developed for hillslopes with only a few for a complete watershed.

##### **2.5.2.1.1. Hillslope Models :**

Freeze (1969) developed a finite difference technique for unidirectional flow recharging a water table, and then (Freeze, 1972) for two dimensional subsurface flow from hillslopes to a stream. The work generalized the few data then available on the effect of soil conductivity and hillslope form on the magnitude of subsurface storm flow. Only in soils with particularly high conductivities did subsurface contributions dominate the storm hydrographs (Dunne, 1983).

Beven (1977) used the finite element method of solving the Richard's equation applied to the same problem, and in addition to the variables examined by Freeze, he emphasized the role of initial moisture conditions and topography in affecting the speed and magnitude of

subsurface contributions to stream flow. Neiber (1979,1982) also developed a finite element model for predicting hillslope runoff. Neiber tested his model against previous mathematical solutions and laboratory data. Adequate representation of transient saturated-unsaturated flow in the laboratory was achieved only after hysteresis was taken into account. The model did best under wet conditions, in which soil water content was greater than about 30% by volume (Sloan et al., 1983).

#### **2.5.2.1.2 Watershed Models :**

In an effort to meet the need of a hydrological model that reflected the actual physical runoff processes involved, Troendle and Hewlett (1979) developed a variable source area simulator (VSASI). Their concept was that instantaneous streamflow is the sum of subsurface flow, precipitation on channel and saturated area, and overland flow from virtually impervious area. Later on Bernier (1982) improved the model (VSAS2). However, Troendle (1985) concluded that VSAS2 was still a prototype that was limited by several major impediments. These include the inadequate description of the hydrological properties and spatial distribution of soils, and the initialization of simulations with inaccurate soil moisture contents. Burke and Gray (1983) developed a completely coupled finite element computer model to solve Richard's equation for saturated-unsaturated subsurface flow, and the Saint Venant equations for the open channel and overland flow components. Due to computational limitations the model was applied to a single conceptually derived hillslope.

#### **2.5.2.2. Lumped Conceptual Models :**

Because of the complexity of using completely physically based



numerical models, approximate models have been developed for the prediction of both subsurface and saturation overland flow. To meet the need of simpler models Nieber (1982) developed a one dimensional model using Richard's equation. Nieber (1982) also evaluated a simpler model that used the Boussinesq's equations. The Boussinesq's equations assume that the hydraulic gradient is equal to the slope of the free water surface. A further approximation is to assume that the hydraulic gradient at any point is equal to the bed slope. Beven (1982) evaluated these approximations and extended the solution to include vertical flow in the unsaturated zone and non-homogeneous but uniformly varying soil conditions (Sloan et al., 1983).

Sloan et al.(1983) performed a comparison of several models including the one dimensional model of Neiber (1982), the kinematic wave model of Beven (1982) and a simple kinematic storage model. Their study showed that the simple kinematic storage model gave the best results with high effective hydraulic conductivities. As a result they concluded that simple conceptual models can adequately simulate runoff from steep-sloped forested watersheds and are the most economical to use because of the greater complexity involved in describing a natural watershed, and the cost of running computer programs of complex models.

At the same time Beven and Wood (1983) introduced a new conceptual variable contributing area model based on a saturation deficit concept. They applied their model to several watersheds in England and in the United States. They concluded that the results obtained from the study were sufficiently encouraging to suggest that the model was worthy of further investigation.

From an examination of several subsurface models, it was concluded that the saturation deficit model of Beven and Wood (1983) and the kinematic storage model of Sloan et al. (1983) both represent the state of the art in conceptual models of subsurface flow. A description of the kinematic storage model and the saturation deficit model is included in the following sections.

#### 2.5.2.2.1. Hillslope Model (Kinematic Storage Model) :

Sloan et al. (1983) developed a simple kinematic storage model with the assumption that hydraulic gradient was equal to bed slope. The continuity equation is the basis of his model and can be written as :

$$\frac{dS}{dt} = I - q \quad (2.34)$$

or in explicit finite difference form as,

$$\frac{S_2 - S_1}{\Delta t} = I - (q_1 + q_2)/2 \quad (2.35)$$

where  $\Delta t = t_2 - t_1$ ,  $S$  is the drainable volume of water stored in the saturated zone per unit width,  $q$  is the discharge from the profile per unit width,  $I$  is the vertical input from the unsaturated zone per unit width and subscripts 1 and 2 refer to the beginning and end of the time period respectively.

$I$  is given by,

$$I = iL \quad (2.36)$$

where  $i$  is the input from unsaturated zone per unit area and  $L$  is the slope length.

Assuming that the water table is linear between the outlet face and the upper boundary (Figure 2.1),

$$S = Lh(\theta_s - \theta_d)/2 \quad (2.37)$$

where  $h$  is the depth of water table at the outlet,  $L$  is the slope length,  $\theta_s$  is the saturated water content and  $\theta_d$  is the water content at field capacity.

Discharge per unit cross-sectional area  $V$  is given by Darcy's law,

$$V = K_s \frac{\partial h}{\partial x} = K_s \sin\alpha \quad (2.38)$$

where  $K_s$  is the saturated hydraulic conductivity,  $\partial h/\partial x$  is the hydraulic gradient and  $\sin\alpha$  is the bed slope.

Discharge per unit width  $q$  is given by,

$$q = hV \quad (2.39)$$

substituting equations (2.37) and (2.39) into equation (2.35), the head at the outlet at the end time increment  $\Delta t$ , can be found explicitly by,

$$h = \frac{h_1 [L(\theta_s - \theta_d)/\Delta t - V]/2 + iL}{2 [L(\theta_s - \theta_d)/\Delta t + V]/2} \quad (2.40)$$

The discharge per unit width at the end of time increment  $\Delta t$  can then be found by :

$$q_2 = h_2 V \quad (2.41)$$

Surface runoff is easily accounted for in this model through the addition of an extra term in the storage equation (equation 2.37). The water table still remains hinged at point D (Figure 2.2). When water table intersects the soil surface, equations (2.37) and (2.39) become,

$$S = [DLs + (L - L_s)D/2][\theta_s - \theta_d] \quad (2.42)$$

$$q = iLs + DV \quad (2.43)$$

where  $L_s$  is the saturated slope length and  $D$  is the hillslope soil depth to an impermeable layer.

Substituting equations (2.42) and (2.43) into equation (2.35),

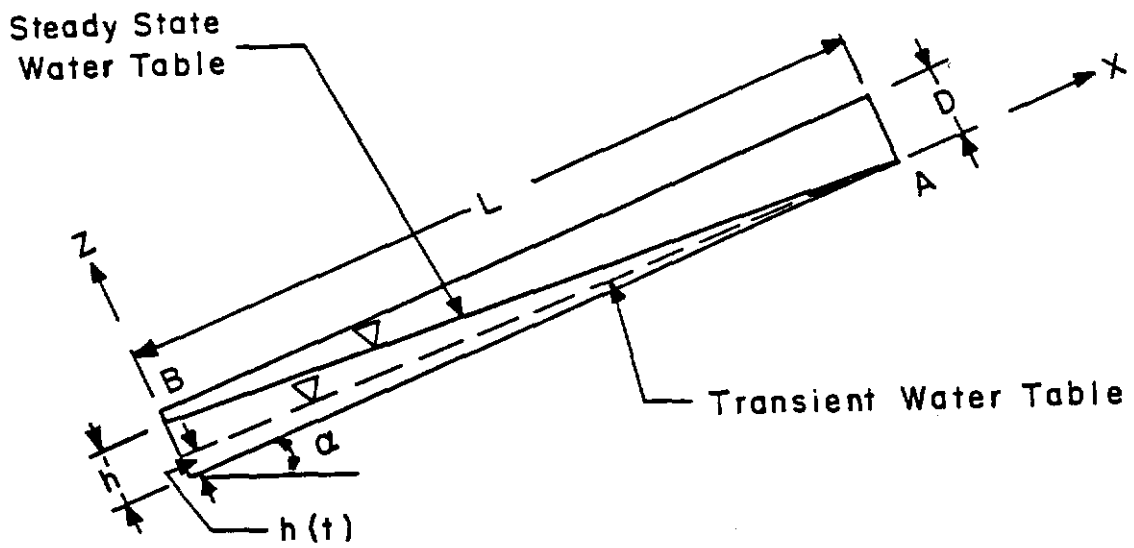


Figure 2.1 Kinematic Storage Model Without Saturation Overland Flow

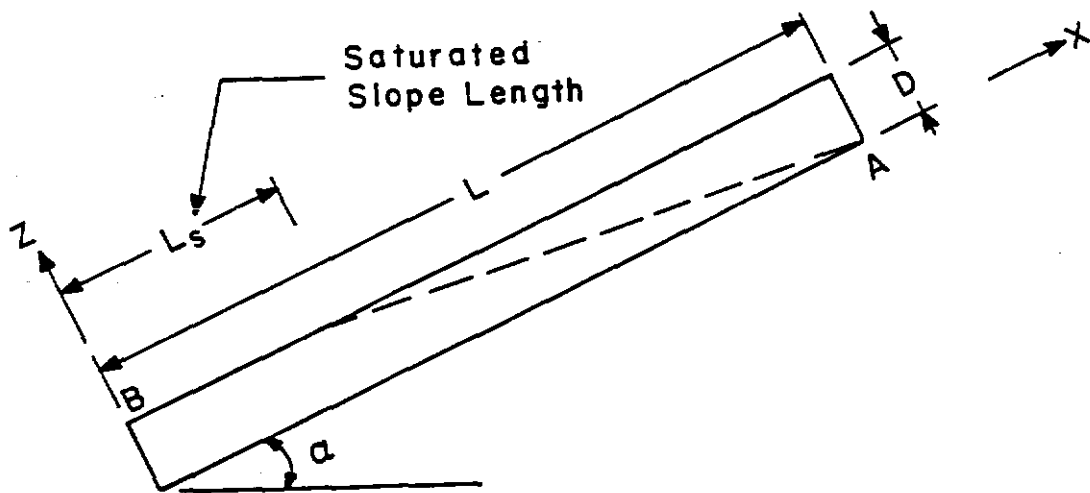


Figure 2.2 Kinematic Storage Model With Saturation Overland Flow

the saturated slope length at the end of time increment  $\Delta t$ , after watertable intersects the soil surface, can be found explicitly by,

$$Ls_2 = \frac{Ls_1 [D(\theta_s - \theta_d)/\Delta t - i]/2 + iL - DV}{[D(\theta_s - \theta_d)/\Delta t + i]/2} \quad (2.44)$$

The discharge per unit width at the end of time increment  $\Delta t$  can then be found by,

$$q_2 = iLs_2 + DV \quad (2.45)$$

#### 2.5.2.2.2. Watershed Model (Saturation Deficit Model) :

Beven and Wood (1983) developed a non-Hortonian flow model following the work of Beven and Kirkby (1976, 1979). In their model they assumed that at any point in the catchment, downslope flow per unit width  $q$ , is related to saturation deficit  $S$  by,

$$q = K_0 \tan\beta e^{(-S/m)} \quad (2.46)$$

where  $K_0$  is the saturated hydraulic conductivity,  $\tan\beta$  is the local surface slope angle and  $m$  is a constant. Saturation deficit is defined as the storage deficit below full saturation due to soil drainage alone and excluding the additional deficits that would result from evapotranspiration. At full saturation,  $S = 0$  so that,

$$q = K_0 \tan\beta \quad (2.47)$$

Therefore,  $K_0 \tan\beta$  is the transmission capacity of the soil profile at full saturation. Therefore, the aforementioned relationship allows the soil hydraulic conductivity to vary with depth but assumes that the local hydraulic gradient is everywhere equal to the surface slope angle. Assuming a steady input rate  $R$ , then at any point :

$$q = Ra \quad (2.48)$$

where  $a$  is the upslope area draining past that point per unit width of slope or contour length.

From equations (2.46) and (2.48),

$$S = -m \ln[(a/\tan\beta)/(K_0/R)] \quad (2.49)$$

The saturated area may then be defined as the area for which  $S < 0$  (noting that deficits are positive) or

$$a/\tan\beta > K_0/R$$

In order to determine the average saturation deficit for the entire catchment, the catchment is first divided into a number of subareas based on the  $\ln(a/\tan\beta)$  distribution of the catchment (see Figure 2.3). The saturation deficit is then calculated for each subarea using equation (2.49). The average storage deficit of the catchment is thus equal to the sum of the deficits in each subarea divided by the total area of the catchment and is given by:

$$\bar{S} = A^{-1} \int_0^A S \, da = A^{-1} \int_0^A \ln[(a/\tan\beta)/(K_0/R)] \, da \quad (2.50)$$

It is further assumed that  $K_0$  and  $m$  are constants i.e. the soil is homogeneous and of uniform depth and since  $R$  is not a function of  $A$ , therefore,

$$\bar{S} = -m\lambda - m \ln(R/K_0) \quad (2.51)$$

where,

$$\lambda = A^{-1} \int_0^A \ln(a/\tan\beta) \, da \quad (2.52)$$

or,

$$\lambda = 1/A \sum \ln(a/\tan\beta) \Delta A \quad (2.53)$$

is a constant for the catchment, dependent only on the topography and  $\Delta A$  is the area of each subarea.

From equation (2.49)

$$\ln(R/K_0) = -S/m - \ln(a/\tan\beta) \quad (2.54)$$

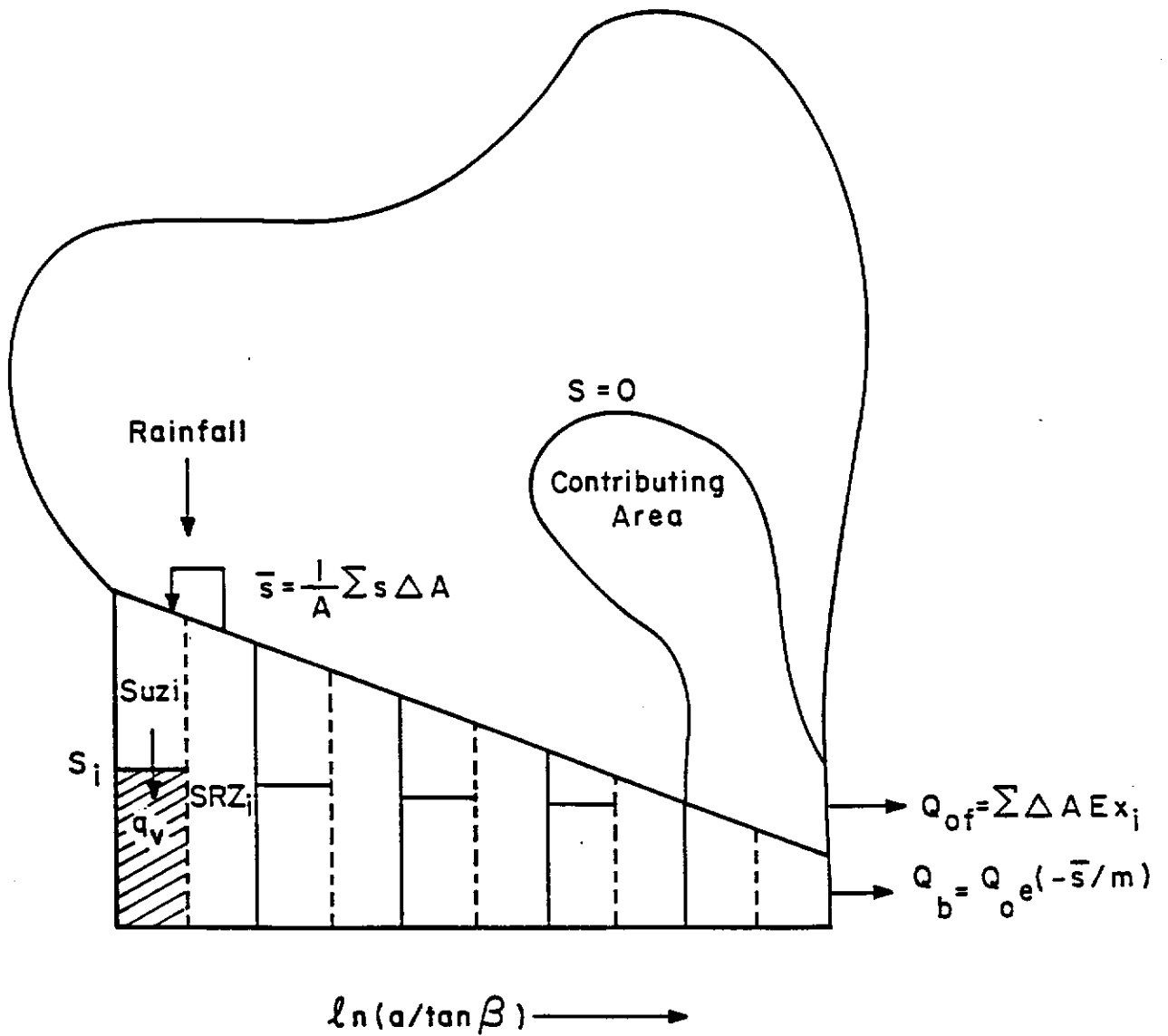


Figure 2.3 Conceptual Representation of Saturation Deficit Model

so that

$$\bar{S} = -m\lambda + S + m \ln(a/\tan\beta) \quad (2.55)$$

or,

$$S = \bar{S} + m\lambda - m \ln(a/\tan\beta) \quad (2.56)$$

Equation (2.56) not only gives a relationship for predicting saturated areas for any value of  $S$  but also for predicting the saturation deficits anywhere in the catchment.

A further assumption is made that subsurface drainage from the complete basin  $Q_b$  is described by a similar exponential function to equation (2.46), involving the average deficit  $\bar{S}$  i.e.,

$$Q_b = Q_0 e^{(-\bar{S}/m)} \quad (2.57)$$

i.e., 
$$\bar{S} = -m \ln(Q_b/Q_0) \quad (2.58)$$

so that  $m$  is then a parameter of the recession curve of the catchment and can easily be calculated from a minimum of discharge measurements. If a value of initial catchment discharge  $Q_i$  is available prior to a storm, than an initial value for  $\bar{S}$  for the catchment can be computed using equation (2.58). Then using equation (2.56)  $S$  can be computed. Values of  $S < 0$  will indicate the initial saturated contributing area, while elsewhere the deficit to be filled before saturation is predicted for each value of  $\ln(a/\tan\beta)$ . For any area of soil at or near saturation, the unsaturated zone delay will be minimal, and will increase upslope for points of higher initial deficit i.e. lower  $\ln(a/\tan\beta)$  value. Assuming that the delay in the unsaturated zone is directly proportional to deficit at a point, then the input to the saturated zone at that point,  $q_v$ , may be described by,



$$q_v = \text{Suz} / (t_d S) \quad (2.59)$$

where  $S$  is the predicted saturation deficit,  $t_d$  is the time delay per unit of deficit and  $\text{Suz}$  is the storage in the unsaturated zone in excess of some "field capacity" value below which vertical drainage may be neglected on the time scale of the storm hydrograph.

The sum of vertical flows weighted by the area associated with each  $\ln(a/\tan\beta)$  increment will give the total reduction ( $Q_{uz} = \sum q_v a$ ) in the catchment average deficit  $\bar{S}$  during a time period. The subsurface outflow from the saturated zone  $Q_b$  can be calculated using.

$$Q_b = Q_0 e^{(-\bar{S}/m)} \quad (2.60)$$

where  $\bar{S}$  is the average saturation deficit from the previous time step.

A water balance calculation for  $\bar{S}$  produces a new end of time step value as shown in the following equation :

$$\bar{S}_{\text{new}} = \bar{S}_{\text{old}} - Q_{uz} + Q_b \quad (2.61)$$

The new value of  $\bar{S}$  is then used to calculate new values of  $S$  using equation (2.56). In this calculation, there is no water balance error involved since the incremental change in  $\bar{S}$  is equal to the areally weighted sum of changes in the  $S$  values. Thus, recalculation of saturation deficits  $S$  predicted from  $\bar{S}$  at each time step makes allowances for downslope flows, and during drainage, the recovery of saturation deficits between closely spaced events.

Surface flow may be generated due to a calculated value of  $S=0$  which represents the saturation excess mechanism of runoff production. Areas of high values of  $\ln(a/\tan\beta)$ , i.e., areas of convergence or low slope angle, will saturate first and as the catchment becomes wetter the area contributing surface flow will increase. Calculated surface flow at any

time step is simply the sum of water in excess of any deficit in each  $\ln(a/\tan\beta)$  increment and is given by

$$Q_{of} = \sum \Delta A * Ex_i \quad (2.62)$$

where  $\Delta A$  is the subarea area and  $Ex_i$  is the water excess in subarea  $i$ .

## CHAPTER 3

### MODEL COMPARISONS

#### 3.1 Introduction :

In order to evaluate the performance of the kinematic storage model and the saturation deficit model both models were embedded into HEC-1, a comprehensive hydrologic software package developed by the US Army Corps of Engineers. Once this was accomplished the modified version of HEC-1 was used to evaluate the hydrologic response of four watersheds. The four watersheds are identified in Table 3.1 and Figures 3.1-3.4. A general description of the geological and hydrological characteristics of the four watersheds is provided in the following sections.

#### 3.2 Physiography And Topography :

Both Sandlick creek and Crane creek lie in the Tug Fork basin which encompasses nearly 1,560 square miles of Kentucky, Virginia and West Virginia. Nearly the entire Tug Fork basin is in the Kanawha section of the Appalachian Plateau physiographic province as defined in Fenneman and Johnson (1984).

The topography of the Tug Fork basin is characterized by narrow river valleys bordered by steeply rising mountains. The rock underlying is Lee formation consisting of sandstone, conglomerate, shale, siltstone, coal, and underclay. It is characterized by massive beds of orthoquartzite that locally contains lenses of conglomerate. In places sandstone makes up more than 80 percent of the formation. Rocks are typically sandstone that are light gray, fine to coarse grained, thin to thick bedded, and locally massive. The sandstone contains white- weathering feldspar, mica and carbonaceous

**TABLE 3.1 WATERSHED CHARACTERISTICS**

<b>Watershed</b>	<b>Area</b>	<b>Disturbed Area</b>	<b>Watershed Slope</b>	<b>Saturated Hydraulic Conductivity</b>
	<b>acres</b>	<b>%</b>	<b>%</b>	<b>inch/hr</b>
Crane Creek, W.Va.	346	0	50	2.50
R.F. Sandlick, W.Va.	776	0	46	3.75
L. Millseat, Ky	205	0	42	4.80
Cane Branch, Ky	429	12	20	2.77





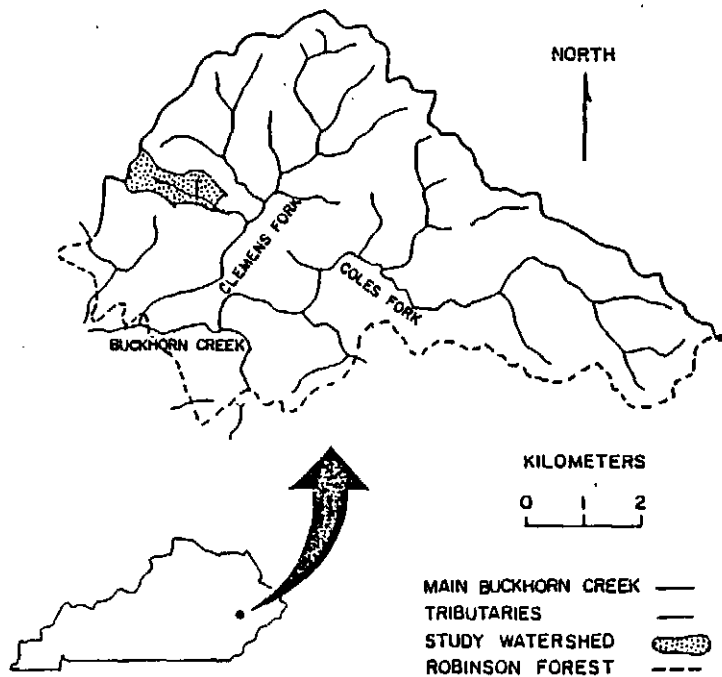


Figure 3.3a Location Map : Little Millseat Watershed, Ky.

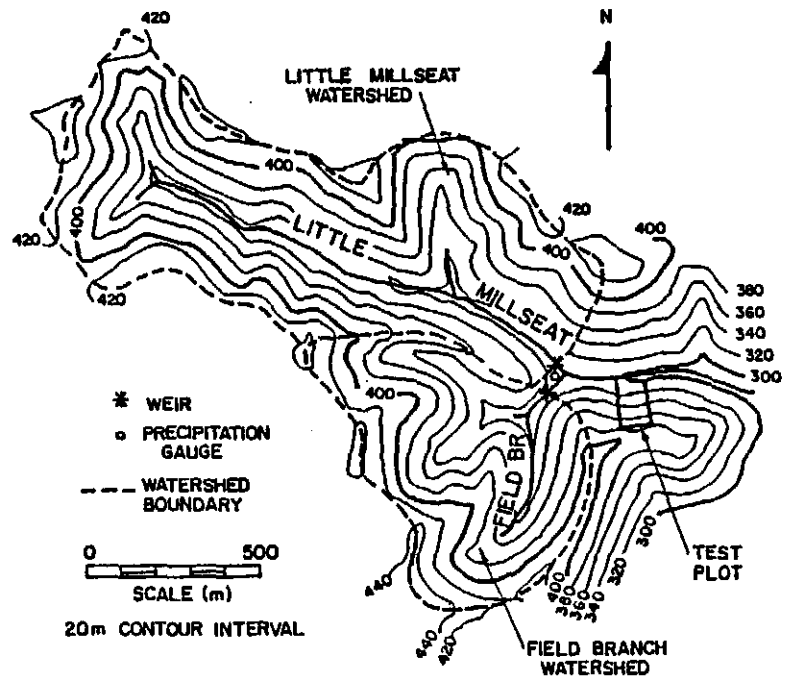


Figure 3.3b Topographic Map : Little Millseat Watershed, Ky.





grains.

Little Millseat watershed is located in University of Kentucky's Robinson Forest, a 15,000 acre research forest. The watershed is characterized by steep slopes and narrow valleys. The bedrock is composed of alternating layers of sandstones, siltstones, shales, and interbedded layers of coal from the Breathitt formation of the Pennsylvanian Age (Hutchins, et. al., 1976; Hanson, 1977).

Cane Branch watershed is located in the Cumberland Plateau physiographic section of southeastern Kentucky. The topography of the watershed is characterized by narrow, winding ridges and deep, steep-sided, narrow valleys. The bedrock is Lee Formation of the Pennsylvanian Age consisting of sandstone, siltstone, claystone, quartz conglomerate and coal (Musser, 1963).

### **3.3 Land Use :**

Most of the area in Sandlick Creek and Crane Creek watersheds is classified as forest land, primarily deciduous. The vegetation on Little Millseat is dominated by the oak-hickory type. Except for a small area of strip mining, the Cane Branch watershed is completely forested with a mix of hardwoods and pines.

### **3.4 Soil Classification :**

Most of the soils in Sandlick Creek and Crane Creek watershed are of Clymer-Dekalb-Jefferson soil association. These are deep to moderately deep, well-drained acid soils occupying the higher mountains of the Appalachia. These soils are formed from the residuum of acid sandstone and shale.

The soils of Little Millseat consist mostly of Shelocta, Gilpin, Dekalb, Sequoia and Cutshin soil types (Smith, 1982), and have moderately

rapid to rapid permeabilities (USDA, 1965). The Shelocta-Cutshin series, a cove association, varies in depth from about 1.22 m to 1.83 m; the Shelocta-Gilpin association averages 1.40 m deep, and the Dekalb-Sequoia series, a ridge top association, is the shallowest with a 1.00 m average depth (Smith, 1982). The deepest soils occur along the upslope sides of benches and in cove sites, while rock outcrops are common along slopes and outslope edges of benches (Springer and Coltharp, 1978).

The soils of Cane Branch watershed consist of Muskingum, Hartsells, Johnsborg, Tilsit and Enders soil types (Musser, 1963). Soils in the watershed are silt loam in texture.

### 3.5 Hydrology :

The Crane Creek and Sandlick watersheds as stated previously are characterized by steep slopes and narrow valleys ; thus reducing the runoff travel time from the head waters to the lower parts of the area. Intense storms and steep slopes cause severe flooding in the area. Floods are usually of short duration but large magnitude.

Hydrograph peaks from Little Millseat watershed are sharp, rather than the more rounded peaks that have been observed from most forested watersheds where subsurface flow controls runoff (Curtis, 1972). Curtis (1972) believed that this was due to shallow soils, steep slopes, and horizontal impervious bedrock. The flashy nature of watersheds in this area was reported by Springer and Coltharp (1978). Mean annual streamflow and mean annual quickflow are about 65 and 25% of mean annual precipitation, respectively (Nuckols, 1982). Quickflow volume account for almost one-half of the precipitation occurring in the winter, while in the fall and summer only 13 to 16% of precipitation is converted to quickflow. Nuckols (1982) believed that during the spring, summer, and fall the major

portion of precipitation was routed through the terrestrial system (subsurface flow). In all seasons quickflow runoff consistently accounts for nearly one-half of the total runoff volume per season, indicating that channel precipitation and the near-channel precipitation must be the primary contributor to stream flow for the watershed (Nuckols, 1982).

Runoff in Cane Branch watershed averages about 22 inches annually. The monthly runoff varies greatly during the year. Runoff in February averages about 4.5 inches and is the highest; next in order of magnitude are runoff in March with about 4.0 inches and in January with about 3.5 inches. More than half of the annual runoff generally occurs during these 3 consecutive months. The month of largest flow is generally October, with runoff averaging between 0.1 and 0.2 inch. Most floods occur during January, February and March.

### **3.6 Hydrologic Data :**

Rainfall and associated runoff events from the previously described watersheds were used to test the applicability of the runoff models available in HEC-1 for steeply sloping forested watersheds. The Crane Creek and Right Fork Sandlick watersheds were monitored by USGS and the data available are for a time increment of five minutes for a period of about two years. Using this data base, four rainfall events were identified for use with the Crane Creek Watershed while two events were identified for use with the Right Fork Sandlick watershed. Little Millseat watershed is maintained by University of Kentucky and data used were for three rainfall-runoff events. The rainfall-runoff data of one event for Cane Branch was provided by Dr. B. Wilson, Agriculture Engineering Department, Oklahoma State University. The precipitation hyetographs for the ten rainfall events for the four watersheds are

provided in Appendix A.

### **3.7. Description of HEC-1 :**

HEC-1 (HEC-1 Users Manual, 1986) is a versatile and comprehensive hydrologic model developed by the US Army Corps of Engineers, The Hydrologic Engineering Center, Davis, California. It is designed to simulate the surface runoff response of a river basin to precipitation by representing the basin as an interconnected system of hydrologic and hydraulic components. Each component models an aspect of the precipitation-runoff process within a portion of the basin; referred to as a subbasin. Representation of a component requires a set of parameters which specify the particular characteristics of the component and mathematical relations which describe the physical process. The result of the modeling process is the computation of streamflow hydrographs at desired locations in the river basin.

#### **3.7.1 Assumptions And Limitations Of HEC-1 :**

In HEC-1, a river basin is represented as an interconnected group of sub-areas. The assumption is made that the hydrologic processes can be represented by model parameters which reflect average conditions within a sub-area.

There are several important limitations of the model. Simulations are limited to a single storm due to the fact that provision is not made for soil moisture recovery during period of no precipitation. The model results are in terms of discharge and not stage, although stages can be printed out by the program based on a user specified rating curve. Stream flow routings are performed by approximate methods and do not reflect the full St. Venant equations

which are required for very flat river basin.

### 3.7.2 Steps To Use HEC-1 :

The following steps are taken to perform any computation using HEC-1:

- i) A river basin is subdivided into an interconnected system of stream components using topographic maps.
- ii) The basin is subdivided into a number of subbasins. Each subbasin is intended to represent an area of the watershed which on the average has the same hydrologic/hydraulic properties.
- iii) Each subbasin is represented by a combination of model components. Among the components available are : subbasin runoff, river routing, reservoir routing, diversion and pump components.
- iv) The subbasin and their components are linked together to represent the connectivity of the river.

### 3.7.3 Capabilities Of HEC-1 :

HEC-1 is a versatile program with a whole range of capabilities. Among the more important ones are:

#### 1) Storm Hydrograph Generation :

The following options are available :

- a) Direct input to the program.
- b) Clark unit hydrograph method.
- c) Snyder unit hydrograph method.
- d) SCS dimensionless unit hydrograph method.

There are several infiltration options available for use with the hydrograph generation options. They are listed below :

- a) Initial and uniform loss rate.
- b) Exponential loss rate.
- c) SCS curve number method.

d) Holtan's loss rate.

2) Channel Routing :

Options available are :

a) Muskingum method.

b) Kinematic wave method.

3) Reservoir Routing :

Options available are :

a) Modified Puls method.

b) Working R and D method.

c) Level-pool reservoir routing method.

4) Parameter Calibration :

a) Unit hydrograph parameters.

b) Loss rate parameters.

5) Dam Safety Analysis

6) Flood Damage Analysis

7) Flood Control System Optimization

**3.7.4 Modified Version of HEC-1 :**

One of the major drawbacks of HEC-1 is the absence of any hydrograph generation option using a variable source area model which combines subsurface flow and saturation overland flow. The kinematic storage model (Sloan et al., 1983) and the saturation deficit model (Beven and Wood, 1983) described in detail in chapter 2 are variable source area models. Both the models have components for subsurface flow and saturation overland flow. These two models were incorporated into HEC-1 and are now available in HEC-1 as new options to generate storm runoff hydrograph.

### **3.8. Non-Hortonian Flow Models :**

Once the two subsurface flow models were embedded into HEC1, they were used to evaluate the hydrologic response of the four watersheds to a series of 10 different storms. The results of this analysis are discussed in the following sections.

#### **3.8.1. Results :**

The two different non-Hortonian models were applied to each of the four watersheds listed in table 3.1. The results of the analysis are shown in tables 3.2a and 3.2b. The results were obtained by calibrating the model parameters in order to get the best possible match between the simulated response and the observed response. The calibrated parameters for the kinematic storage model include the saturated hydraulic conductivity and the difference between saturated and field capacity water contents. The calibrated parameters for the saturation deficit model include the subsurface flow at zero deficit, the recession constant, the initial subsurface flow, the maximum value of the SRZ store, and the time delay constant.

Table 3.2a contains the optimized parameters for each storm event for both the models. Table 3.2b provides a comparison between the observed and predicted hydrologic statistics for each model. The runoff hydrographs for both the models for each storm event are provided in figures 3.5 to 3.14.

For both the Crane Creek and Right Fork Sandlick watersheds, the kinematic storage and the saturation deficit models tend to overpredict the volume. As regards peak discharge, both the subsurface flow models tend to substantially underpredict. In general, time of peak is not predicted very well by either the kinematic storage model or the

TABLE 3.2a OPTIMIZED PARAMETERS : NON-HORTONIAN MODELS

Watershed	Storm No.	Parameters						
		KSM		SDM				
		$K_s$	$(\theta_s - \theta_d)$	$Q_0$	$m$	$Q_i$	SRmax	$U_0$
Crane Creek	1	10.96	0.15	0.093	0.18	.00017	4.25	0.58
	2	7.48	0.27	1.044	0.18	.00387	1.66	0.004490
	3	2.45	0.16	1.155	0.17	.00209	0.88	0.001650
	4	5.98	0.45	0.749	0.27	.00200	0.42	0.000317
R.F. Sandlick Creek	1	6.55	0.27	0.119	0.46	.00150	1.25	0.000288
	2	19.17	0.40	1.452	0.20	.00370	0.31	0.000013
L. Millseat	1	2.97	0.16	5.870	0.14	.00890	0.01	0.000011
	2	52.14	0.39	0.128	0.48	.00376	1.03	2.13
	3	1.43	0.30	1.830	0.19	.00180	1.49	0.000045
Cane Branch	1	42.45	0.28	0.300	0.42	.00116	0.32	18.32

Definition of Parameters :

- $K_s$  : Saturated hydraulic conductivity.
- $\theta_s - \theta_d$  : Difference between saturated and field capacity water contents.
- $Q_0$  : Subsurface flow when storage deficit is zero.
- $m$  : Recession constant.
- $Q_i$  : Initial subsurface flow.
- SRmax : Maximum value of SRZ store.
- $U_0$  : Time delay constant.



**TABLE 3.2b STATISTICS OF SELECTED HYDROLOGIC PARAMETERS :  
NON-HORTONIAN MODELS**

Watershed	Storm No.	Hydrologic Parameters								
		Volume			Peak			Time of Peak		
		KSM	SDM	OBS	KSM	SDM	OBS	KSM	SDM	OBS
Crane Creek	1	0.192	0.175	0.175	3.29	4.12	4.10	8.42	10.00	10.75
	2	0.047	0.047	0.040	1.56	3.91	3.90	1.00	1.00	1.08
	3	0.017	0.017	0.015	1.30	1.24	1.90	0.83	0.83	1.42
	4	0.014	0.014	0.013	0.84	0.82	1.30	2.08	0.08	2.42
R.F. Sandlick Creek	1	0.009	0.010	0.009	1.26	1.38	2.00	3.92	0.08	1.92
	2	0.062	0.066	0.052	3.01	6.06	6.60	3.17	2.33	1.42
L. Millseat	1	0.314	0.289	0.261	1.28	2.13	2.28	10.50	0.50	2.50
	2	3.292	3.043	2.351	11.90	19.58	16.61	50.00	38.00	48.50
	3	0.059	0.063	0.055	0.44	0.50	0.74	17.50	34.50	7.00
Cane Branch	1	1.160	1.156	0.866	68.46	69.98	58.88	10.00	10.25	10.75

**Definitions :**

KSM : Kinematic storage model values.

SDM : Saturation deficit model values.

OBS : Observed values.

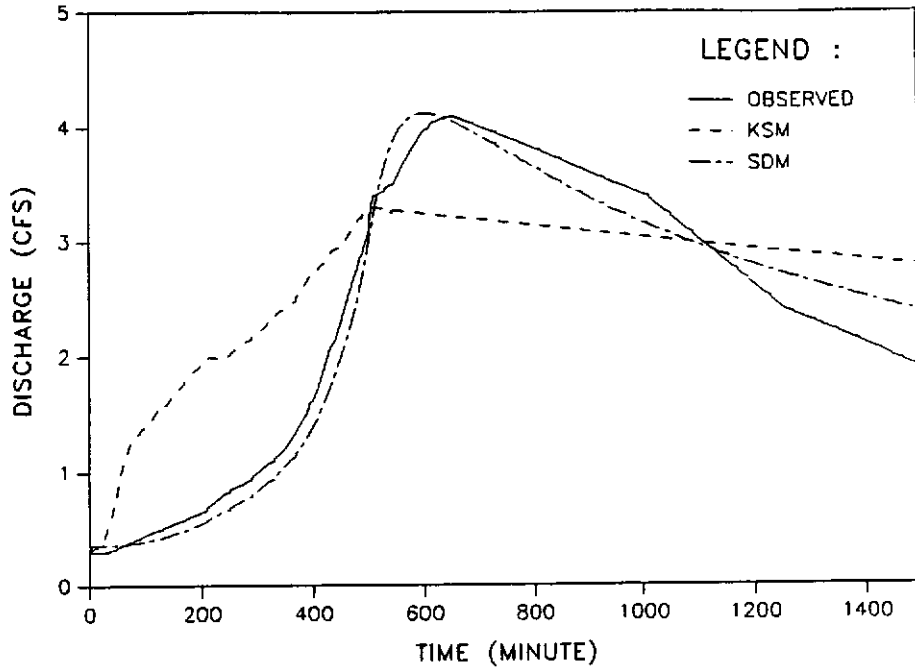


Figure 3.5a Crane Creek : Storm 1 : Non-Hortonian Models With Optimization

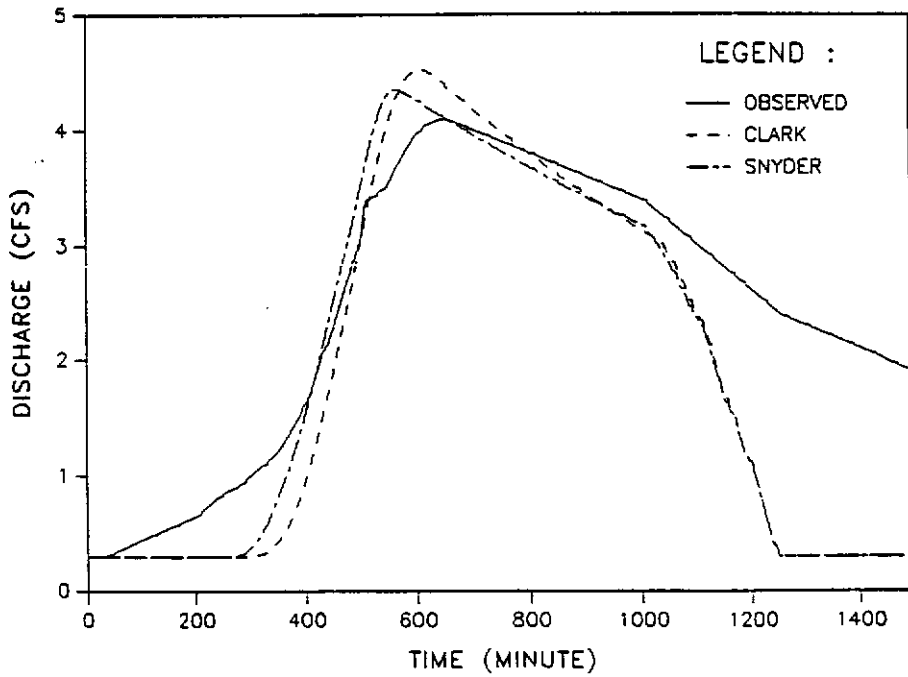


Figure 3.5b Crane Creek : Storm 1 : Hortonian Models With Optimization

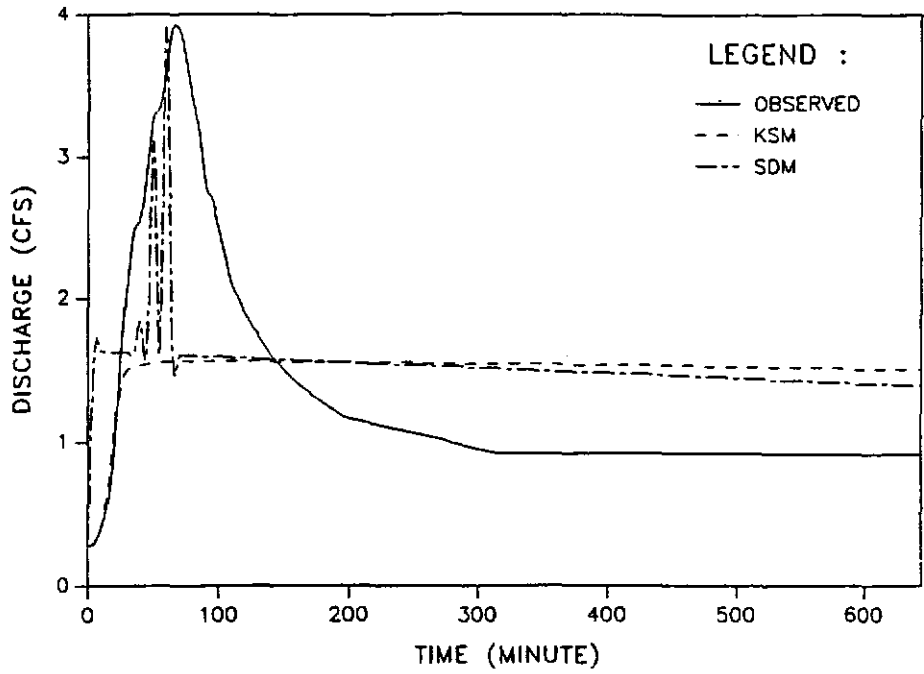


Figure 3.6a Crane Creek : Storm 2 : Non-Hortonian Models With Optimization

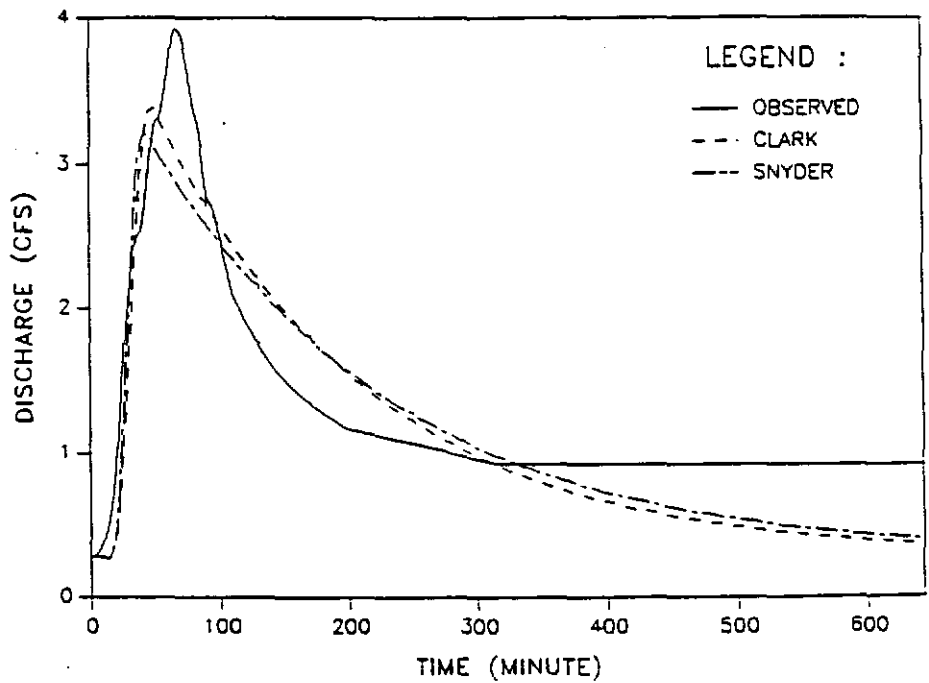


Figure 3.6b Crane Creek : Storm 2 : Hortonian Models With Optimization

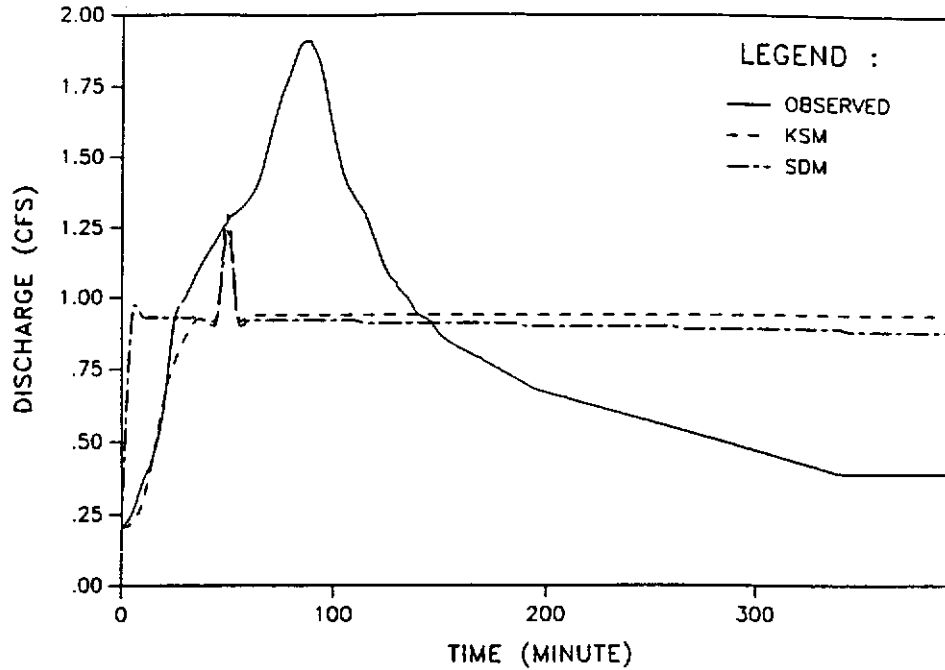


Figure 3.7a Crane Creek : Storm 3 : Non-Hortonian Models With Optimization

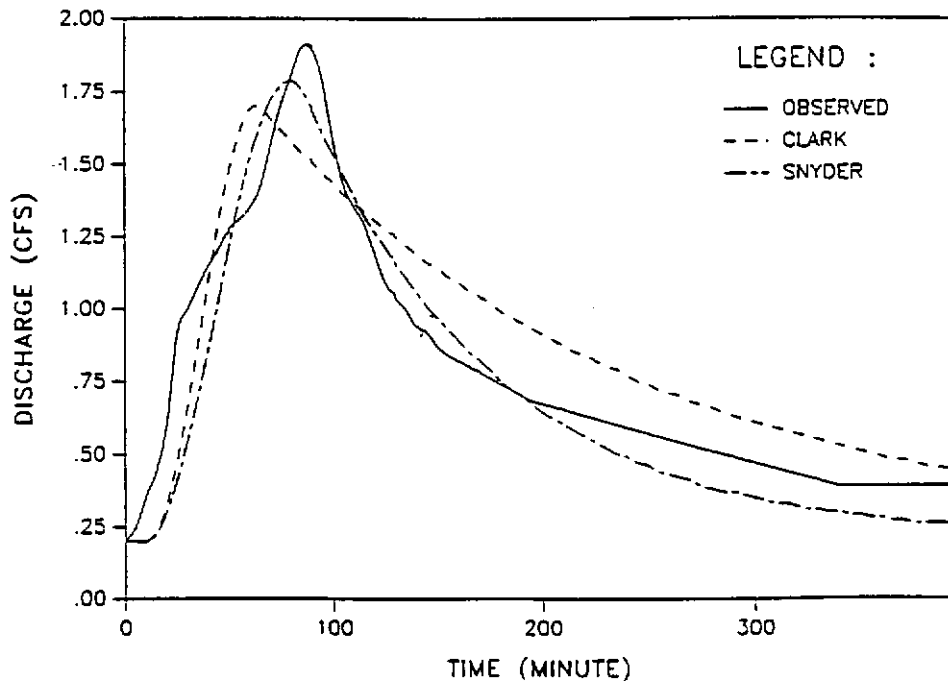


Figure 3.7b Crane Creek : Storm 3 : Hortonian Models With Optimization

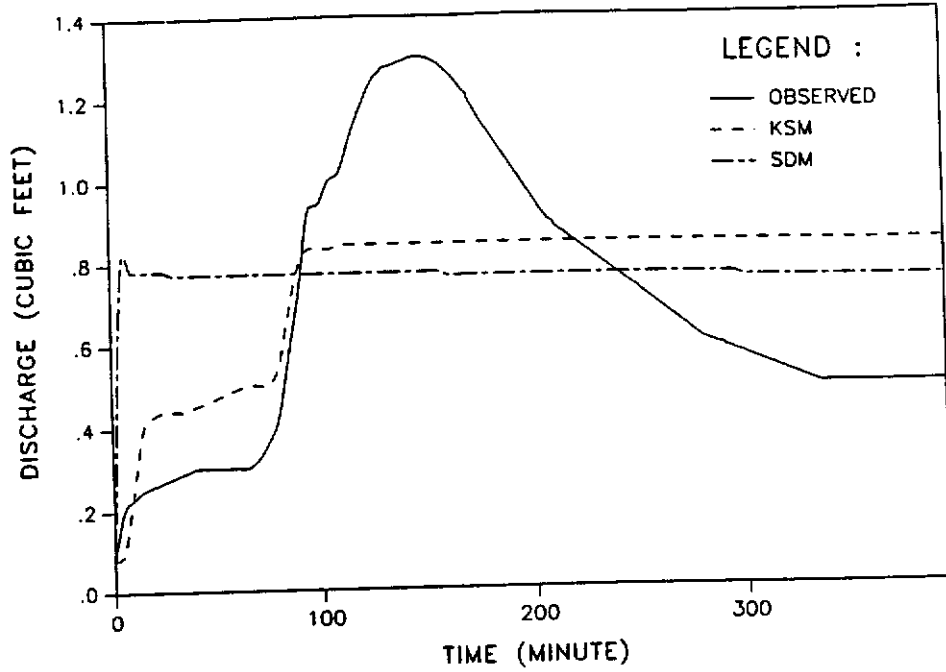


Figure 3.8a Crane Creek : Storm 4 : Non-Hortonian Models With Optimization

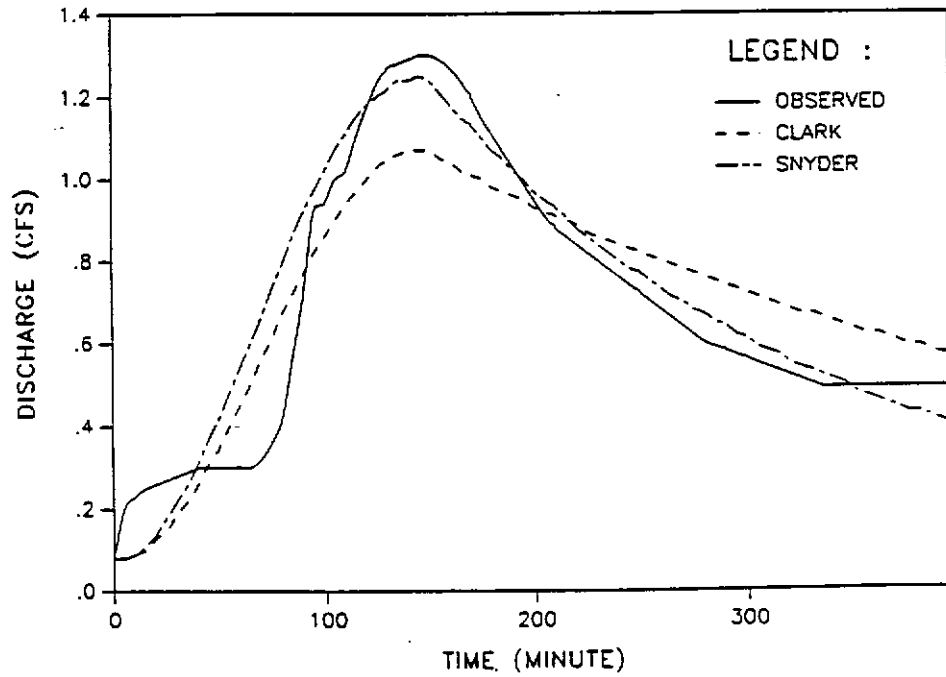


Figure 3.8b Crane Creek : Storm 4 : Hortonian Models With Optimization

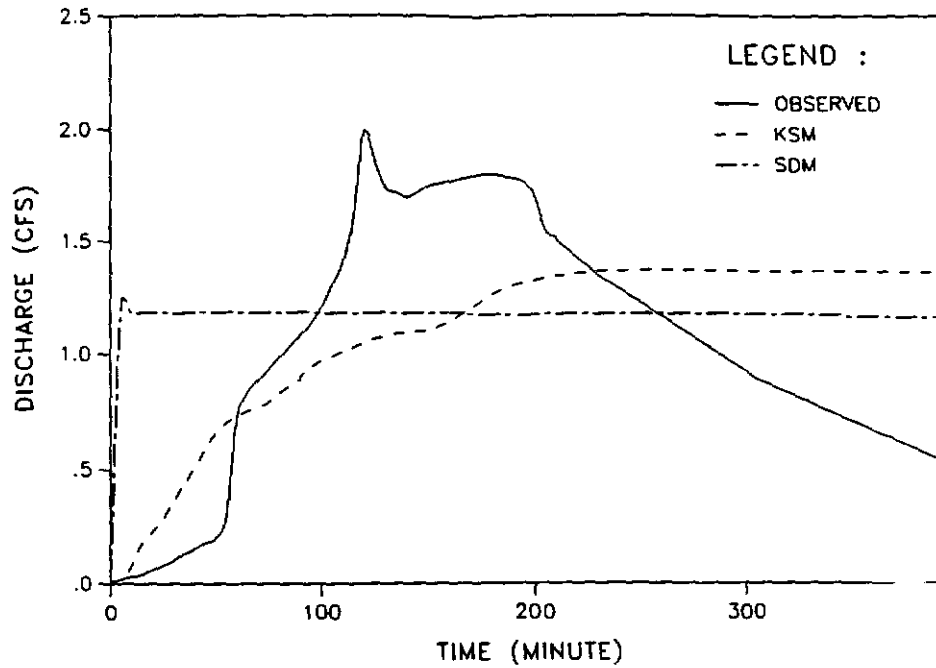


Figure 3.9a R.F. Sandlick Creek : Storm 1 : Non-Hortonian Models With Optimization

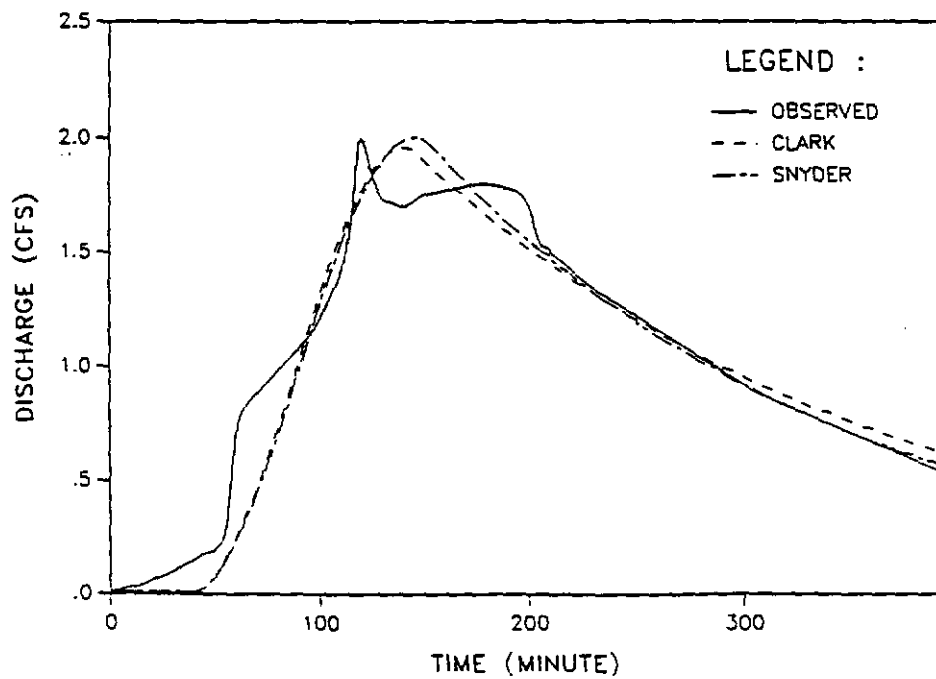


Figure 3.9b R.F. Sandlick Creek : Storm 1 : Hortonian Models With Optimization

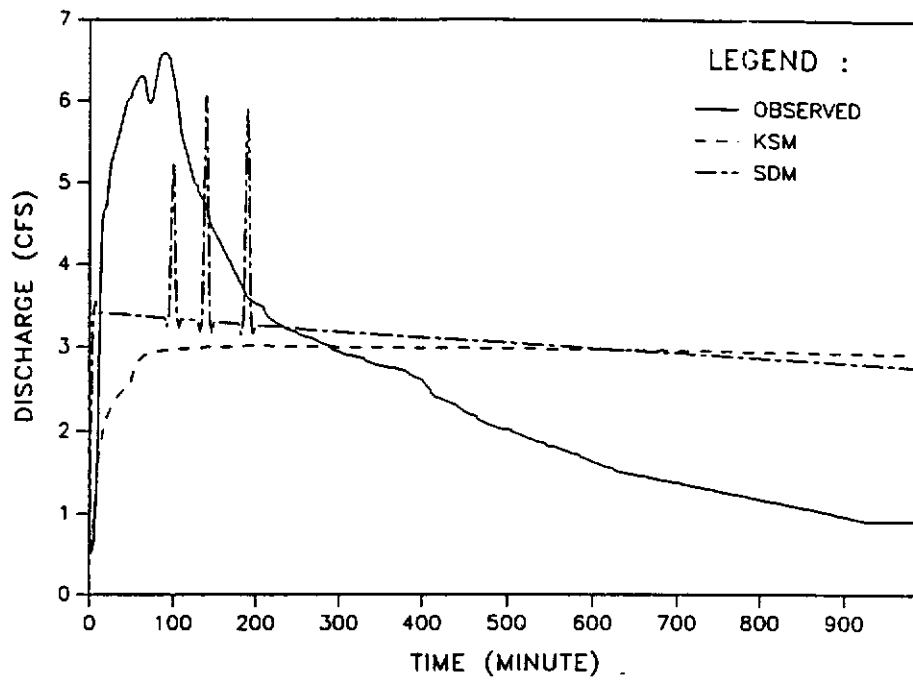


Figure 3.10a R.F. Sandlick Creek : Storm 2 : Non-Hortonian Models With Optimization

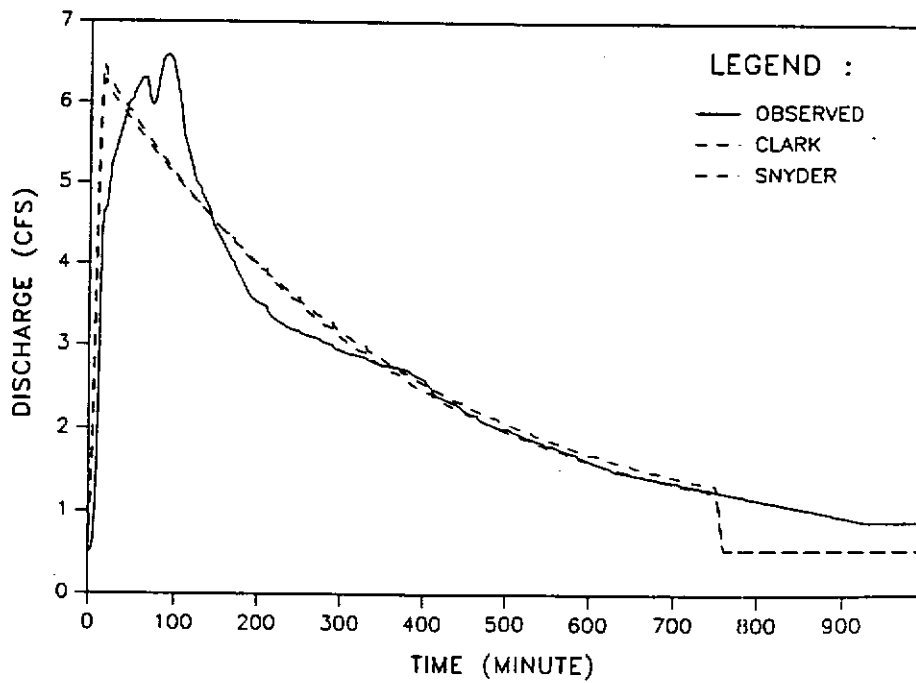


Figure 3.10b R.F. Sandlick Creek : Storm 2 : Hortonian Models With Optimization

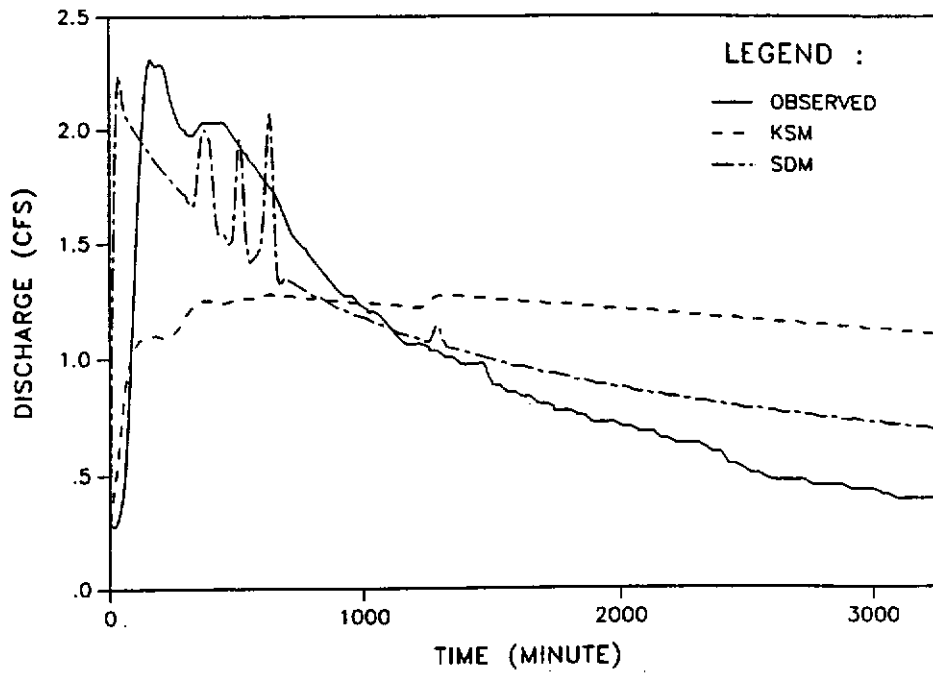


Figure 3.11a Little Millseat : Storm 1 : Non-Hortonian Models With Optimization

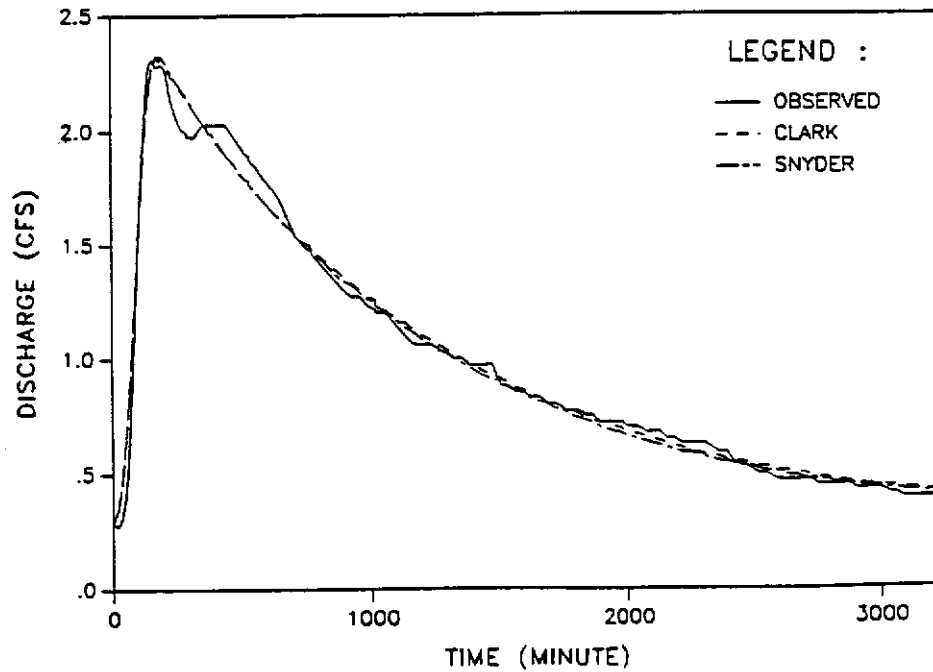


Figure 3.11b Little Millseat : Storm 1 : Hortonian Models With Optimization



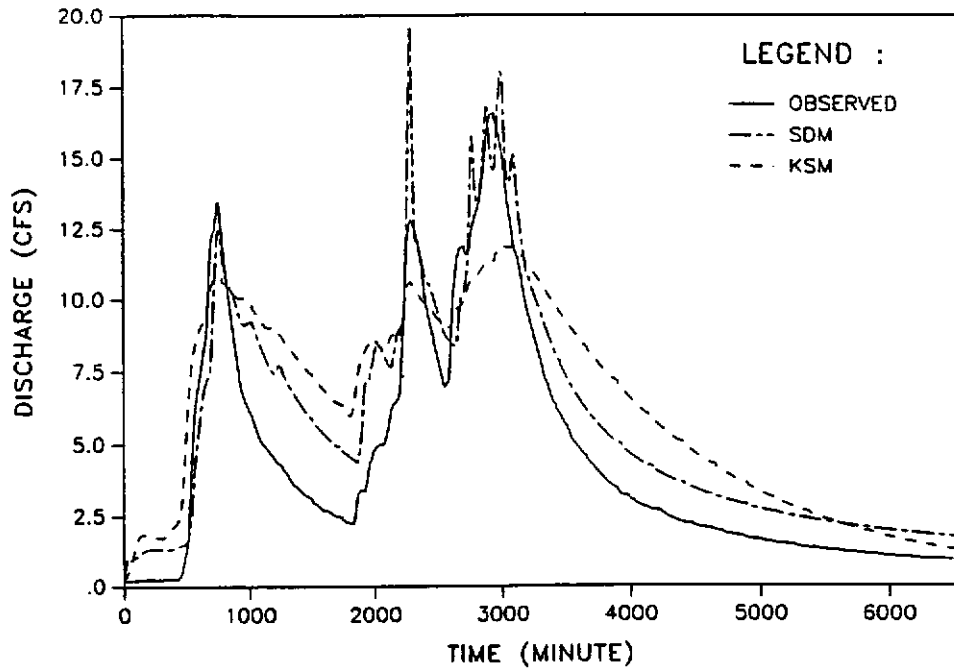


Figure 3.12a Little Millseat : Storm 2 : Non-Hortonian Models With Optimization

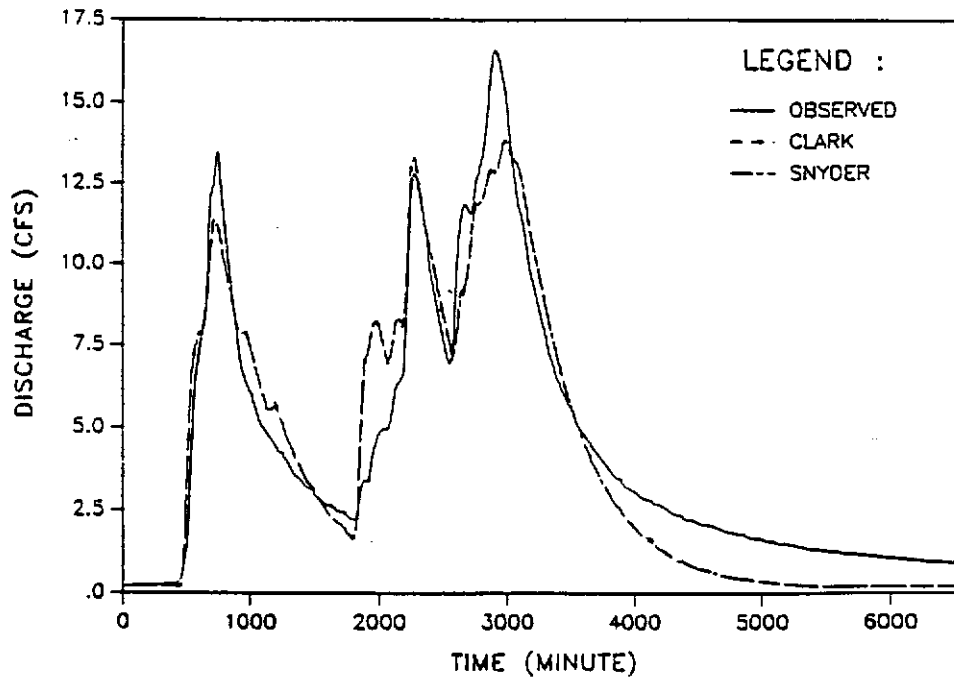


Figure 3.12b Little Millseat : Storm 2 : Hortonian Models With Optimization

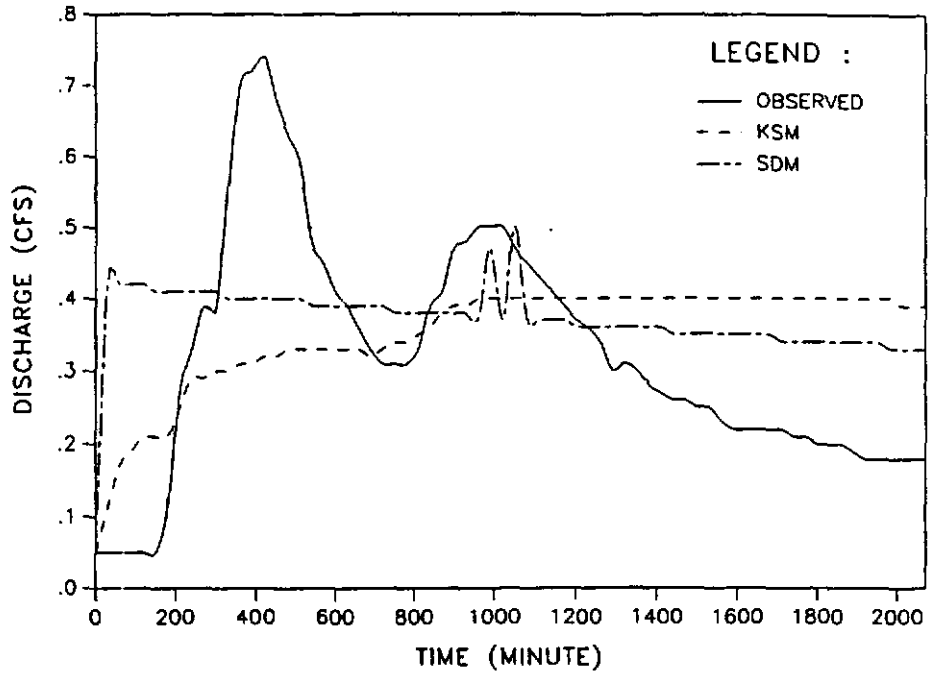


Figure 3.13a Little Millseat : Storm 3 : Non-Hortonian Models With Optimization

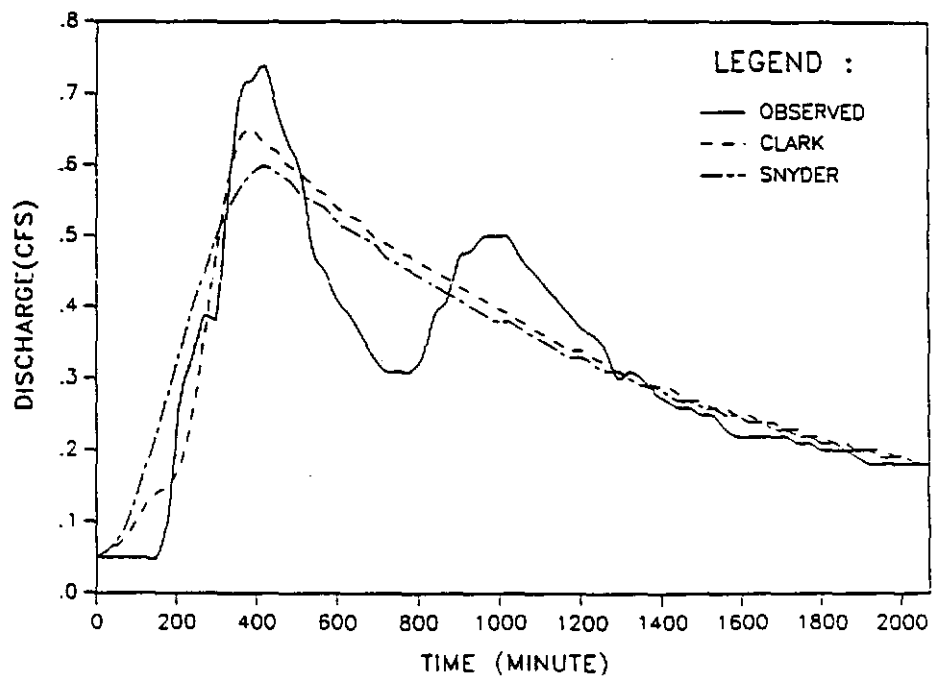


Figure 3.13b Little Millseat : Storm 3 : Hortonian Models With Optimization

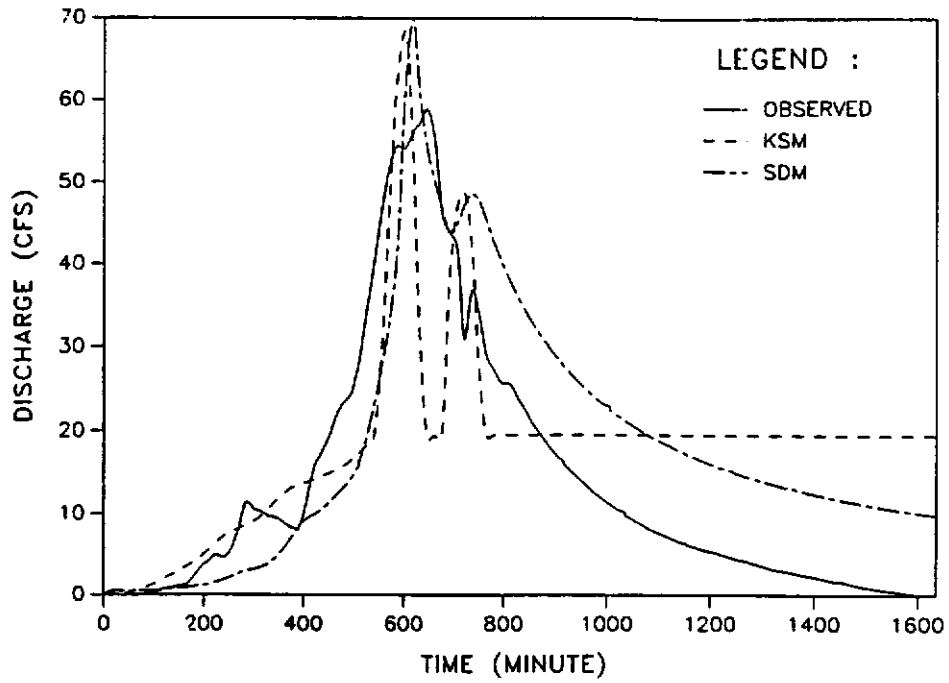


Figure 3.14a Cane Branch : Storm 1 : Non-Hortonian Models With Optimization

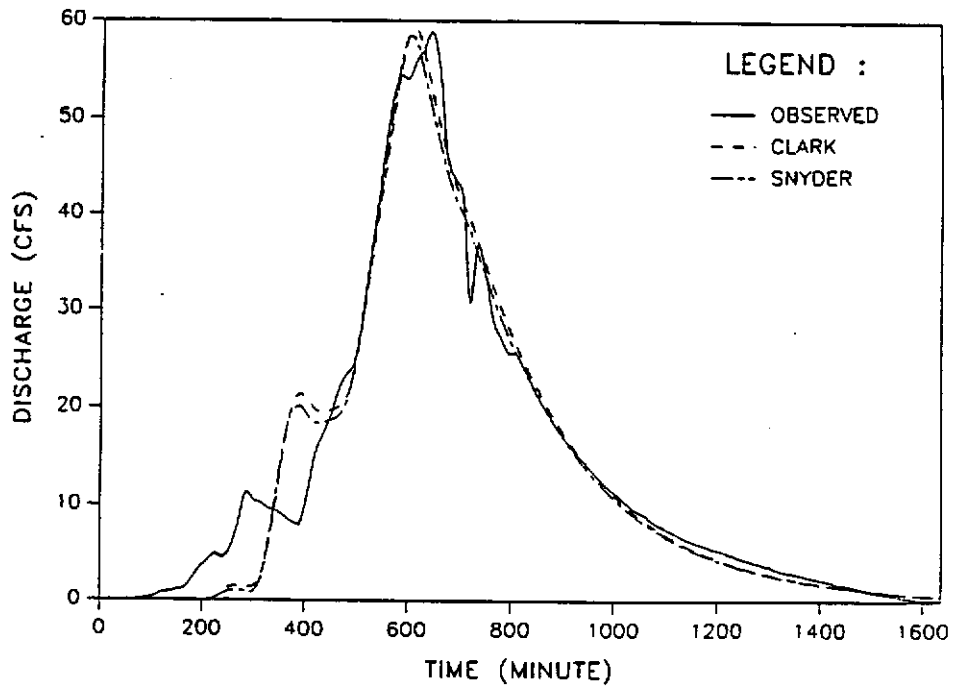


Figure 3.14b Cane Branch : Storm 1 : Hortonian Models With Optimization

saturation deficit model. The saturation deficit model performed very poorly. From table 3.2a, it can be seen that for both models the optimized parameter values are substantially different for different storm events for the same watershed. An examination of the storm hydrographs on figures 3.5 to 3.10 show that for all storm events, both the kinematic storage and saturation deficit models performed very poorly showing a very delayed response to precipitation which is in sharp contrast to the observed response.

Similar conclusions can be reached for the four storm events associated with the Little Millseat watershed and the Cane Branch watershed. From the plots (Figs. 3.11 to 3.14), it can be seen that, in general, the kinematic storage and saturation deficit models produce a very delayed response with almost a constant discharge throughout the time base of flow.

### **3.8.2 Discussion of the Results :**

The extensive review of literature dealing with the hydrology of steeply sloping forested watersheds in humid regions suggested that overland flow is a rare occurrence in these areas. Rainfall-runoff data were analyzed for four watersheds, two in West Virginia and two in Eastern Kentucky using two subsurface models. The hydraulic conductivities for these watersheds were high enough that one would not expect saturation from above to occur except in isolated area and on rare occasions of very intense rainfall. However, when optimization of the rainfall-runoff process was carried out, neither one of the subsurface flow models did very well indicating the probable absence of any substantial micropore subsurface flow.

### **3.9 Hortonian Flow Models :**

In order to compare the performance of the non-Hortonian based models to Hortonian based models, results from both the kinematic storage model and the saturation deficit model were compared with the results obtained using Snyder's unit hydrograph method and Clark's unit hydrograph method. The results of this comparison are discussed in the following sections.

#### **3.9.1. Results :**

Both Clark's and Snyder's models were applied to the four watersheds. The results of the analysis are shown in tables 3.3a and 3.3b. The runoff hydrographs for both the models for each storm event are provided in figures 3.5 to 3.14. As before, both models were calibrated in order to obtain the closest match between the simulated events and the observed events. The calibrated parameters for Clark's model include the final infiltration rate, the initial storage potential, the time of concentration, and the storage coefficient. The calibrated parameters for Snyder's model include the final infiltration rate, the initial storage potential, the time lag, and the peaking coefficient.

For both the Crane Creek and Right Fork Sandlick watersheds, Clark's and Snyder's models either underpredict or match the observed runoff volume. As regards peak discharge, Clark's and Snyder's model tend to overpredict. In general, Clark's and Snyder's model gave good estimation of the time of peak. From table 3.3a, it can be seen that for both models the optimized parameter values are substantially different for different storm events for the same watershed. An examination of the storm hydrographs on figures 3.5 to 3.10 show that for all storm events, Clark's model gave a very good match, closely followed by Snyder's model.

**TABLE 3.3a OPTIMIZED PARAMETERS : HORTONIAN MODELS**

Watershed	Storm No.	Parameters							
		Clark				Snyder			
		fc	S	Tc	R	fc	S	Tlag	Cp
Crane Creek	1	0.01	0.65	2.27	15.91	0.00	0.67	1.46	0.07
	2	0.37	2.49	0.48	2.77	0.08	2.74	0.43	0.13
	3	0.01	2.55	0.85	3.01	0.10	2.48	1.14	0.51
	4	0.12	2.89	2.33	5.75	0.23	2.87	2.34	0.50
R.F. Sandlick Creek	1	0.15	1.12	1.87	3.42	0.06	1.26	1.82	0.38
	2	0.30	2.51	0.09	5.16	0.29	2.52	0.21	0.04
L. Millseat	1	0.31	0.20	2.60	18.21	0.18	0.44	2.91	0.15
	2	0.01	0.86	0.50	7.53	0.01	0.87	1.06	0.14
	3	0.05	0.92	2.96	18.41	0.19	0.65	6.80	0.29
Cane Branch	1	0.09	0.63	0.55	3.64	0.09	0.64	0.60	0.15

**Definition of Parameters :**

- fc : Final infiltration rate.
- S : Initial storage potential.
- Tc : Time of concentration.
- R : Storage coefficient.
- Tlag : Time of lag.
- Cp : Peaking coefficient.

**TABLE 3.3b STATISTICS OF SELECTED HYDROLOGIC PARAMETERS :  
HORTONIAN MODELS**

Watershed	Storm No.	Hydrologic Parameters								
		Volume			Peak			Time of Peak		
		CLK	SNY	OBS	CLK	SNY	OBS	CLK	SNY	OBS
Crane Creek	1	0.135	0.138	0.175	4.53	4.35	4.10	10.08	9.42	10.75
	2	0.035	0.036	0.040	3.38	3.20	3.90	0.83	0.75	1.08
	3	0.017	0.014	0.015	1.70	1.79	1.90	1.08	1.33	1.42
	4	0.014	0.014	0.013	1.08	1.25	1.30	2.42	2.42	2.42
R.F. Sandlick Creek	1	0.009	0.009	0.009	1.99	1.94	2.00	2.50	2.50	1.92
	2	0.040	0.038	0.052	6.39	6.19	6.60	.25	.25	1.42
L. Millseat	1	0.263	0.260	0.261	2.32	2.33	2.28	3.00	3.00	2.50
	2	2.193	2.177	2.351	13.85	13.85	16.61	50.00	50.00	48.50
	3	0.057	0.057	0.055	0.65	0.60	0.74	6.50	7.00	7.00
Cane Branch	1	0.852	0.832	0.866	59.08	58.52	58.88	10.25	10.00	10.75

**Definitions :**

CLK : Clark's model values.

SNY : Snyder's model values.

OBS : Observed values.

Similar conclusions can be reached for the four storm events associated with the Little Millseat watershed and the Cane Branch watershed. From the plots (Figs. 3.11 to 3.14), it can be seen that for Clark's and Snyder's models the regeneration of the hydrographs is again excellent.

### **3.9.2. Discussion of Results :**

It was suggested earlier that in steeply sloping forested watersheds Hortonian overland does not usually occur. However, the optimized results of the eleven rainfall events in four watersheds do show that two Hortonian runoff models, Clark's and Snyder's models perform very well suggesting at least a quick response flow mechanism in play.

### **3.10 Parameter Estimation for Hortonian Models :**

As discussed earlier, Hortonian overland flow is generally thought to be absent in steeply sloping forested watersheds considered in this research. However, when the two Hortonian models were applied to these watersheds, the models did quite well when the model parameters were optimized. As a result, a decision was made to evaluate the performance of the two Hortonian models with estimated parameter values. Parameter estimates for the four watersheds were obtained using available precipitation records, soil classification maps and climatological data. The following sections describe the procedures employed in the data reduction.

#### **3.10.1. Loss Rate Parameters :**

For both Clark's and Snyder's models the rainfall excess was determined using Holtan's infiltration equation. Holtan's infiltration equation involves four different parameters: a land use coefficient  $a$ , an exponent  $n$ , a final infiltration rate  $f_c$ , and the initial storage



potential S. Estimates of these four parameters were obtained as follows.

#### **3.10.1.1 Land Use Coefficient :**

The land use coefficient a was assumed to be unity for the forested watersheds considered in this research.

#### **3.10.1.2 Infiltration Exponent :**

The infiltration exponent n was assumed to have a value of 1.4.

#### **3.10.1.3. Final Infiltration Rate :**

To estimate the final infiltration rate for each watershed, the dominant soil type was first identified. For Crane creek and R.F. Sandlick this was done using information from Kiesler et al. (1983), for Cane Branch from Musser (1963) and SCS (1970), and for Little Millseat from SCS (1982) and Sloan (1983). Using this information the corresponding hydrologic soil group (A,B,C or D) was obtained for each watershed (Soil Conservation Service, 1972). Once the soil group was determined, fc was approximated from Musgrave (1955). An average value for each watershed was used. The values of fc for the four watersheds are shown in Table 3.4.

#### **3.10.1.4 Initial Storage Potential :**

The initial storage potential for a particular rainfall event was determined using the following procedure. A heavy rainfall event was identified several days prior to the heavy storm event, soil was assumed to be at field capacity after the heavy rainfall event has occurred and then soil-moisture accounting was done allowing evapotranspiration from the soil using the following equation (Holtan et al., 1975) :

$$ET = GI * K * EP * [(S_{max} - S) / AW_{max}]^n \quad (3.1)$$

where ET is evapotranspiration potential (in/day), GI is the growth index of crops in % of maturity, K is the ratio of GI to pan evaporation, EP is

the pan evaporation (in/day),  $S_{max}$  is the maximum storage potential (in),  $S$  is the available storage potential (in), and  $AW_{max}$  is the maximum available water for evapotranspiration (in). The exponent  $n$  is defined by the following equation :

$$n = AW_{max}/GW_{max} \quad (3.2)$$

Where  $GW_{max}$  is the maximum gravity water in the soil profile (in).

Antecedent precipitation data for Crane creek and R.F. Sandlick creek were obtained from the USGS. Antecedent precipitation data for Little Millseat and Cane Branch were approximated using precipitation data for nearby stations available from NOAA (1960, 1985, 1986). Pan evaporation and temperature data for all four watersheds were estimated using climatological data for nearby stations (NOAA, 1960, 1981, 1982, 1985, 1986). Growth index  $GI$  for the watersheds were approximated using information in Veismann et al. (1977) and mean monthly temperature. The ratio of  $GI$  to pan evaporation i.e.,  $K$  was assumed to be 1.6 i.e. the lower limit for forested watersheds (Veismann et al., 1977) for Crane creek, R.F. Sandlick creek and Little Millseat. For Cane Branch  $K$  was assumed to be 88% of 1.6 i.e., 1.41 since 88% of the watershed is undisturbed. Data to estimate  $S_{max}$ ,  $GW_{max}$  and  $AW_{max}$  for Crane creek and R.F. Sandlick creek were obtained from Scott (1984) and Kiesler et al. (1983). For Little Millseat, these values were obtained from Sloan (1983) and SCS (1982); and for Cane Branch, from Musser (1963), SCS (1970) and Wilson et al. (1984). Initial storage potential values for the ten storm events are shown in Table 3.4.

### 3.10.2. Unit Hydrograph Parameters :

Clark's model require two parameters, time of concentration  $t_c$  and storage coefficient  $R$ , as input to the model. Snyder's model also require

two parameters, time of lag  $T_{lag}$  and peaking coefficient  $C_p$ . The estimation of these four parameters are described below.

#### **3.10.2.1 Time of Concentration :**

Time of concentration  $t_c$  for the watersheds were approximated by the upland method using the following equation (Soil Conservation Service, 1972):

$$t_c = L/(3600 V) \quad (3.3)$$

where  $t_c$  is the time of concentration (hours),  $L$  is the hydraulic length (ft) and  $V$  is the velocity (ft/s). Hydraulic lengths for Crane creek and R.F. Sandlick creek were obtained from Scott (1984), for Little Millseat from Sloan (1983), and for Cane Branch from Wilson et al. (1984). Velocity  $V$  for all watersheds was estimated using the watershed slopes from (Soil Conservation Service, 1972). The values of  $t_c$  for the four watersheds are shown in Table 3.4.

#### **3.10.2.2 Storage Coefficient :**

Storage coefficient  $R$  was assumed equal to the time of lag. The values of  $R$  for the four watersheds are shown in Table 3.4.

#### **3.10.2.3 Time of Lag :**

Time of lag  $T_{lag}$  was assumed to be 60% of time of concentration. Table 3.4 shows the time of lag for the four watersheds.

#### **3.10.2.4 Peaking Coefficient :**

Peaking coefficient  $C_p$  was assumed 0.70 for Crane creek which has a very steep slope (50%). This was based on values of  $C_p$  cited in literature ranging from 0.40 to 0.80 (Veissman et al., 1977). Using this value as the reference,  $C_p$  for other watersheds were estimated based on their slopes. The values of  $C_p$  for the four watersheds are also shown in Table 3.4.

TABLE 3.4 ESTIMATED PARAMETERS VALUES : HORTONIAN MODELS

Watershed	Storm No.	Parameters											
		Clark						Snyder					
		a	n	fc	S	tc	R	a	n	fc	S	Tlag	Cp
Crane Creek	1	1.0	1.4	.225	3.91	1.12	0.67	1.0	1.4	.225	3.91	0.67	0.70
	2	1.0	1.4	.225	5.47	1.12	0.67	1.0	1.4	.225	5.47	0.67	0.70
	3	1.0	1.4	.225	5.67	1.12	0.67	1.0	1.4	.225	5.67	0.67	0.70
	4	1.0	1.4	.225	5.37	1.12	0.67	1.0	1.4	.225	5.37	0.67	0.70
R.F. Sandlick Creek	1	1.0	1.4	.220	5.09	1.71	1.03	1.0	1.4	.220	5.09	1.03	0.68
	2	1.0	1.4	.220	4.84	1.71	1.03	1.0	1.4	.220	4.84	1.03	0.68
L. Millseat	1	1.0	1.4	0.16	5.54	0.90	0.54	1.0	1.4	0.16	5.54	0.54	0.65
	2	1.0	1.4	0.16	5.53	0.90	0.54	1.0	1.4	0.16	5.53	0.54	0.65
	3	1.0	1.4	0.16	5.90	0.90	0.54	1.0	1.4	0.16	5.90	0.54	0.65
Cane Branch	1	1.0	1.4	0.14	3.83	1.30	0.78	1.0	1.4	0.14	3.83	0.78	0.52

Definition of Parameters :

- a : Land use coefficient.
- n : Infiltration exponent.
- fc : Final infiltration rate.
- S : Initial storage potential.
- tc : Time of concentration.
- R : Storage coefficient.
- Tlag : Time of lag.
- Cp : Peaking coefficient.

### 3.10.3. Results :

Both Clark's and Snyder's models were applied to the four watersheds using real data. Table 3.4 contains the realistic parameter values for the two Hortonian models. It was found that using realistic model parameters neither Clark's model nor Snyder's model was able to produce any rainfall excess and the runoff hydrograph consisted entirely of the base flow.

### 3.10.4. Discussion of the Results :

Despite the good performance of the two Hortonian models with optimized parameters, the models failed to generate any rainfall excess when realistic data were used. This means that all rainfall infiltrated into the soil, thus indicating the distinct possibility of a quick response subsurface flow mechanism of runoff hydrograph generation.

### 3.11 Conclusions :

As mentioned previously, the high hydraulic conductivity values for the watersheds tested do not indicate the presence of Hortonian overland flow. In case of Little Millseat watershed, field observations support this conclusion. For the four rainfall events cited, evidence of Hortonian overland flow was never observed. Also when realistic values of infiltration rate and subsurface storage potential were used, Clark's and Snyder's models did not produce any rainfall excess, all precipitation was infiltrated thus in fact corroborating field observations that no overland flow occurred. Furthermore, the kinematic storage model and the saturation deficit model (slow response subsurface models) performed poorly indicating the probable absence of any substantial micropore flow. Therefore, the good performance of Clark's and Snyder's models and the poor performance of the slow response subsurface models suggest the

necessity for developing a subsurface flow model which can account for the quick response of the watersheds. The proposed model will therefore incorporate macropore flow (quick response subsurface flow) in addition to micropore flow (slow response subsurface flow). This topic will be addressed in the next chapter.

## CHAPTER 4

### A COMPREHENSIVE CONCEPTUAL MODEL FOR FORESTED WATERSHEDS

#### 4.1 Introduction :

From the discussions in the previous chapter it is apparent that both Beven and Wood's saturated deficit model and Sloan et al.'s kinematic storage model were inadequate in predicting the rapid hydrologic response of the forested watersheds. Although both Snyder's and Clark's models were able to produce better correlations between the observed and predicted hydrographs, the resulting hydrologic parameters were not realistic. As a result an alternative model structure is proposed which incorporates a rapid response mechanism (macropore flow) while still maintaining the predominantly observed flow mechanism of subsurface flow.

#### 4.2. General Description of the Model :

The comprehensive hydrologic model developed in this research is based on a storage approach. A fundamental assumption of the model is that the catchment under study may be subdivided into several subcatchment units which are relatively homogeneous in their hydrologic response and which therefore may be modeled separately. This subdivision is carried out on the basis of the channel network, not only because it is a convenient and objective method, but also because routing from the subcatchment outflow through the channel network may have a significant influence on the final distribution of the catchment discharge (Surkan, 1968; Kirkby, 1976).

The simulated discharges from each subcatchment are routed through the channel to the catchment outflow. The model structure reflects the variable source area concept unifying all the possible runoff generation processes from Hortonian overland flow to subsurface flow

including macropore flow. The subcatchment model is shown in figures 4.1 and 4.2. The model comprises three storage components : a macropore store, a micropore store and a surface store. These storage components are described in the following sections.

#### 4.2.1. Macropore Store :

The macropore store has a maximum value of  $S_{mpmax}$  which represents the maximum amount of water that can be held in the soil macropores.  $S_{mpmax}$  does not however represent the limiting storage value to produce macropore flow as will be explained later. With the initiation of a rainfall event, a fraction of the rainfall is considered diverted to the macropore store. The remaining rainfall may either infiltrate the soil micropores or run off the catchment as overland flow. The fraction which enters the macropores is a function of the type and density of vegetation as well as percent of area having vegetal openings on the soil surface. If at any time the macropore store exceeds its maximum value, an overflow from the macropore store to the micropore store occurs.

#### 4.2.2. Micropore Store :

The micropore store comprises a gravity water store and an available water store. The available water store has a maximum value of  $AW_{max}$  and the gravity water store,  $GW_{max}$ . The rate at which rain water infiltrates the soil micropores is a function of the storage potential of the micropore store (Holtan, 1961). The initial storage potential is a function of maximum storage potential and the antecedent moisture condition of the soil. As soon as the available water store becomes full, additional rain water begins to fill up the gravity water store. The flow through the soil micropores is termed  $Q_{mi}$  and is an outflow from the gravity water store.



#### 4.2.3. Surface Store :

The surface store accounts for overland flow due both to Hortonian type of flow as well as saturation overland flow. The assumptions are that Hortonian overland flow occurs whenever the rainfall rate exceeds the infiltration rate and saturation overland flow occurs whenever gravity water in the subsurface store exceeds one-half of the maximum gravity water store.

#### 4.3 Detailed Description of the Model :

##### 4.3.1. Macropore Storage :

The continuity equation for flow through macropore store can be written as,

$$\frac{dS_{mp}}{dt} = \bar{R}_{mp} - \bar{Q}_{mp} \quad (4.1)$$

where  $S_{mp}$  is the effective macropore storage,  $\bar{R}_{mp}$  is the average rate of the vertical input into the macropore store and  $\bar{Q}_{mp}$  is the average rate of outflow from the macropores.

Equation (4.1) can be written in explicit finite difference form as,

$$\frac{S_{mp_2} - S_{mp_1}}{\Delta t} = (P_{mp_1} + P_{mp_2}) / (2\Delta t) - (Q_{mp_1} + Q_{mp_2}) / 2 \quad (4.2)$$

where  $\Delta t = t_2 - t_1$ ,  $Q_{mp}$  is the outflow from the macropores ( $LT^{-1}$ ) and subscripts 1 and 2 refer to the beginning and end of the time period respectively. The definitions of  $S_{mp}$  and  $P_{mp}$  will vary depending on whether any gravity water is present in the micropore store. Therefore, in this regard, two scenarios are possible (Figs. 4.1 and 4.2).

When gravity water is absent (Scenario I),  $S_{mp}$  is given by,

$$S_{mp} = S_{mpss} \quad (4.3)$$

where  $S_{mpss}$  is volume of the water in the macropore store.  $P_{mp}$  is the

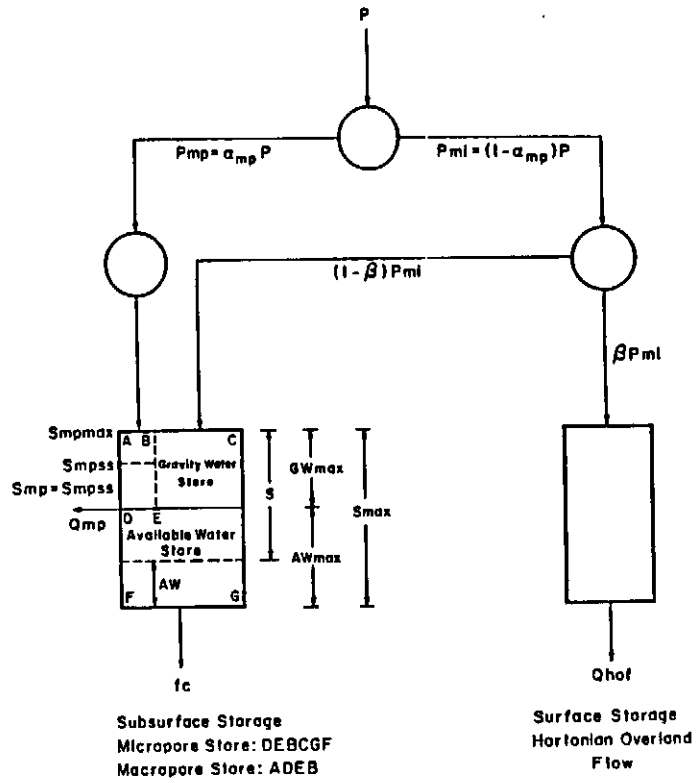


Figure 4.1 Comprehensive Watershed Model  
Scenario I: Gravity Water Absent

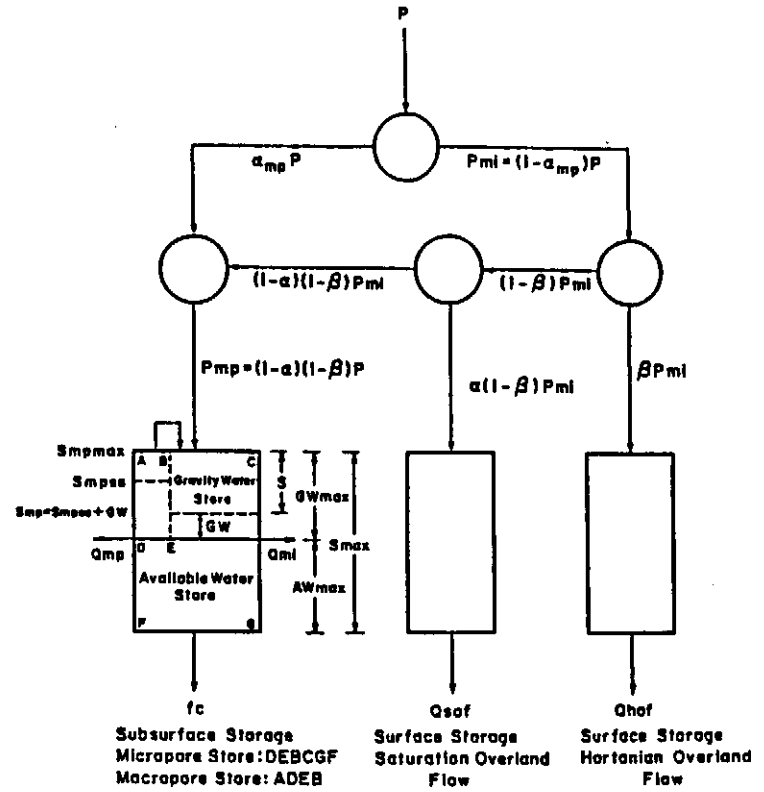


Figure 4.2 Comprehensive Watershed Model  
Scenario II: Gravity Water Present

vertical input into the macropore store and is given by,

$$P_{mp} = \alpha_{mp} P \quad (4.4)$$

where  $P$  is the rainfall and  $\alpha_{mp}$  is the fraction of the precipitation entering the soil macropores.

When gravity water is present (Scenario II),  $S_{mp}$  is given by

$$S_{mp} = S_{mpss} + GW \quad (4.5)$$

where  $S_{mpss}$  is the volume of water in the macropore store and  $GW$  is the volume of water in the gravity water store.  $P_{mp}$  is the vertical input into the combined macropore-gravity water store and is given by,

$$P_{mp} = (1 - \alpha)(1 - \beta)P \quad (4.6)$$

where  $\alpha$  is the fraction of the rainfall contributing to saturation overland flow,  $\beta$  is the fraction of the rainfall contributing to Hortonian overland flow, and  $P$  is the amount of rainfall.

If the macropore store is considered as a linear reservoir, then the corresponding storage-discharge relationship can be written as,

$$S_{mp} = C_{mp} Q_{mp} \quad (4.7)$$

where  $C_{mp}$  is defined as the macropore storage constant (T). This constant is a function of soil type, length and depth of hillslope and the watershed slope.

Substituting equation (4.7) in equation (4.2) and rearranging,

$$\frac{C_{mp}(Q_{mp2} - Q_{mp1})}{\Delta t} = \frac{(P_{mp1} + P_{mp2})}{(2\Delta t)} - \frac{(Q_{mp1} + Q_{mp2})}{2} \quad (4.8)$$

Solving equation (4.8) explicitly we have,

$$Q_{mp2} = [(P_{mp1} + P_{mp2}) - Q_{mp1}\Delta t + 2C_{mp} Q_{mp1}] / (2C_{mp} + \Delta t) \quad (4.9)$$

Then  $S_{mp2}$  at the end of time step  $\Delta t$  is computed by,

$$S_{mp2} = C_{mp}/Q_{mp2} \quad (4.10)$$

If there is no gravity water, the macropore store acts independently of the gravity water store. If however, gravity water is present, it is

assumed that an instantaneous inflow takes place from the gravity water store to the macropore store in order to maintain flow in the macropores. This affects the gravity water store in the following way,

$$GW^{new} = GW^{old} + (1 - \alpha)(1 - \beta)Pm_i - \overline{\overline{Q_{mp}}} \Delta t \quad (4.11)$$

where  $\overline{\overline{Q_{mp}}}$  is the average value of  $Q_{mp}$  over the time step.

If the computed value of  $GW^{new}$  using equation (4.11) is less than zero, it means that there is not enough water in the gravity store to provide the entire amount of macropore flow. As a result,  $GW^{new}$  takes a value of zero and additional water for macropore flow is supplied by the macropore store. This leads to the following changes in the macropore store and the gravity store,

$$Smpss^{new} = Smpss^{old} + \alpha_{mp} P - GWD \quad (4.12)$$

$$GW^{new} = 0 \quad (4.13)$$

where GWD is equivalent to the absolute value of equation (4.11).

If however, the computed value of  $GW^{new}$  using equation (4.11) is greater than zero, this means that the entire amount of water for macropore flow is supplied by the gravity store. For this case, the gravity water store is given by equation (4.11) and the macropore store is then affected as follows,

$$Smpss^{new} = Smpss^{old} + \alpha_{mp} P \quad ; \quad Smpss^{new} \leq Smpmax \quad (4.14)$$

where  $Smpmax$  is the maximum macropore storage value and is given by,

$$Smpmax = \alpha_{smp} Smax \quad (4.15)$$

where  $\alpha_{smp}$  is the ratio of macroporosity to microporosity and  $Smax$  is the maximum micropore storage potential.  $Smax$  is given by,

$$Smax = Gwmax + Awmax \quad (4.16)$$

If at any time  $Smpss$  exceeds  $Smpmax$ , excess water is diverted from the macropore store to the gravity water store. This results in the

following changes in the gravity store and the macropore store,

$$GW^{new} = GW^{old} + (Smpss^{new} - Smpmax) \quad (4.17)$$

$$Smpss^{new} = Smpmax \quad (4.18)$$

where  $GW^{old}$  in equation (4.17) is actually the  $GW^{new}$  value calculated using either equation (4.11) or (4.13) depending on the circumstances.

#### 4.3.2. Micropore Storage :

The micropore storage comprises a gravity water store with a maximum value of  $GW_{max}$  and an available water store with a maximum value of  $AW_{max}$ . Two scenarios are also possible with micropore store depending on the absence or presence of gravity water. If gravity water is absent (Scenario I), then using Holtan's approach (Holtan, 1961) the following equation can be written for the rate of infiltration into the soil micropores,

$$f = a(S-F)^n \quad (4.19)$$

where  $f$  is the rate of infiltration into soil micropores ( $LT^{-1}$ ),  $S$  is the maximum storage potential of soil after accounting for antecedent moisture condition ( $L$ ),  $F$  is the accumulated infiltration ( $L$ ),  $a$  is a coefficient for land use pattern and  $n$  is an exponent assumed to be a constant for a given soil.

The current storage potential  $S$  is given by,

$$\dot{S} = S - F \quad (4.20)$$

Now, using equations (4.19) and (4.20),

$$S - \dot{S} = a\dot{S}^n \Delta t \quad (4.21)$$

or,

$$F(\dot{S}) = a\dot{S}^n \Delta t - S + \dot{S} \quad (4.22)$$

differentiating,

$$F'(\dot{S}) = n a \dot{S}^{n-1} \Delta t + 1 \quad (4.23)$$

Equation (4.23) can be solved by Newton's method using,

$$\dot{S}_i = \dot{S}_{i-1} - F(\dot{S}_{i-1}) / F'(\dot{S}_{i-1}) \quad (4.24)$$

where  $i$  refers to iteration step in the solution process.

Micro pore flow is assumed to be zero if gravity water is absent. However, with the continuation of the storm, as soon as the available water becomes full, additional rainwater begins to fill up the gravity water store. This marks the beginning of scenario II and the ensuing flow through the soil micropores. The micropore flow (slow response subsurface flow) is termed  $Q_m$  and is an outflow from the gravity water store. The outflow (per unit area) from the gravity water store through the micropores is given by Darcy's law as,

$$Q_s = K_s i h \quad (4.25)$$

where  $Q_s$  is the micropore flow per unit area ( $LT^{-1}$ ),  $K_s$  is the saturated hydraulic conductivity of soil ( $LT^{-1}$ ) and  $i$  is the hydraulic gradient.

For the proposed model, the hydraulic gradient is assumed to be equal to the bed slope. Using the conceptual hillslope (Fig. 2.1) used by Sloan et al. (1983) as mentioned previously, equation (4.25) can be written as,

$$Q_s = K_s \sin(a) h \quad (4.26)$$

where  $h$  is the equivalent water level in the conceptual hillslope ( $L$ ). The variable  $h$  is assumed proportional to gravity water store and given by,

$$h = (2GW/GW_{max})D \quad (4.27)$$

where  $D$  is the depth of hillslope ( $L$ ). From equations (4.26) and (4.27),

$$Q_s = K_s \sin(a) (2GW/GW_{max})D \quad (4.28)$$

Therefore, the flow per unit width may be expressed as,

$$Q_s/l = (K_s \sin(a)) (D/l) (2GW/GW_{max}) \quad (4.29)$$

or, 
$$Q_{mi} = C_{ss} C_g (2GW/GW_{max}) \quad (4.30)$$

where,

$$Q_{mi} = Q_s/l \quad (4.31)$$

$$C_{ss} = K_s \sin(a) \quad (4.32)$$

$$C_g = D/l \quad (4.33)$$

Where  $C_{ss}$  is termed the micropore flow velocity ( $LT^{-1}$ ) and  $C_g$  is termed the geometric factor of the watershed.

A water balance calculation is then made to find the new beginning of time step gravity water storage in the following manner,

$$GW^{beg} = GW^{end} - \bar{Q}_{mi} \Delta t \quad ; \quad GW^{beg} \geq 0 \quad (4.34)$$

where  $\bar{Q}_{mi}$  is the average  $Q_{mi}$  value over the time step.

#### 4.3.3. Surface Storage :

The surface storage accounts for overland flow. Overland flow may comprise two components : Hortonian overland flow and saturation overland flow.

##### 4.3.3.1. Hortonian Overland Flow :

Hortonian overland flow occurs whenever rainfall rate exceeds infiltration rate. This may be expressed as,

$$dP_{mi}/dt > f \quad (4.35)$$

where  $f$  is the rate of infiltration ( $LT^{-1}$ ). The definitions of  $P_{mi}$  varies depending on the state of the gravity water store. If it is empty,  $P_{mi}$  is the fraction of rainfall which either infiltrates the micropores or runs off as overland flow ( $L$ ) and is given by,

$$P_{mi} = (1 - \alpha_{mp}) P \quad (4.36)$$

where  $\alpha_{mp}$  is the fraction of rainfall falling into the soil macropores and  $P$  is the amount of rainfall ( $L$ ).

If the gravity water store is not empty,  $P_{mi}$  equals the amount of

precipitation and therefore given by,

$$P_{mi} = P \quad (4.37)$$

#### 4.3.3.2 Saturation Overland Flow :

Saturation overland flow occurs whenever gravity water store exceeds one half of maximum gravity water storage. This may be expressed as,

$$GW > 0.50 GW_{max} \quad (4.38)$$

where  $GW$  is the gravity water store in the micropore store ( $L$ ) and  $GW_{max}$  is the maximum gravity water storage ( $L$ ). The above conclusion is based on the conceptual hillslope (figure 2.1) used in the development of the kinematic storage model of Sloan et al. (1983). They assumed that saturation overland flow occurs over the conceptual hillslope as soon as the water table which is hinged at point A intersects the ground surface (point B). Equation (4.38) can be obtained by assuming that the maximum possible storage in the hillslope is equal to the maximum gravity water storage.

#### 4.3.3.3 Distribution of Overland Flow :

Depending on the rainfall rate and the amount of gravity water storage, the fraction of rainfall which becomes overland flow is given by,

$$\gamma = \alpha(1 - \beta)P_{mi} + \beta P_{mi} \quad (4.39)$$

where,

$$\alpha = (2GW - GW_{max})/GW_{max} \quad (4.40)$$

$$\text{and,} \quad \beta = 1 \text{ if } dP_{mi}/dt > f \quad (4.41)$$

$$\beta = 0 \text{ if } dP_{mi}/dt < f \quad (4.42)$$

Equation (4.40) is also derived using the conceptual hillslope (Fig. 2.2) used by Sloan et al. (1983).



There may be four combinations of the situations as described above :

i)  $GW < 0.50 GW_{max}$  and  $dP_{mi}/dt < f$  :  $\alpha = 0$  and  $\beta = 0$ ; therefore there is no overland flow.

ii)  $GW < 0.50 GW_{max}$  and  $dP_{mi}/dt > f$  :  $\alpha = 0$  and  $\beta = 1$ ; therefore there is only Hortonian overland flow.

iii)  $GW > 0.50 GW_{max}$  and  $dP_{mi}/dt < f$  :  $\alpha > 0$  and  $\beta = 0$ ; therefore there is only saturation overland flow.

iv)  $GW > 0.50 GW_{max}$  and  $dP_{mi}/dt > f$  :  $\alpha > 0$  and  $\beta = 1$ ; therefore there is Hortonian overland flow as well as saturation overland flow.

## CHAPTER 5

### COMPREHENSIVE MODEL RESULTS

#### 5.1. Introduction :

In order to assess the utility of the new comprehensive watershed model, it was embedded into HEC-1. Subsequently the model was applied to the four watersheds mentioned in chapter three.

#### 5.2. Modified Version of HEC-1 :

As stated in chapter three, the two slow response subsurface models, the kinematic storage model and the saturation deficit model, were unable to predict with reasonable accuracy the hydrologic response of the four steeply sloping forested watersheds even with optimized parameters. In contrast, the two Hortonian models, Clark's and Snyder's models, were able to predict accurately the hydrologic response of the watersheds with optimized parameters. However, the final parameter values were unrealistic and also different for different rainfall events for the same watershed. Moreover, with realistic data the Hortonian models were unable to generate any rainfall excess. The good performance of the Hortonian models with optimization and their subsequent inability to produce any rainfall excess (with realistic data) led to the conclusion that a quick response subsurface flow mechanism is responsible for storm hydrograph generation in the modeled watersheds. As a result a comprehensive watershed model was developed which incorporated all of the possible flow mechanism inclusive of a quick response subsurface flow mechanism. This model was incorporated into HEC-1 and is now available in HEC-1 as a new option to calculate runoff hydrograph.

### 5.3. Comprehensive Model Application :

Once the comprehensive watershed model was embedded into HEC-1, it was used to evaluate the hydrologic response of the four watersheds to the set of 10 different storms mentioned in chapter three. The data reduction and the results of the analysis are discussed in the following sections.

#### 5.3.1. Data Reduction :

The comprehensive watershed model (COMWAM) requires as input nine parameters: three for the infiltration model component,  $a$ ,  $n$  and  $S$ , three for the micropore model component,  $GW_{max}$ ,  $C_{ss}$ , and  $C_g$ , and three for the macropore model component,  $\alpha_{mp}$ ,  $\alpha_{smp}$  and  $C_{mp}$ . All these parameters have been defined in chapter four.

Infiltration model parameters and the micropore model parameter  $GW_{max}$  were estimated in the same way as stated in chapter three. The micropore model parameters  $C_{ss}$  and  $C_g$  were estimated using values of watershed slope, length, depth and saturated hydraulic conductivity of soil. These data were all obtained from the sources referred to in chapter three. The values of all these parameters are shown in Table 5.1. Since at this point no method has been devised to estimate the macropore model parameters, a decision was made to obtain estimates of these parameters through model calibration.

#### 5.3.2. Results :

The comprehensive watershed model was applied to the four watersheds. The results of the analysis are shown in Tables 5.2 and 5.3. Table 5.2 contains the optimized macropore model parameters for each storm event. Table 5.3 provides a comparison between the observed and predicted hydrologic statistics for the model. The runoff hydrographs for each storm event are provided in Figures 5.1 to 5.10.

**TABLE 5.1 ESTIMATED PARAMETER VALUES :  
COMPREHENSIVE WATERSHED MODEL**

Watershed	Storm No.	Parameters						
		a	n	S	Smax	GWmax	Css	Cg
Crane Creek	1	1.0	1.4	3.91	9.77	3.47	1.12	.00195
	2	1.0	1.4	5.47	9.77	3.47	1.12	.00195
	3	1.0	1.4	5.67	9.77	3.47	1.12	.00195
	4	1.0	1.4	5.37	9.77	3.47	1.12	.00195
R.F. Sandlick Creek	1	1.0	1.4	5.09	7.56	2.68	1.57	.00067
	2	1.0	1.4	4.84	7.56	2.68	1.57	.00067
L. Millseat	1	1.0	1.4	5.54	10.16	4.78	1.86	.00576
	2	1.0	1.4	5.53	10.16	4.78	1.86	.00576
	3	1.0	1.4	5.90	10.16	4.78	1.86	.00576
Cane Branch	1	1.0	1.4	3.83	7.23	2.64	0.54	.00435

**Definition of parameters :**

- a : Land use coefficient.
- n : Infiltration exponent.
- S : Initial storage potential.
- Smax : Maximum storage potential.
- GWmax : Maximum gravity water store.
- Css : Micropore flow velocity.
- Cg : Geometric factor of watershed.

**TABLE 5.2 OPTIMIZED PARAMETERS : COMPREHENSIVE WATERSHED MODEL**

Watershed	Storm No.	Parameters			
		CWM			
		$\alpha_{mp}$	$\alpha_{smp}$	Cmp	S
Crane Creek	1	0.08	0.87	23.71	3.98
	2	0.04	0.01	3.64	5.95
	3	0.02	0.33	3.13	4.36
	4	0.02	0.07	5.75	4.70
R.F. Sandlick Creek	1	0.01	0.95	3.84	4.50
	2	0.04	0.57	4.49	5.71
L. Millseat	1	0.22	0.87	15.22	5.65
	2	0.43	0.32	7.70	5.91
	3	0.05	0.96	14.26	5.95
Cane Branch	1	0.22	0.28	3.12	4.07

**Definition of Parameters :**

- $\alpha_{mp}$  : Fraction of precipitation entering soil macropores.
- $\alpha_{smp}$  : Ratio of macroporosity to microporosity.
- Cmp : Macropore storage constant.
- S : Initial storage potential.

**TABLE 5.3 STATISTICS OF SELECTED HYDROLOGIC PARAMETERS :  
COMPREHENSIVE WATERSHED MODEL**

Watershed	Storm No.	Hydrologic Parameters					
		Volume		Peak		Time of Peak	
		CWM	OBS	CWM	OBS	CWM	OBS
Crane Creek	1	0.177	0.175	4.18	4.10	8.42	10.75
	2	0.039	0.040	3.06	3.90	0.58	1.08
	3	0.016	0.015	1.60	1.90	0.58	1.42
	4	0.014	0.013	1.12	1.30	1.58	2.42
R.F. Sandlick Creek	1	0.010	0.009	1.51	2.00	3.17	1.92
	2	0.051	0.052	6.13	6.60	1.08	1.42
L. Millseat	1	0.264	0.261	2.06	2.28	5.50	2.50
	2	2.276	2.351	15.03	16.61	50.00	48.50
	3	0.059	0.055	0.53	0.74	4.00	7.00
Cane Branch	1	0.977	0.866	59.76	58.88	10.25	10.75

**Definitions :**

CWM : Comprehensive watershed model values.

OBS : Observed values.

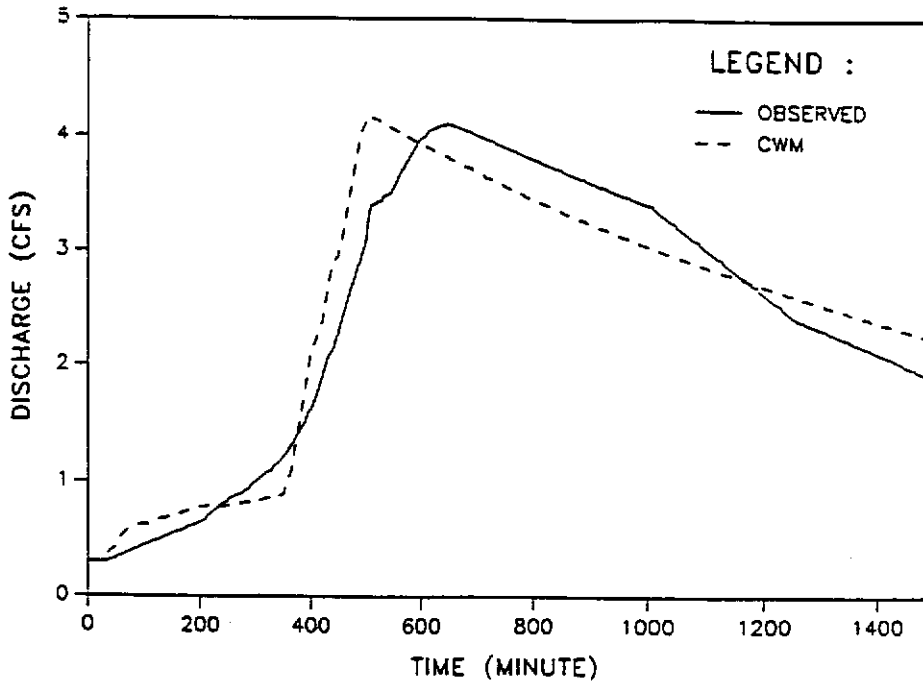


Figure 5.1 Crane Creek : Storm 1 : Comprehensive Watershed Model

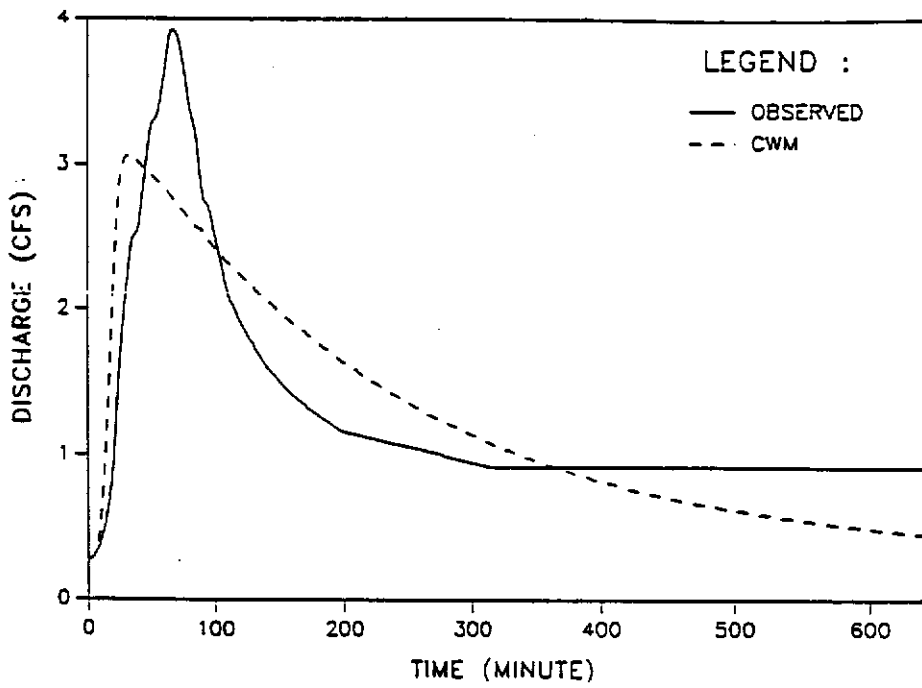


Figure 5.2 Crane Creek : Storm 2 : Comprehensive Watershed Model

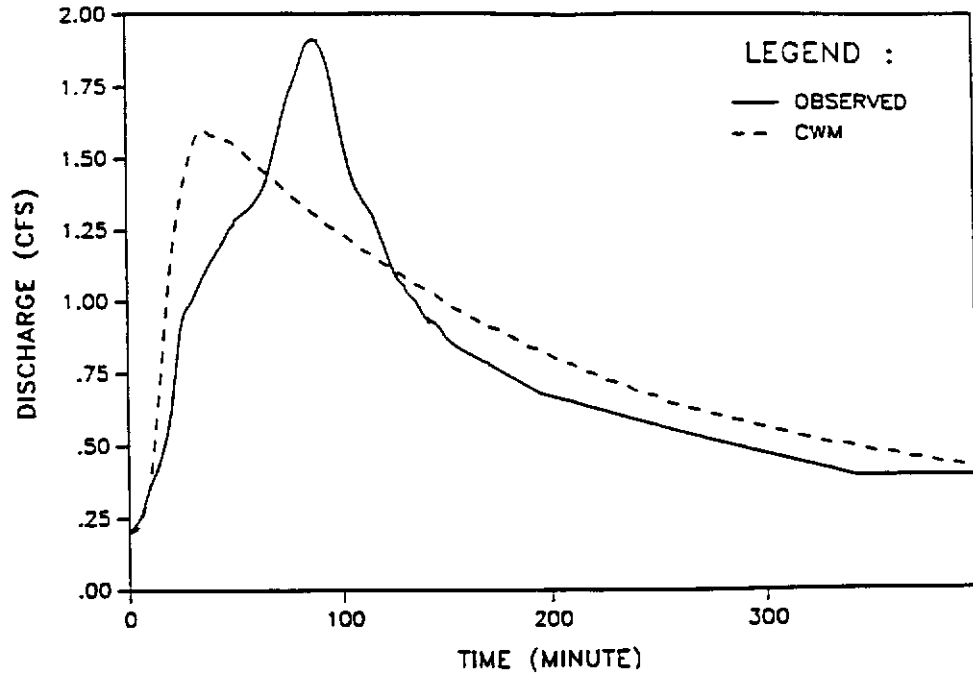


Figure 5.3 Crane Creek : Storm 3 : Comprehensive Watershed Model

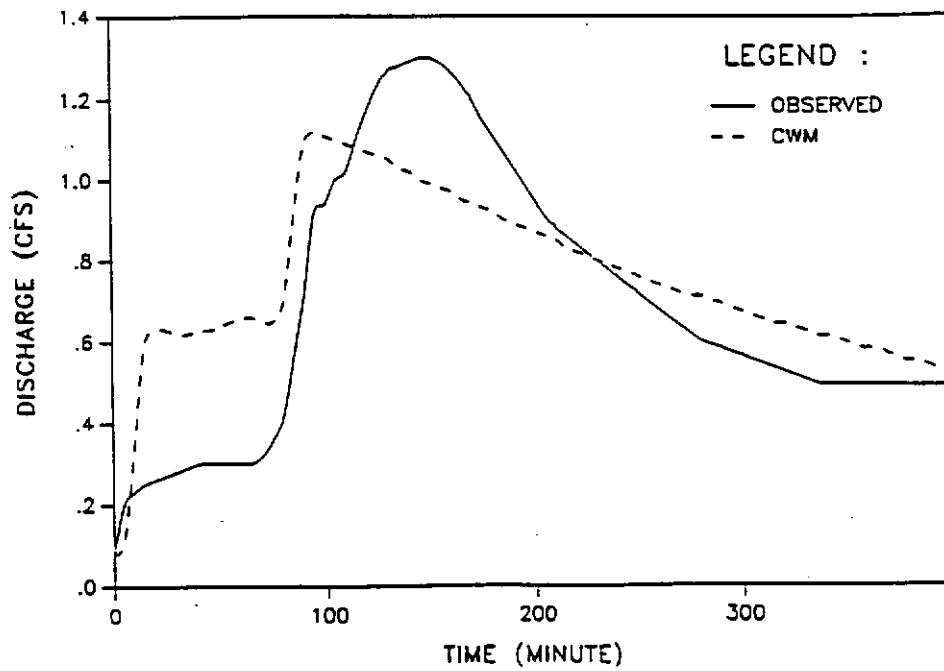


Figure 5.4 Crane Creek : Storm 4 : Comprehensive Watershed Model



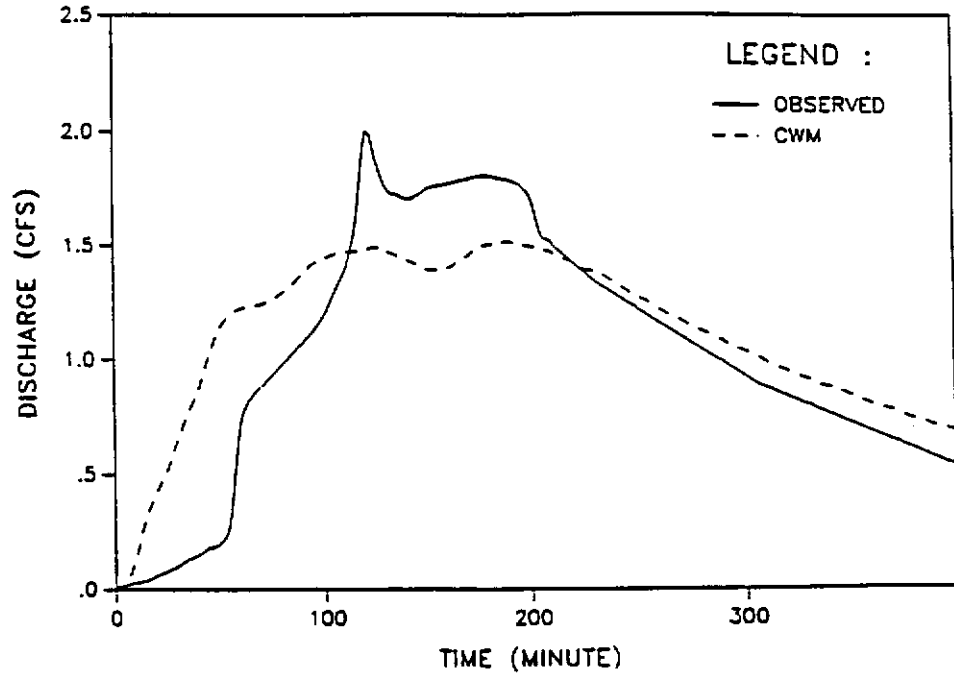


Figure 5.5 R.F. Sandlick Creek : Storm 1 : Comprehensive Watershed Model

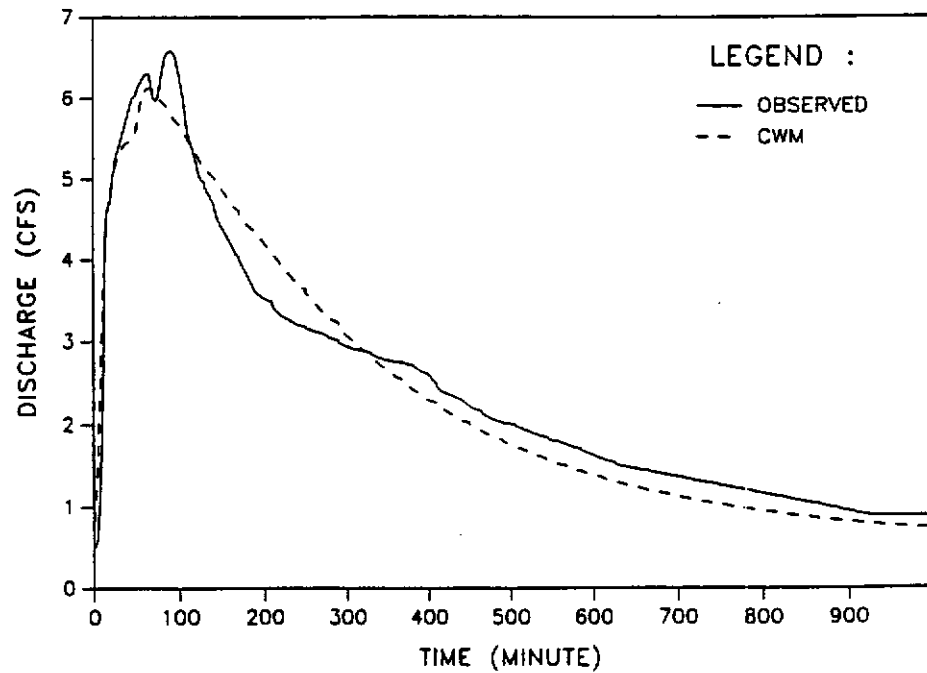


Figure 5.6 R.F. Sandlick Creek : Storm 2 : Comprehensive Watershed Model

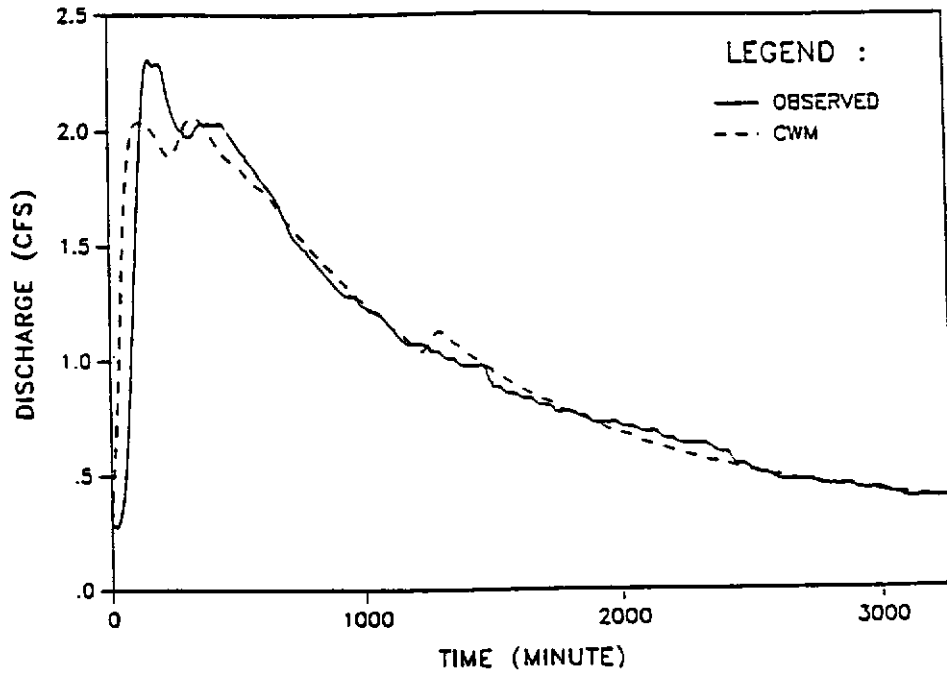


Figure 5.7 Little Millseat : Storm 1 : Comprehensive Watershed Model

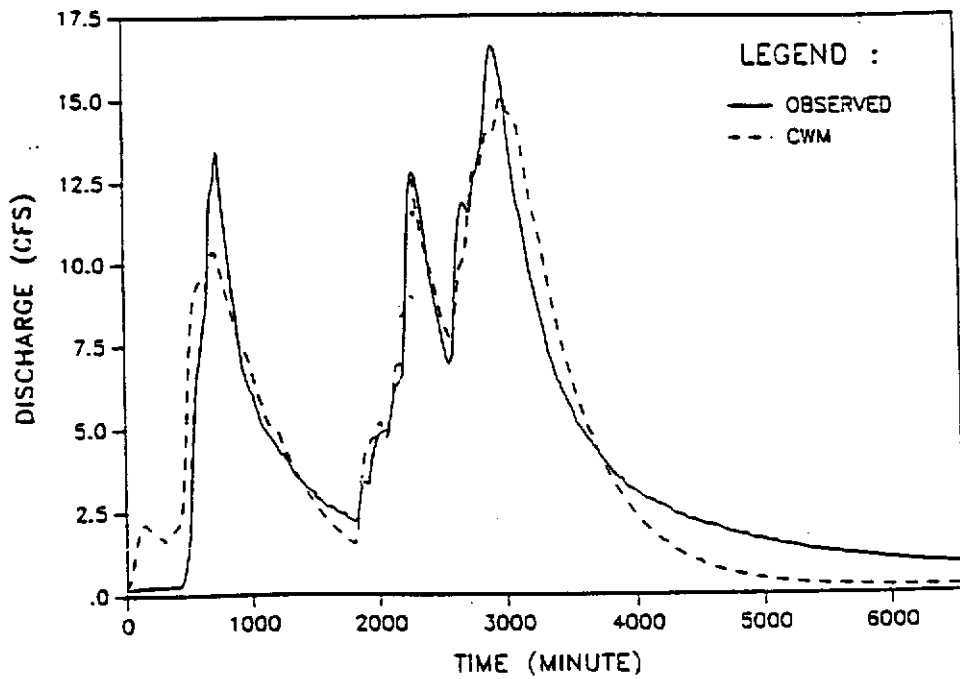


Figure 5.8 Little Millseat : Storm 2 : Comprehensive Watershed Model

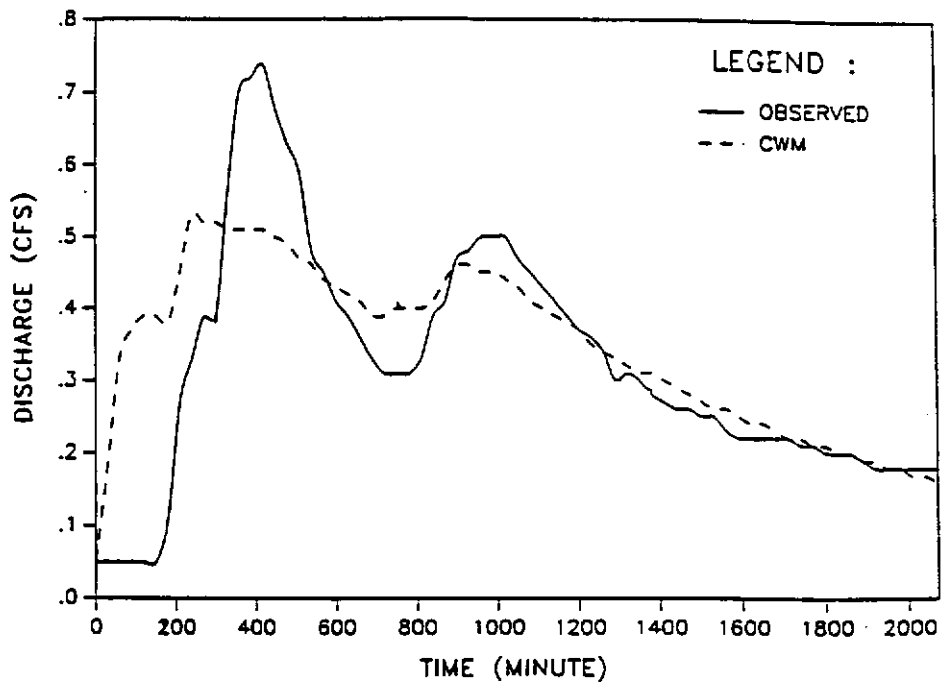


Figure 5.9 Little Millseat : Storm 3 : Comprehensive Watershed Model

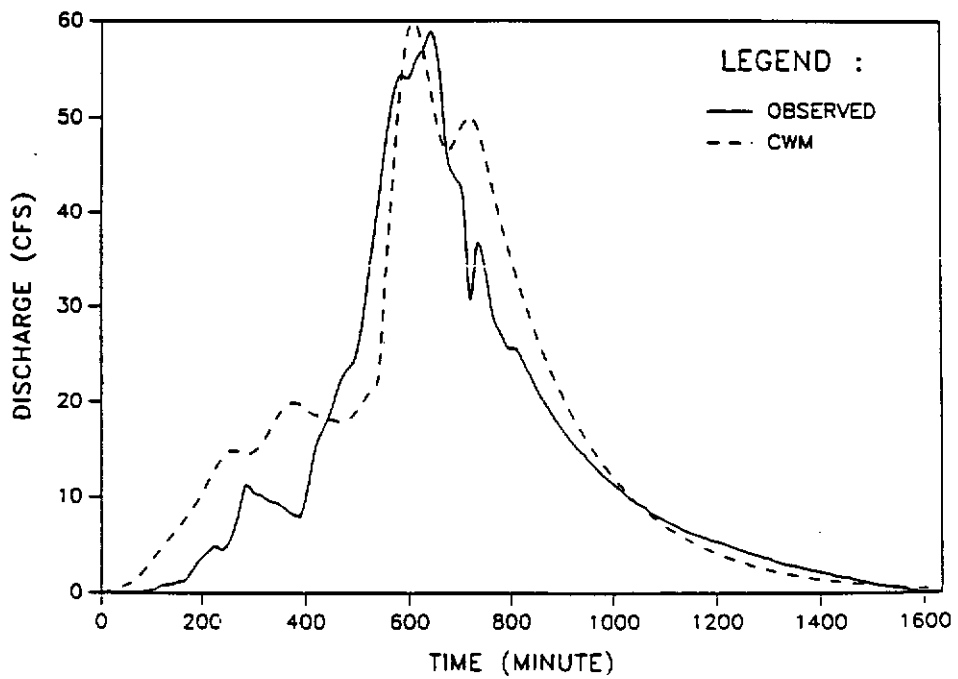


Figure 5.10 Cane Branch : Storm 1 : Comprehensive Watershed Model

For all four watersheds, the comprehensive watershed model tends to overpredict the volume. As regards peak discharge, the model tends to slightly underpredict. In general, the time of peak for the predicted hydrographs is shorter than that for the observed hydrographs thus indicating a quicker response of peak flow using the model. From the plots (Figs. 5.1 to 5.10), it can be seen that the hydrographs produced with the model match the general characteristics of the observed hydrographs fairly well.

### **5.3.3. Discussion of Results :**

The comprehensive model developed in this research gives better performance than both the slow response subsurface models with optimized parameters and the Hortonian models with realistic parameters. It would appear that the rapid flow response which was observed in the four watersheds may be adequately predicted by the use of a conceptual model which incorporated a quick response (macropore) flow mechanism. In the proposed model the macropore flow response was simulated using a linear reservoir model.

## CHAPTER 6

### SUMMARY AND CONCLUSIONS

#### 6.1. Summary :

The objective of this research was to develop a watershed model to simulate the hydrologic response of steeply sloping forested watersheds. As part of this objective, two non-Hortonian and two Hortonian models were tested with data from selected watersheds in West Virginia and eastern Kentucky. This was done in order to understand the different mechanisms of flow responsible for storm hydrograph generation in this type of watersheds. Based on the understanding of the flow processes involved, an attempt was made to develop a comprehensive watershed model which incorporated all possible runoff generation mechanisms including quick response subsurface flow (macropore flow).

The two non-Hortonian models tested were the kinematic storage model (Sloan et al., 1983) and the saturation deficit model (Beven and Wood, 1983). Both of these models were embedded in HEC-1, a hydrologic software package developed by Corps of Engineers, Davis, California. The models were applied to ten different storms in four watersheds in order to assess their applicability to the prediction of the hydrologic response of steeply sloping forested watersheds. The results show that models which account only for slow response subsurface flow (micropore flow) were unable to regenerate runoff hydrographs in the four forested watersheds considered in this research.

The two Hortonian models tested were Clark's unitgraph model and Snyder's unitgraph model (available in HEC-1). These models were also applied to the previously mentioned ten storms. The results demonstrate

that with parameter optimization, these two models can simulate with substantial accuracy the hydrologic response of this type of watersheds. However, the parameter values so obtained are very unrealistic. Furthermore, with realistic data, these models did not work for these watersheds because of the absence of any rainfall excess.

The failure of the slow response subsurface models and the success of the Hortonian models with optimized parameters led to the conclusion of a possible quick response subsurface flow mechanism being in play. This backdrop provided the justification for developing a comprehensive watershed model which incorporates a quick response macropore flow mechanism.

Based on the conclusions from the testing of the two non-Hortonian and the two Hortonian models, a simple conceptual comprehensive watershed model was developed for predicting storm hydrograph from small, steeply sloping forested watersheds. The conceptual model incorporates all types of flow processes including macropore flow (quick response subsurface flow). Once the conceptual model was developed it was embedded in the HEC-1 watershed program in order to provide a more comprehensive framework for modeling large tributary watersheds.

An evaluation of the resulting model was made using the data from the previously mentioned four watersheds in West Virginia and eastern Kentucky. The model predicted with reasonable accuracy the response of these watersheds to precipitation. The correlation of runoff volume, peak flow and time of peak between observed and predicted hydrographs was good. The results indicate that the model is capable of simulating the hydrologic response of this type of watersheds while at the same time depicting the actual flow mechanism in play.

## 6.2. Conclusions :

The conclusions reached from this study may be outlined as follows:

- a) The primary process involved in the runoff generation of the modeled steeply sloping forested watersheds was subsurface quick flow (macropore flow).
- b) Slow response subsurface models like the kinematic storage model and the saturation deficit model were inadequate for simulating the runoff response of the modeled watersheds.
- c) Hortonian models like Clark's and Snyder's models were inoperative for the modeled watersheds with realistic data because of the absence of any rainfall excess. However, with complete parameter optimization, these models performed quite well although the final parameter values were unrealistic.
- d) Watershed models delineating the actual physical process are necessary in order to better understand the flow mechanism involved in steeply sloping forested watersheds.
- e) The comprehensive watershed model developed in this research predicts with reasonable accuracy the hydrologic response of steeply sloping forested watersheds taking into account the actual flow processes involved.

## 6.3. Recommendations for Future Research :

- a) The model developed during the current study may serve as the starting point in the future development of more useful simple conceptual comprehensive watershed models which would include all possible flow processes.
- b) No method has been developed so far to estimate the parameters of the macropore component of the comprehensive model. These include  $\alpha_{mp}$ ,  $\alpha_{smp}$

and  $C_{mp}$ . To develop guidelines for evaluating these parameters, tests on a physical hillslope model under a controlled environment are recommended. It should be understood that even with tests on a hillslope and even after developing guidelines for estimating  $\alpha_{mp}$ ,  $\alpha_{smp}$  and  $C_{mp}$ , the fact remains that the model developed in this research is a conceptual one and hence does not entirely explain the physics of macropore flow.

c) For reasons mentioned in recommendation (b) and as a natural sequel to the present model, efforts should be directed towards developing a more physically based model which considers the physical flow relationships embedded in macropore flow. Experimentations on a physical hillslope under controlled conditions can then be utilized more effectively in relating the parameters of the model to the hydrologic and geomorphologic characteristics of the hillslope. Better correlations among the model parameters and the watershed characteristics will certainly enhance the ability to predict the hydrologic response of the watershed while taking into account the actual flow mechanism in play. More importantly however, it is hoped that these correlations will lead to an increased understanding of the source and movement of pollutants within the watershed. As a result, it is expected that improved management practices may be identified for the proper management of the watershed.



## REFERENCES

- Aubertin, G.M., 1971 : Nature and Extent of Macropores in Forest Soils and Their Extent on Subsurface Water Movement. For. Serv. Res. Pap. NE (U.S.) 192 ps, 33 p.
- Barcelo, M.D. and Nieber, J.L., 1981 : Simulation of the Hydrology of Natural Pipes in a Soil Profile. Am. Soc. of Ag. Engr. Paper No. 81-2028, St. Joseph, MI 49085.
- Barcelo, M.D. and Nieber, J.L., 1982 : Influence of a Soil Pipe Network on Catchment Hydrology. Am. Soc. of Ag. Engr. Paper No. 82-2027, St. Joseph, MI 49085.
- Bernier, P.Y., 1982 : VSAS2: A Revised Source Area Simulator for Small Forested Basins. Ph.D Dissertation , Univ. of Georgia, Athens.
- Beven, K.J., 1977 : Hillslope Hydrographs by the Finite Element Method. Earth Surface Processes, 2, 13-28.
- Beven, K.J., 1981 : Micro-, Meso-, Macro-porosity and Channeling Flow in Soils. Soil Sci. Soc. Am. J., 45, 1245.
- Beven, K., 1982 : On Subsurface Storm Flow : Predictions with Simple Kinematic Theory for Saturated and Unsaturated Flows. WRR, 18(6), 1627-1633.
- Beven, K.J. and Kirkby, M.J., 1976 : Towards a Simple Physically-Based Variable Contributing Area Model of Catchment Hydrology. School of Geogr., Univ. of Leeds, Leeds, Work Pap. No. 154.
- Beven, K.J. and Kirkby, M.J., 1979 : A Physically-Based Variable Contributing Area Model of Basin Hydrology. Hydrol. Sci. Bull., 24, 43-69.
- Beven, K. and Germann, P., 1981 : Water Flow in Soil Macropores, 2, A Combined Flow Model. J. Soil Sci., 32, 15-29.
- Beven, K. and Germann, P., 1982 : Macropores and Waterflow in Soils. WRR, 18(15), 1311-1325.
- Beven, K. and Wood, E.F., 1983 : Catchment Geomorphology and the Dynamics of Runoff Contributing Areas. J. Hydrol., 65, 139-158.
- Burke, C.B. and Gray, D.D., 1983 : Hillslope Runoff Processes: A Finite Element Model. Report No. CE-HSE-83-11, 148 p., Hydraulics and Systems Engg., School of Civil Engg., Purdue Univ., West Lafayette, Indiana 47907.
- Clark, C.O., 1945 : Storage and the Unit Hydrograph. ASCE Trans., 110, 1419-1446.
- Corbett, E.S., 1979 : Hydrological Evaluation of the Stormflow Generation Process on a Forested Watershed. Ph.D Thesis, Office of Water Res. and Tech., Washington, D.C., NTIS : PB80-129133, 125 p.

- Crawford, N.H. and Linsley, R.K., 1966 : Digital Simulation in Hydrology : Stanford Watershed Model IV. Tech. Rept. No. 39, Dept. of Civil Engr., Stanford Univ., CA, 210 p.
- Cunge, J.A., 1969 : On the Subject of a Flood Propagation Computation Method (Muskingum Method). J. Hydraulic Res., 7(2), 205-230.
- Curtis, W.R., 1972 : Strip-Minng Increases Flood Potential of Mountain Watersheds. Watersheds in Transition, Amer. Water Resour. Assoc., pp. 357-360.
- Diskin, M.H., 1967 : On the Solution of the Muskingum Method of Flood Routing Equation. J. Hydrol., 5, 286-289.
- Dooce, J.C.I. and Harley, B.M., 1967 : Linear Routing in Uniform Open Channels. International Hydrology Symposium, Fort Collins.
- Dunne, T., 1983 : Relation of Field Studies and Modelling in the Prediction of Runoff. J. Hydrol., 65, 25-48.
- Dunne, T. and Black, R.G., 1970 : Partial Area Contributions to Storm Runoff in a Small New England Watershed. WRR, 6, 1296-1311.
- Dunne, T., Moore, T.R., and Taylor, C.H., 1975 : Recognition and Prediction of Runoff Producing Zones in Humid Regions. Hydrol. Sci. Bull., 20, No. 3, 305-327.
- Engman, E.T. and Rogowski, A.S., 1974 : A Partial Area Model for Storm Flow Synthesis. WRR, 10(3), 464-472.
- Fenneman, N.M. and Johnson, D.W., 1946 : Physical Divisions of the United States. U.S. Geological Survey Map.
- Fread, D.L., 1985 : Channel Routing : Chapter 14, Hydrological Forecasting, Edited by M.G. Anderson and T.P. Burt, Copyright 1985, John Wiley and Sons Ltd.
- Freeze, R.A., 1972 : Role of Subsurface Flow in Generating Surface Runoff 2, Upstream Source Areas. WRR, 8(5), 1272-1283.
- Freeze, R.A., 1969 : The Mechanism of Natural Groundwater Recharge and Discharge: 1. One-Dimensional, Vertical, Unsteady, Unsaturated Flow Above A Recharging or Discharging Groundwater Flow System. WRR, 5, pp. 153-171.
- Germann, P. and Beven, K., 1981a : Water Flow in Soil Macropores, 1, An Experimental Approach. J. Soil Sci., 32, 1-13.
- Germann, P. and Beven, K., 1981b : Water Flow in Soil Macropores, 3, A Statistical Approach. J. Soil Sci., 32, 31-39.
- Germann, P. and Beven, K., 1985 : Kinematic Wave Approximation to Infiltration into Soils with Sorbing Macropores. WRR, 21(7), pp. 990-996.

Green, W.H. and Ampt, G.A., 1911 : Studies on Soil Physics, I -- Flow of Air and Water Through Soils. J. Agri. Res., 4, pp. 1-24.

Hanson, C.T., 1977 : Relationship of Soil and Site Characteristics to Soil Moisture Regimes in a Forested Watershed. Unpub. M.S. Thesis, Univ. of Kentucky, Lexington, Ky.

HEC-1 Users Manual, 1986 : Hec-1 Flood Hydrograph Package, U.S. Army Corps of Engineers, Users and Programmers Manual.

Hewlett, J.D., 1961 : Soil Moisture as a Source of Base Flow from Steep Mountain Watersheds. Southeastern Forest Experiment Station Pap. No. 132, USDA-Forest Service, Asheville, NC, 11 p.

Hewlett, J.D. and Hibbert, A.R., 1967 : Factors Affecting the Response of Small Watersheds to Precipitation in Humid Areas. W.E. Sopper and H.W. Lull (Editors), Forest Hydrology, Pergamon, Oxford, pp. 275-290.

Hewlett, J.D. and Troendle, C.A., 1975 : Non-point and Diffused Water Sources : A Variable Source Area Problem. Watershed Management, Logan, Utah, ASCE, pp. 21-45.

Holtan, H.N., 1961 : A Concept for Infiltration Estimates in Watershed Engineering. USDA, ARS-41-51, 25 p.

Holtan, H.N., England, C.B., and Shanholtz, V.O., 1965 : Concepts in Hydrologic Soil Grouping. Pap. No. 65-739, Winter Meeting of ASAE, Chicago, Ill.

Holtan, H.N., Stiltner, G.J., Henson, W.H., and Lopez, N.C., 1975 : USDAHL-74 Revised Model of Watershed Hydrology. USDA, ARS Tech. Bull. No. 1518, Washington, D.C.

Horton, R.E., 1933 : The Role of Infiltration in the Hydrologic Cycle. Trans. AGU, 14, 460-466.

Hursh, C.R. and Brater, E.F., 1941 : Separating Storm Hydrographs from Small Drainage Areas into Surface and Subsurface Flow. EOS Trans. AGU, 22, 802-870.

Hutchins, R.B., Blevins, R.L., Hill, J.H., and White, E.H., 1976 : The Influence of Soils and Microclimate on Vegetation of Forested Slopes in Eastern Kentucky. Soil Sci., 12(4), 239-241.

Hyami, S., 1951 : On the Propagation of Flood Waves, Bulletin No. 1, Disaster Prevention Research Institute, Kyoto Univ., Japan.

Isaacson, E.J., Stoker, J.J., and Troesch, B.A., 1954 : Numerical Solution of Flood Prediction and River Regulation Problems: Report 2, Numerical Solution of Flood Problems in Simplified Models of the Ohio River and the Junction of the Ohio and Mississippi Rivers. Report No. IMM-205, Institute of Mathematical Sciences, New York University, New York.

Jones, J.A.A., 1971 : Soil Piping and Stream Channel Initiation. WRR, 7, 602-610.

Jones, J.A.A., 1975 : Soil Piping and the Subsurface Initiation of Stream Channel Networks. Unpub. Ph.D Thesis, University of Cambridge, England, 467 p.

Kiesler, J., Quinones, F., Mull, D., and York, K., 1983 : Hydrology of Area 13, Eastern Coal Province, Kentucky, Virginia and West Virginia. USGS WRI Open File Rept. 82-505.

Kirkby, M.J., 1976 : Tests of the Random Network and Its Application to Basin Hydrology. Earth Surface Processes, 1(3), 197-212.

Kirkby, M.J., Callen, J., Weyman, D.R., and Wood, J., 1976 : Measurement and Modelling of Dynamic Contributing Areas in Very Small Catchments. Working Pap. 167, School of Geogr., Univ. of Leeds.

Li, R.M., Simons, D.B., and Stevens, M.A., 1975 : Nonlinear Kinematic Wave Approximation for Water Routing. WRR, 11(2), pp 245.

Lighthall, M.H. and Whitman, G.B., 1955 : On Kineamtic Waves, 1. Flood Movement in Long Rivers. Proc. R. Soc., London Ser. A., 229, 281-316.

Linsley, R.K., Jr., Kohler, M.A., and Paulhus, L.H., 1975 : Hydrology For Engineers. New York, McGraw-Hill Book Company.

McCarthy, G.T., 1938 : The Unit Hydrographs and Flood Routing. Unpub. Manuscript, North Atlantic Division, U.S. Army Corps of Engineers.

Mosley, M.P., 1979 : Streamflow Generation in a Forested Watershed, New Zealand. WRR, 15, 795-806.

Mosley, M.P., 1982 : Subsurface Flow Velocities Through Selected Forest Soils, South Island, New Zealand. J. Hydrol., 55, 65-92.

Musgrave, G.W., 1955 : How Much Rain Enters the Soil . Alfred Stefferud (ed.), Water, The Year Book of Agriculture, 1955, U.S. Govt. Printing Office, Washington, D.C., pp 151-159.

Musser, J. J., 1963 : Description of Physical Environment and of Strip-mining Operations in Parts of Beaver Creek Basin, Kentucky. U.S.G.S. Professional Pap. 427-A, 25 p.

Nash, J.E., 1957 : The Form of the Instantaneous Unit Hydrograph. IASH Publication No. 45, 3, 114-121.

Nieber, J.L., 1979 : Hillslope Runoff Characteristics. Ph.D Thesis, Cornell Univ., Ithaca, N.Y., Univ. Microfilms International, Ann Arbor, MI, 260 p.

Nieber, J.L., 1982 : Hillslope Soil Moisture Flow, Approximation by A One-Dimensional Formulation. ASAE Pap. No. 82-2026, St. Joseph, MI.

- NOAA,1960 : Climatological Data, Kentucky, 1960. National Oceanic and Atmospheric Administration.
- NOAA,1981 : Climatological Data, West Virginia, 1981. National Oceanic and Atmospheric Administration.
- NOAA,1982 : Climatological Data, West Virginia, 1981. National Oceanic and Atmospheric Administration.
- NOAA,1985 : Climatological Data, Kentucky. 1985. National Oceanic and Atmospheric Administration.
- NOAA,1986 : Climatological Data, Kentucky, 1986. National Oceanic and Atmospheric Administration.
- Nuckols, J.R., 1982 : The Influence of Atmospheric Nitrogen Influx upon the Stream Nitrogen Profile of Two Relatively Undisturbed Forested Watersheds in the Cumberland Plateau of the Eastern United States. Unpub. Ph.D Dissertation, Univ. of Kentucky, Lexington, KY, 264 p.
- Philip, J.R., 1954 : An Infiltration Equation with Physical Significance. Soil Science Society of America Proceedings, V. 77, pp. 153-157.
- Philip, J.R., 1957 : Numerical Solution of Equations of the Diffusion Type with Diffusivity Concentration Dependent. Australian J. Phys., 10,29.
- Price, R.K., 1974 : Comparison of Four Numerical Methods for Flood Routing. ASCE Journal of the Hydraulics Division, Vol. 100, HY7.
- Retzer, J.L., 1963 : Soil Foramtion and Classification of Forested Mountain Lands in the United States. Soil Sci., 96(1), 68-74.
- Schwab, G.O., Frevert, R.L.K., Edminster, T.W., and Barnes, K.K., 1966 : Soil and Water Conservation Engineering. John Wiley & Sons, Inc., New York.
- Scott, A.G., 1984 : Analysis of Characteristics of Simualted Flows from Small Surface-mined and Undisturbed Appalachian Watersheds in the Tug Fork Basin of Kentucky, Virginia, and West Virginia. U.S.G.S. Water Resources Investigations Rept. 84-4151, 169 p.
- SCS,1970 : Soil Survey of McCreary-Whitley Area, Kentucky.
- SCS,1982 : Soil Survey of Leslie and Perry Counties, Kentucky.
- Sloan, P.G., Moore, I.D., Coltharp, G.B., and Eigel, J.D., 1983 : Modeling Surface and Subsurface Stormflow on Steeply-sloping Forested Watersheds. Rept. 142, 167 p., Water Resour. Inst., Univ. of Ky., Lexington, KY.
- Smith, W.D., 1982 : The Physical and Hydrological Processes of Soils on Field Branch Watershed, Unpub. M.S. Thesis, Univ. of Kentucky, Lexington, KY, 65 p.

Snyder, F.F., 1938 : Synthetic Unit Graphs. Trans. Amer. Geophys. Union, 19, 447-454.

Soil Conservation Service, 1972 : SCS National Engg. Handbook, Section 4, Hydrology.

Springer, E.P., and Coltharp, G.B., 1978 : Some Hydrologic Characteristics of a Small Forested Watershed in Eastern Kentucky. Trans. of the Kentucky Academy of Science, 39(1-2), 31-38.

Stoker, J.J., 1953 : Numerical Solution of Flood Prediction and River Regulation Problems: Report 1, Derivation of Basic Theory and Formulation of Numerical Methods of Attack. Report No. IMM-200, Institute of Mathematical Sciences, New York University, New York.

Surkan, A.J., 1968 : Synthetic Hydrographs : Effects of Network Geometry. WRR, 5, 112-128.

Troendle, C.A., 1985 : Variable Source Area Models, Chapter 12, Hydrological Forecasting, Edited by M.G. Anderson and T.P. Burt, Copyright 1985, John Wiley and Sons Ltd., pp 347-403.

Troendle, C.A. and Hewlett, J.D., 1979 : A Variable Source Area Simulator (VSAS) for Small Forested Watersheds. Unpub. Pap., Univ. of Georgia, Athens, GA, 38 p.

USDA, 1965 : Soil Reports for Fourteen Counties in Eastern Kentucky. USDA, Washington, D.C.

Viessmann, W., Jr., Knapp, J.W., Lewis, G.W., and Harbaugh, T.E., 1977 : Introduction to Hydrology, Harper and Row, New York, 704 p.

Weyman, D.R., 1970 : Throughflow on Hillslopes and Its Relation to the Stream Hydrograph. Bull. Assoc. Sci. Hydrol., 15(3), 25-33.

Weyman, D.R., 1973 : Measurement of the Downslope Flow of Water in a Soil. J. Hydrol., 20, 267-288.

Whipkey, R.Z., 1965 : Subsurface Flow of Forested Slopes. Bull. Int. Assoc. Sci. Hydrol., 10(2), 74-85.

Whipkey, R.Z., 1967 : Theory and Mechanics of Subsurface Storm Flow. Proc. Int. Sym. on Forest Hydrology, Penn. State Univ., Univ. Park, PA, pp 255-260.

Whipkey, R.Z., 1969 : Storm Runoff from Forested Catchments by Subsurface Routes. Intern. Assoc. Sci. Hydrol., 85, 773-779.

Wilson, B.N., Barfield, B.J., Ward, A.D., and Moore, I.D., 1984 : A Hydrology and Sedimentology Watershed Model, Part I : Operational Format and Hydrologic Component. Trans. of the ASAE, 27(5), 1370-1377.

APPENDIX A

PRECIPITATION HYETOGRAPHS

# PRECIPITATION HYETOGRAPH

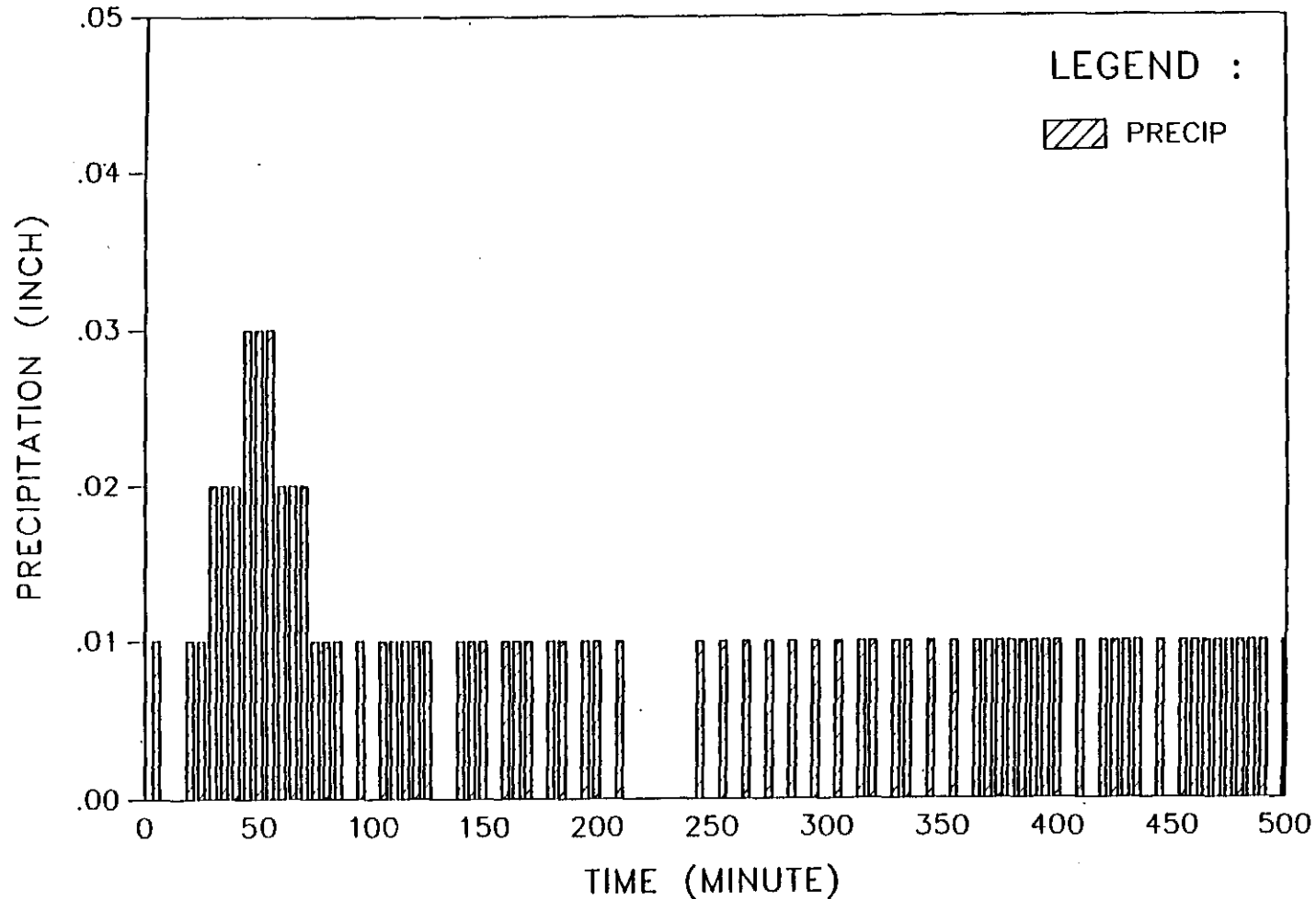


Figure A.1 : Crane Creek : Storm 1



# PRECIPITATION HYETOGRAPH

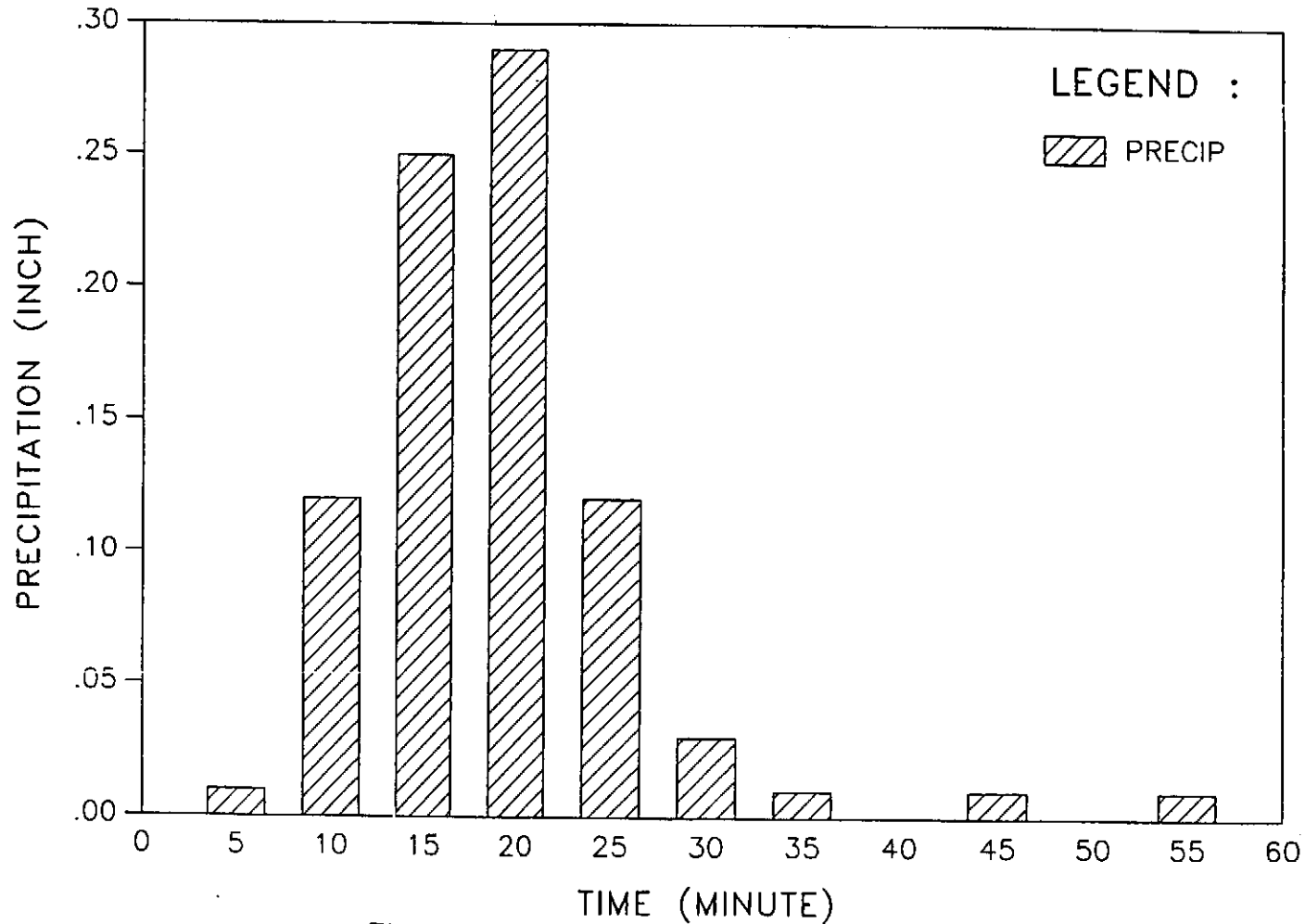


Figure A.2 : Crane Creek : Storm 2

# PRECIPITATION HYETOGRAPH

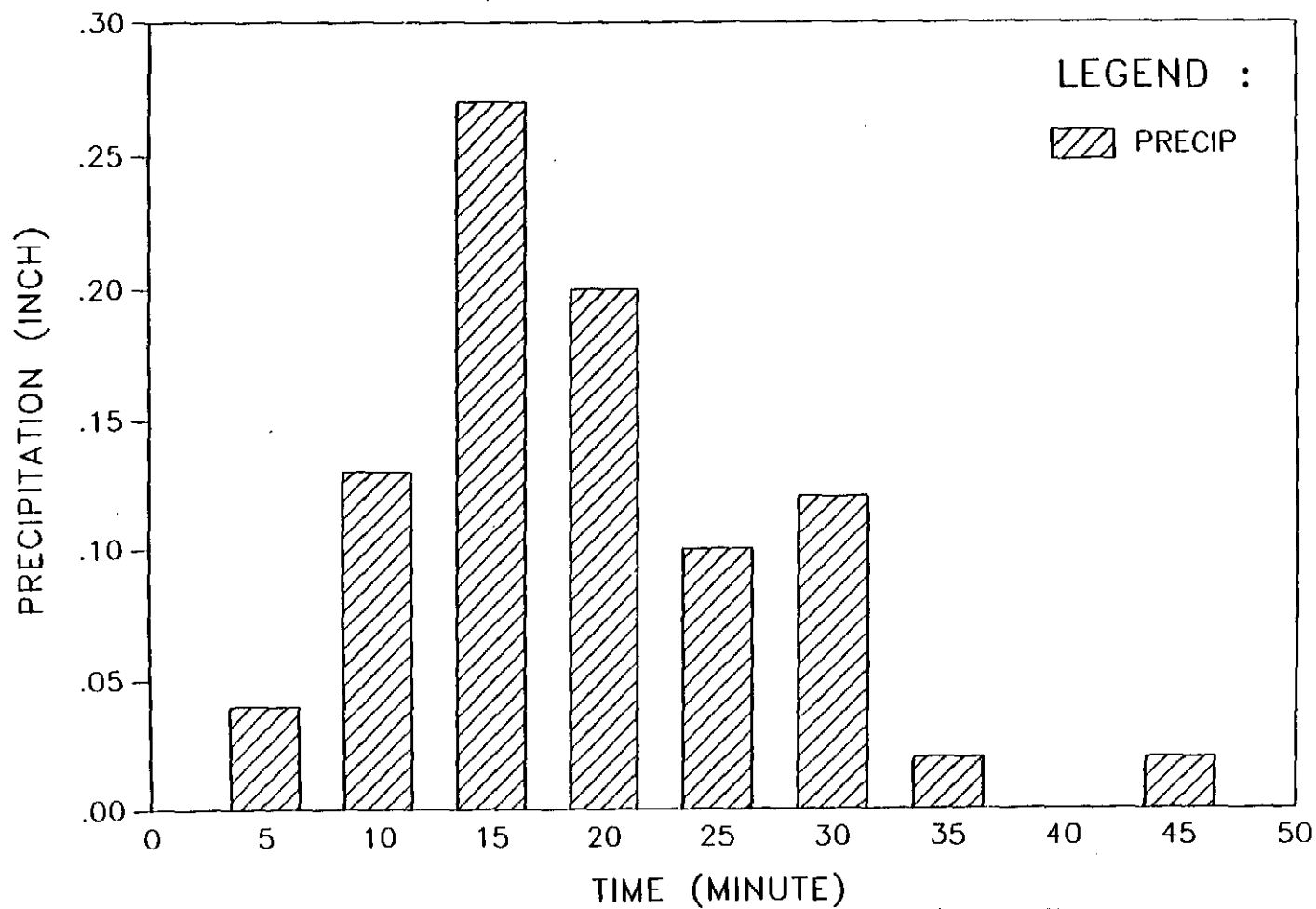


Figure A.3 : Crane Creek : Storm 3

# PRECIPITATION HYETOGRAPH

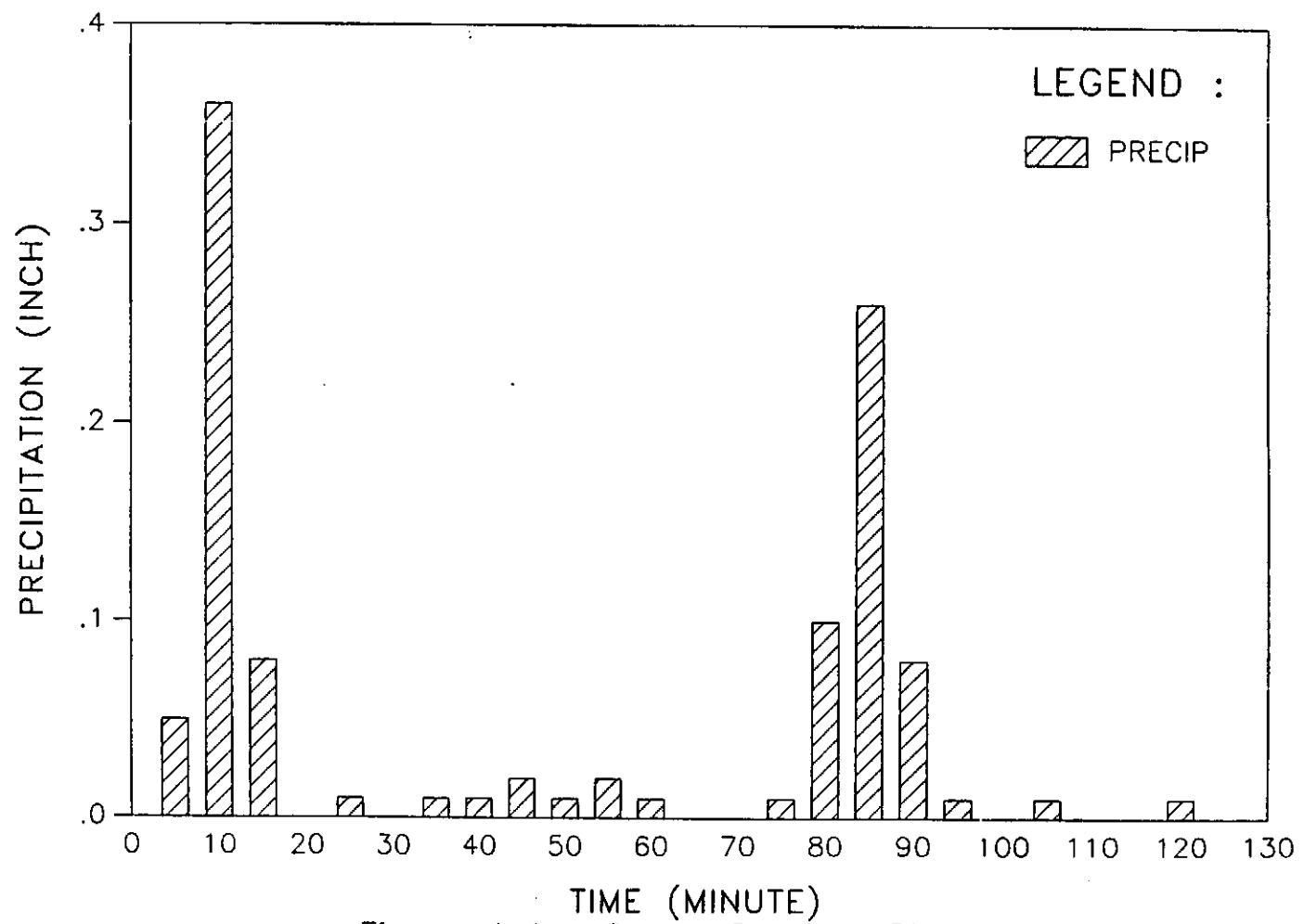


Figure A.4 : Crane Creek : Storm 4

# PRECIPITATION HYETOGRAPH

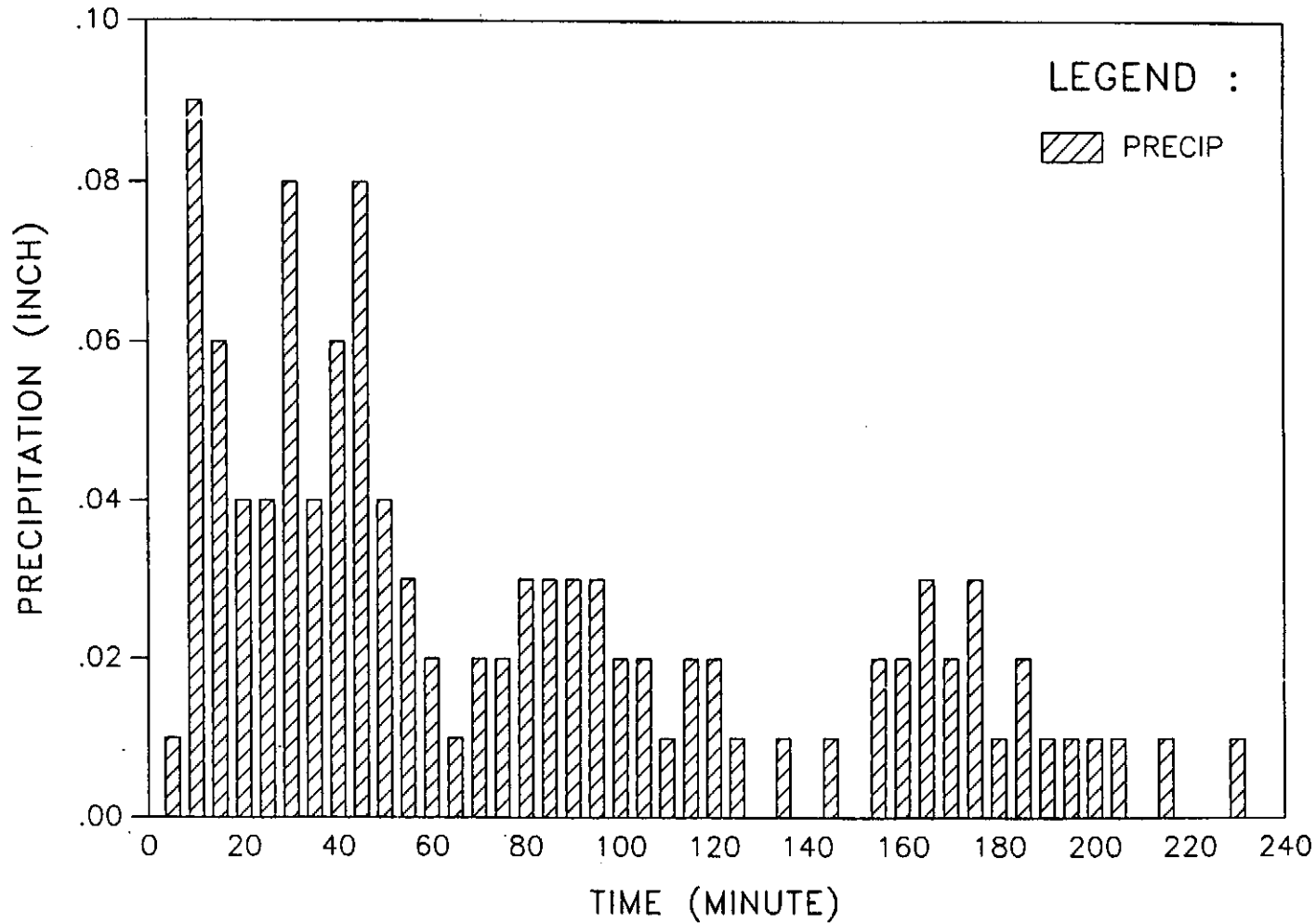


Figure A.5 : R.F. Sandlick Creek : Storm 1

# PRECIPITATION HYETOGRAPH

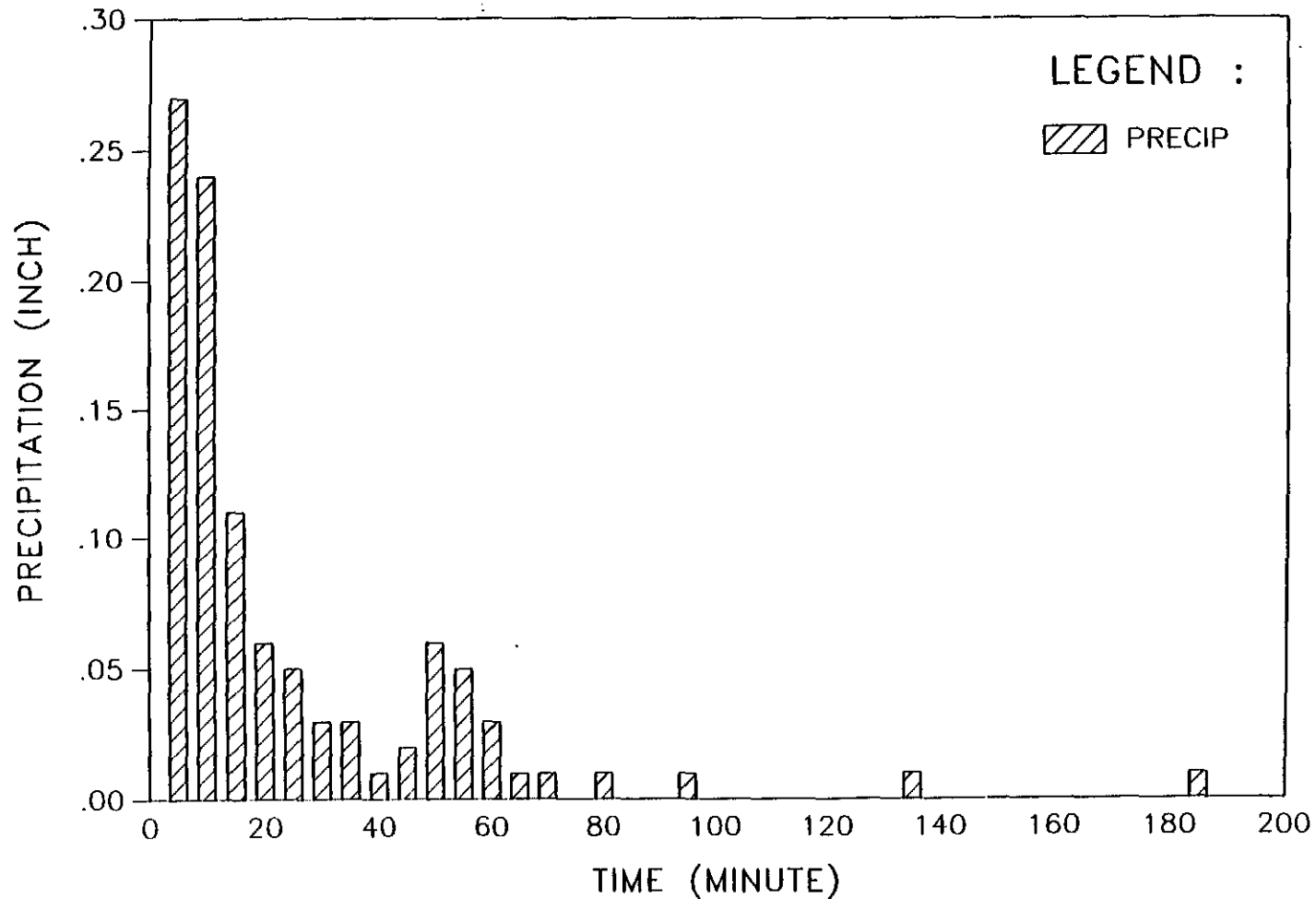


Figure A.6 : R.F. Sandlick Creek : Storm 2

# PRECIPITATION HYETOGRAPH

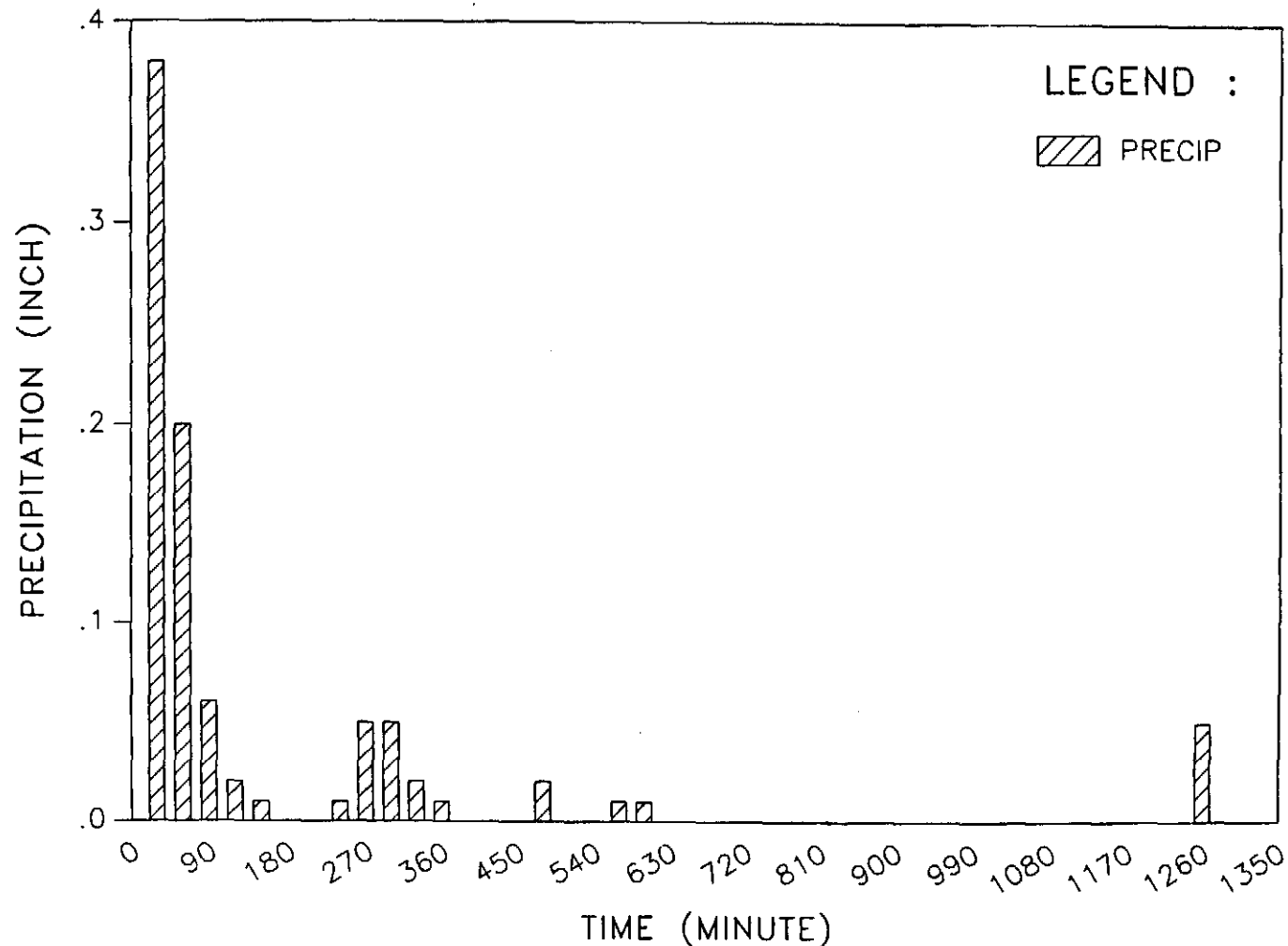


Figure A.7 : Little Millseat : Storm 1

# PRECIPITATION HYETOGRAPH

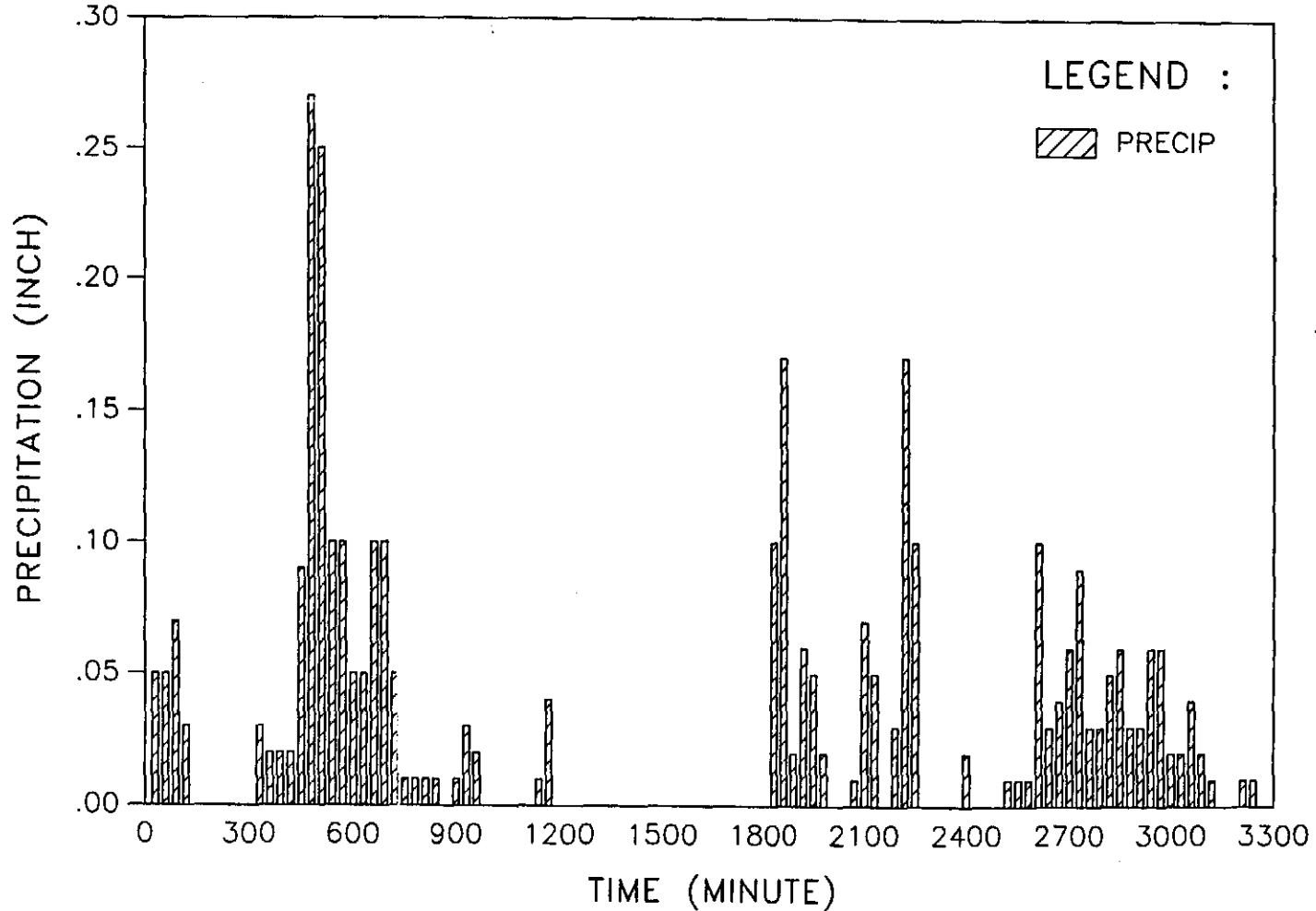


Figure A.8 : Little Millseat : Storm 2

# PRECIPITATION HYETOGRAPH

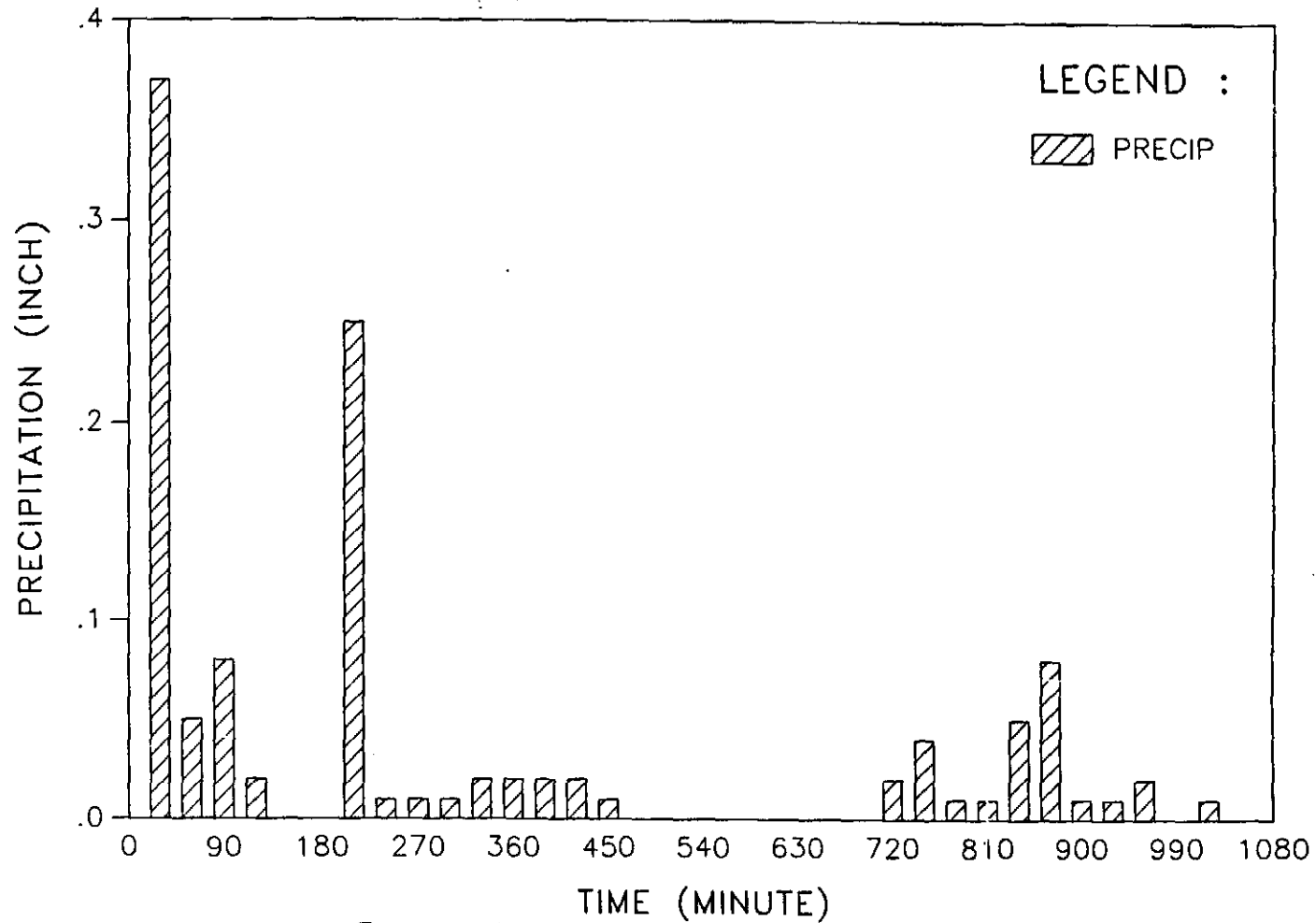


Figure A.9 : Little Millseat : Storm 3



# PRECIPITATION HYETOGRAPH

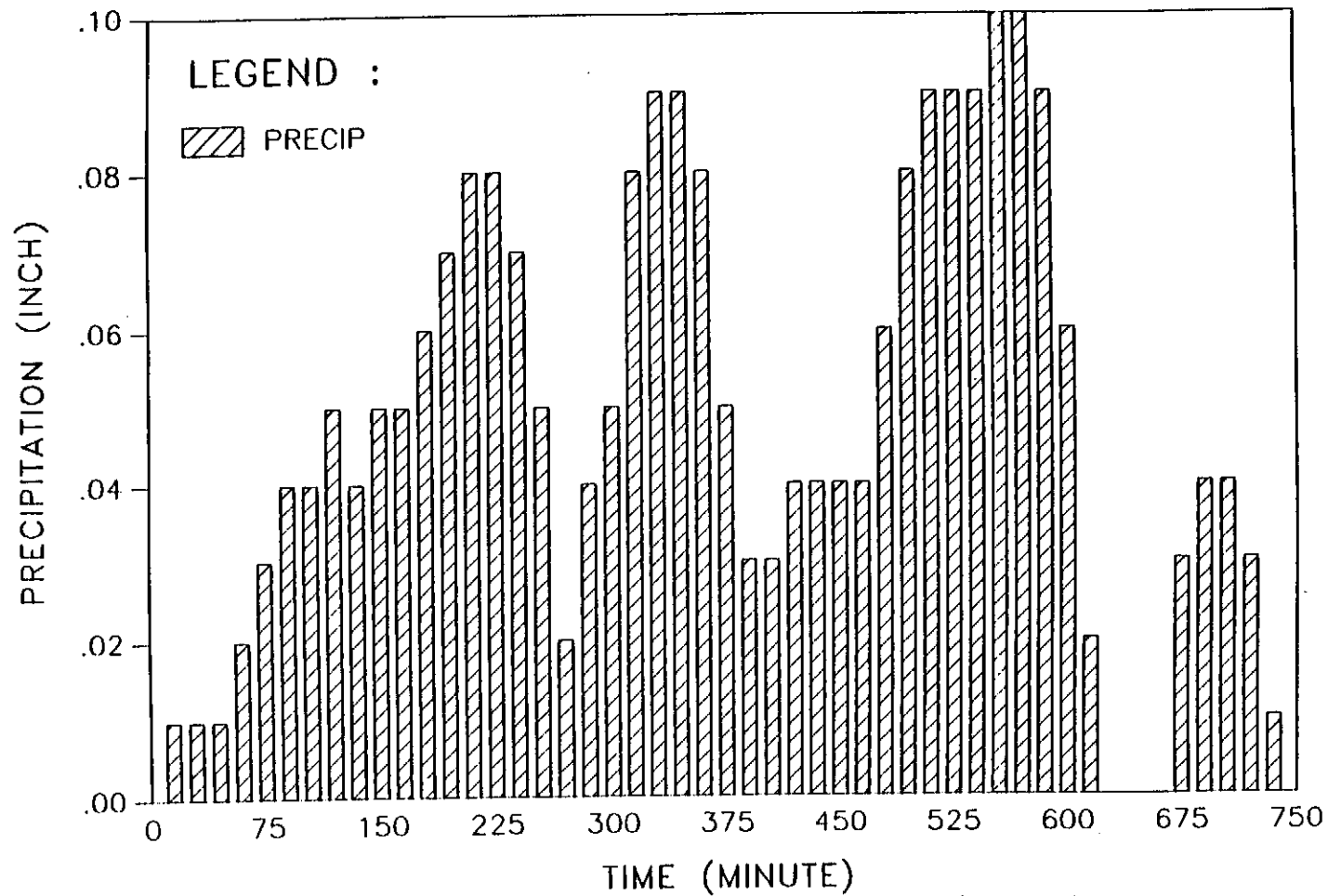


Figure A.10 : Cane Branch : Storm 1